

# Optics and Fluid Dynamics Department annual progress report for 2001

**Bindslev, H.; Hanson, Steen Grüner; Lynov, Jens-Peter; Petersen, Paul Michael; Skaarup, Bitten**

*Publication date:*
2002

*Document Version*
Publisher's PDF, also known as Version of record

Risø-R-1314(EN)

# Optics and Fluid Dynamics Department Annual Progress Report for 2001

**Edited by H. Bindslev, S.G. Hanson, J.P. Lynov
P.M. Petersen and B. Skaarup**

**Risø National Laboratory, Roskilde, Denmark
March 2002**

**Abstract** The Optics and Fluid Dynamics Department performs basic and applied research within three scientific programmes: (1) laser systems and optical materials, (2) optical diagnostics and information processing and (3) plasma and fluid dynamics. The department has core competences in: optical sensors, optical materials, optical storage, biooptics, numerical modelling and information processing, non-linear dynamics and fusion plasma physics. The research is supported by several EU programmes, including EURATOM, by Danish research councils and by industry. A summary of the activities in 2001 is presented.

ISBN 87-550-2993-0 (Internet)
ISSN 0106-2840
ISSN 0906-1797

# Contents

# 1. Introduction

*J.P. Lynov*
*jens-peter.lynov@risoe.dk*

During January–March 2001, an international evaluation panel evaluated Risø National Laboratory. The evaluation was initiated in accordance with the performance contract for the period 1988-2001 between the former Ministry of Information Technology and Research (now part of the Ministry of Science, Technology and Innovation) and Risø. The evaluation of the Optics and Fluid Dynamics Department was very positive and found that the research in the department is of outstanding international class. The full report is available on the homepage of the Ministry of Science, Technology and Innovation at http://www.fsk.dk.

The Optics and Fluid Dynamics Department performs basic and applied research in laser systems, optical sensors and optical materials as well as in plasma and fluid dynamics. The research is conducted as a combination of science and technology with the following core competences:

- Optical sensors
  - Light propagation in complex systems
  - Laser-based sensors
  - Diffractive optical components
  - Phase contrast methods
- Optical materials
  - Polymers
  - Laser ablation
- Optical storage
  - Holographic techniques
  - Optical encryption
- Biooptics
  - Light/tissue interaction
  - Diode laser systems
  - Biosensors
  - Optical tweezers
  - IR spectroscopy
- Numerical modelling and information processing
  - Plasma and fluid dynamics, optics, ultrasound
  - Knowledge-based processing
  - Image processing ("data mining")
- Non-linear dynamics
  - Turbulence
  - Vortex dynamics
  - Parametric processes
  - Photorefractive materials
- Fusion plasma physics
  - Theoretical plasma physics
  - Laser and microwave diagnostics

The output from the research activities is new knowledge and technology. The users are within industry, research communities and government, and the department is responsible for the Danish participation in EURATOM's fusion energy programme.

For the solution of many of the scientific and technological problems the department employs the following key technologies:

- Microtechnology for optical systems
  - Analogue and digital laser recording of holograms
  - Injection moulding of diffractive optical elements
- Optical characterisation
  - Determination of material surfaces
  - Phase contrast measurements
- Temperature calibration and IR measurement techniques
  - Accredited temperature calibration including IR techniques
  - Fourier transform infrared (FTIR) measurements

The department is organised in three scientific programs

- Laser systems and optical materials
- Optical diagnostics and information processing
- Plasma and fluid dynamics

In the following sections, the scientific and technical achievements during 2001 for each of these programmes are described in more detail.

# 2. Laser systems and optical materials

## 2.1 Introduction

*P.M. Petersen*
*paul.michael.petersen@risoe.dk*

The research programme on Laser Systems and Optical Materials (LSO) has its main competence within the areas of laser systems, holographic storage, active and passive polymer technology, laser-assisted deposition, and nonlinear properties of materials. The research initiatives within LSO include fundamental studies of advanced laser systems and optical materials and simultaneously point out new areas for application of lasers and optical materials. The aim is to become one of the leading international research groups within advanced laser systems and optical materials. We have close collaboration with Danish and foreign universities, research institutes and industry. Nationally, we participate in the Danish Polymer Centre and the Center for Biomedical Optics and New Laser Systems. Furthermore, we play an important role in the Danish Graduate School in Nonlinear Science and undertake significant teaching activities at both the University of Copenhagen and the Technical University of Denmark.

Research in the field of nonlinear optics has been a subject of intense investigations for many years. The field covering the dynamics of optical materials is concentrated on both inorganic and organic materials. Among the inorganic materials the efforts have been within photorefractives and semiconductors in which nonlinear effects such as parametric oscillation and amplification, optical phase conjugation, four-wave mixing and two-step gated recording processes have been studied. The organic studies include surface as well as bulk effects. More specifically storage effects, surface relief gratings, molecular reorientation dynamics, electrooptic properties and, finally, rotational effects are being investigated.

The polymer optics activity in LSO is currently involved in activities on the fabrication and replication of diffractive optics, dynamic holographic recording materials, liquid crystalline polymers as well as laser-assisted deposition of transparent coatings (indium tin oxide, ITO) on polymers. The common denominator of these research areas is a strong relation between theory and experimental work.

The research programme also includes a major activity within development of new laser systems. We are currently developing new and improved laser systems for applications in printing, rapid prototyping, biotechnology, materials processing and optical sensing. Our future generations of coherent light sources will be built on recent technological and scientific breakthroughs within improved optical materials and new cavity design. An important research area is the development of new high-power, tuneable semiconductors with high spatial and temporal coherence.

Laser ablation is also performed in LSO with facilities that comprise a vacuum chamber for studying fundamental laser plume properties, a vacuum chamber for thin film production by pulsed laser deposition, and a test chamber for production of polymer films. The facilities are based on UV light from an Nd:YAG laser with pulse energies up to 200 mJ at 355 nm.

Finally, holographic data storage is an important activity that has recently led to collaboration with industry. The activities within optical storage include development and application of polyesters and peptides for optical storage. An important activity is the use of spin-coated polyester films for application in holographic storage.

# 2.2 Nonlinear optics

### 2.2.1 Photorefractive response in polymers

*P.M. Johansen, K.G. Jespersen, T.G. Pedersen (Aalborg University, Denmark), E.V. Podivilov (Institute of Automation and Electrometry, Russia) and B.I. Sturman (Institute of Automation and Electrometry, Russia)*
per.michael.johansen@risoe.dk

The level of physical understanding of the nonlinear process that takes place in polymers and that displays the photorefractive effect is rather low. This feature is primarily due to the complexity of the charge transport in polymers as compared with that in inorganic materials. This complexity rests with factors such as spatial disorder and strong field dependence of the main transport parameters. In previous attempts at explaining the photorefractive effect in polymers, researchers have often combined particular microscopic models previously developed under strong simplifying assumptions for different physical processes and situations. The obvious weakness of this approach has forced experimenters to utilise the simplest known model for inorganic materials even without proper adjustment for the actual case. In order to circumvent this inherent problem we have employed a phenomenological approach to minimise the assumptions underlying the light-induced charge transport in polymers and to express the steady state photorefractive response of polymers through measurable medium characteristics.[1]

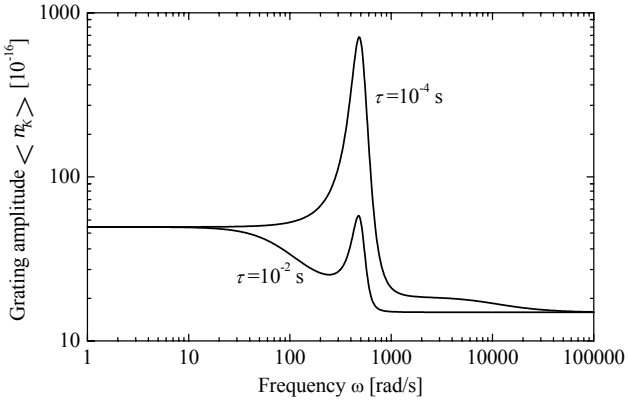


Figure 1. Frequency dependence of the first-order grating amplitude for two different values of τ. The two curves illustrate the cases $\tau\omega_{ac} > 1$ and $\tau\omega_{ac} << 1$, respectively, where $\omega_{ac} \approx$ 500 rad/s is the ac enhancement resonance frequency.

In photorefractive polymers containing rod-shaped nonlinear optical chromophores it has been demonstrated that there exists an orientational enhancement effect that is absent in traditional materials. Basically, the dipole moment of the chromophores couples to the combined applied and induced space-charge fields and this coupling leads to a preferred molecular orientation along the direction of the field. The enhancement effect adds to the usual electro-optic effect and, hence, the modulation of the refractive index increases. We have analysed the enhancement effect by means of a so-called rotational diffusion model and have studied the influence of the rotational response time on the photorefractive response as seen in Figure 1.[2]

1. E. V. Podivilov, B. I. Sturman, P. M. Johansen and T. G. Pedersen, *Opt. Lett.* **26**, 226 (2001).
2. T. G. Pedersen, K. G. Jespersen and P. M. Johansen, *Opt. Mat.* **18**, 95 (2001).

### 2.2.2 Rotational diffusion in active polymers

*K.G. Jespersen, P.M. Johansen, T.G. Pedersen (Aalborg University, Denmark), J. Juul Rasmussen, J. Wyller (Dept. of Mathematical Science, Agricultural University of Norway, Aas, Norway) and V. Naulin*
per.michael.johansen@risoe.dk

Our research is focussed on studying the dynamics of chromophores in a polymer matrix. The topic is relevant for nearly all polymer-based components in, e.g., imaging devices and in telecommunication. Dye containing polymers constitute a model system for investigating molecular dynamics in a viscous polymer matrix. We have extended an existing oriented-gas model to include a molecular field that represents the effect of a polymer matrix and thus describes the temperature dependence of the dynamics. The dynamics have been probed in an ellipsometer set-up that measures the induced birefringence due to an applied ac and/or dc electric field. We have consequently measured the relaxation dynamics of dye molecules and found a rotational diffusion process that depends critically on temperature. Furthermore, we have investigated the frequency response of the chromophores. The response shows a clear dependence on a characteristic rotational diffusion time constant as well as on the temperature via the molecular field of the polymer matrix. Both are in accordance with the extended oriented-gas theory. Future research will include conducting polymers in order to investigate the effect of molecular dynamics on the conductivity.

Application of the rotation diffusion model with the assumption that the molecular field is either parallel or anti-parallel to the applied field results in a rotational diffusion equation. An approximate solution to this equation can be found by means of a Galerkin approximation with respect to a Legendre basis and Fourier series expansion in terms of the Galerkin coefficients. The resulting algebraic system has to be truncated in order to obtain a closed form solution. However, such truncation needs close investigations of the convergence properties. Such studies has been published in Ref. 1 and we have proved that when the ac field is neglected, the equilibrium solutions of the rotational diffusion equation act as a global attractor for any initial distribution. In addition, the decay towards this distribution is a purely exponential decay for small and moderate values of the dc-field strength. When this field exceeds a certain threshold, the relaxation process is characterized as a damped oscillation.

1. J. Wyller, T. G. Pedersen and P. M. Johansen, *J. Phys. A: Mat. Gen.* **34**, 6531 (2001).

## 2.3 Polymer optics

### 2.3.1 A new plotter for small structures - the nanoplotter

*E. Rasmussen*
erling.rasmussen@risoe.dk

Nine years ago we developed a laserplotter, called the holoplotter, capable of manufacturing diffractive structures and masks.[1,2] The plotter has been used to make diffraction gratings, computer-generated holograms and diffractive optics. In general, the main objective has been to produce optical elements that in one single element can replace several conventional

optical elements; a procedure that cannot be made with traditional refractive optics (lenses) or diffractive optical elements.

The resolution of the holoplotter is down to 2.5 μm. For a number of tasks, however, this resolution is insufficient. For the last couple of years Risø has consequently been developing a new plotter called the nanoplotter.

Figure 2. Erling Rasmussen operating the nanoplotter.

The following features of the nanoplotter have been demonstrated:

- An 800 nm writing spot may be plotted in a raster with a resolution of less than 100 nm and with a degree of accuracy of less than 40 nm. Two light sources with wavelengths of 633 nm and 442 nm are available. The plotter is capable of plotting at 255 grey scale levels selected from a palette of 4096 grey levels.
- The maximum plot area is circular - Ø160 mm - or square 100 x 100 mm. The writing speed is up to 10 lines pr. second at 20 megapixels/sec.

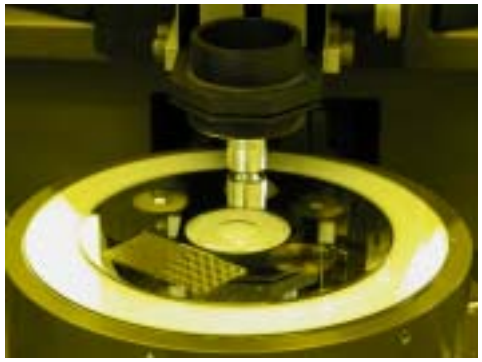

Figure 3. Writing head of the nanoplotter.

A few examples of the application areas of the nanoplotter are the manufacturing of, e.g., specifically designed optical components for two NASA projects, a number of computer-generated holograms for the English research centre DERA, test masks for a Spanish research group, and phase filters for Risø's own research in optical encryption.

For more information, follow this link.

1. Optics and Fluid Dynamics Department's Annual Progress Report for 1992, pp. 11-12. ISBN 87-550-1885-8.
2. Optics and Fluid Dynamics Department's Annual Progress Report for 1994, pg. 8. ISBN 87-550-2044-5.

### 2.3.2 Analytical modelling of two-beam coupling during grating translation in photorefractive media

*H.C. Pedersen, P.M. Johansen and T.G. Pedersen (Aalborg University, Denmark)*
henrik.pedersen@risoe.dk

When determining material parameters of new photorefractive materials, optical measurement techniques are often used. For example, when estimating the effective trap density in photorefractive polymers, a method called the grating translation technique has been used to measure the so-called photorefractive phase shift. The basic set-up is shown in Figure 4.

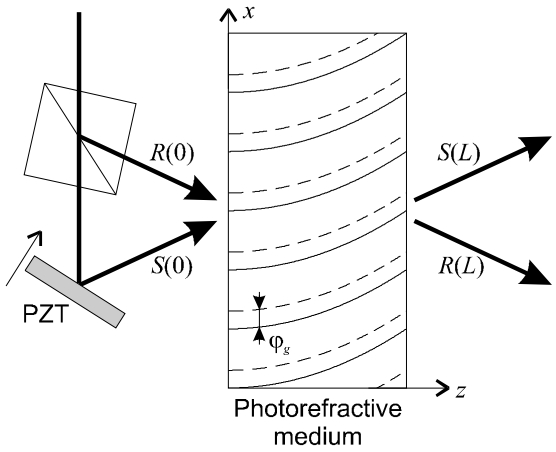


Figure 4. Schematic set-up showing the grating translation technique. The PZT is a piezodriven mirror that can be translated uniformly to induce a linearly increasing phase shift between the reference (R) and signal (S) beams, respectively. $\varphi_g$ is the phase shift between the illuminating light interference pattern and the induced photorefractive grating. This phase shift is called the photorefractive phase shift.

When the photorefractive medium is illuminated by the two crossed laser beams, the beams form a light interference pattern in the medium, which is running in the *x*-direction due to the moving piezo mirror. The light in turn induces a running photorefractive grating which translates at the same speed as the light pattern. However, the light pattern and the grating are generally out of phase. This phase shift has a large effect on the coupling efficiency between the beams and, thereby, the amplification of the signal beam S. If the phase shift is 90˚, the coupling is strongest leading to maximum amplification of the signal beam S. Conversely, if the phase shift is zero or 180˚, there is no amplification.

The grating formation has a certain response time (typically some ms) which means that if one suddenly stops the piezo mirror movement and, thereby, the movement of the light pattern, the grating will continue to run for some ms, enough for the phase shift to go through at least one cycle. Since the phase shift controls the gain, the signal beam is going to oscillate in time. Based on the initial phase, $\varphi_{meas}$, the initial photorefractive phase shift can be deducted.

Theoretically, the relation between $\varphi_{meas}$ and $\varphi_g$ can be derived from the coupled wave equations. Previously, this relation was calculated by using purely numerical methods.[1] In this work we have solved the wave coupling equations analytically leading to an analytical expression for the photorefractive phase shift. Moreover, the analytical work has revealed mistakes in the numerical results published earlier. In Figure 5 $\varphi_{meas}$ has been plotted versus the beam ratio $\beta$, which is the incident reference-to-signal intensity ratio.[2]

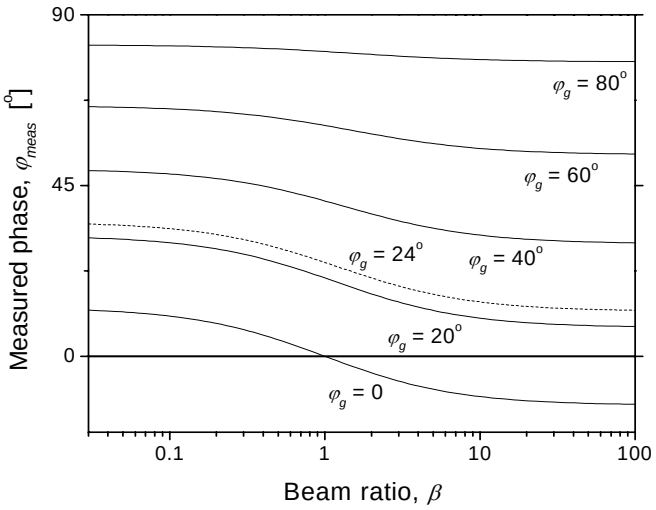


Figure 5. $\varphi_{meas}$ versus beam ratio β for different values of $\varphi_g$.

1. A. Grunnet-Jepsen, C.L. Thomsen, R.J. Twieg and W.E. Moerner, *Appl. Phys. Lett.* 70 (1997) 1515-1517.
2. H.C. Pedersen, P.M. Johansen and T.G. Pedersen, *Opt. Commun.* 192 (2001) 377-385.

### 2.3.3 Propagation of polarised light through azobenzene polyester films

*P. S. Ramanujam, L. Nedelchev*, A. Matharu* (*Optilink A/S, Denmark),*
*L. Nikolova (Bulgarian Academy of Science, Sofia, Bulgaria) and S. Hvilsted*
*(Technical University of Denmark, Denmark)*
*p.s.ramanujam@risoe*

When elliptically polarised light of appropriate wavelength corresponding to the *trans-cis-trans* isomerisation process is incident on thin films of azobenzene polyesters, a helical structure is induced. We have investigated the propagation of the exciting light beam (self-induced) as well as a probe light beam outside the absorption band through the polyester films. We have studied amorphous and liquid crystalline polyesters as well as copolyesters. We have shown[1] that after irradiation amorphous polyester behaves like a classical helical material after irradiation with elliptically polarised light.

1. L. Nedelchev, L. Nikolova, T. Todorov, T. Petrova, N. Tomova, V. Dragostinova, P.S. Ramanujam, S. Hvilsted, *J. Opt. A: Pure Appl. Opt.* **3**, 304 (2001).

### 2.3.4 Polarisation holograms in a "liquid crystal-porous glass" system

*P.S. Ramanujam, O. Yaroshchuk (Institute of Physics of Nasu, Kyiv, Ukraine),*
*K. Otto*, G. Pelzl* and F. Janovski* (*Martin Luther University, Halle, Germany)*
*p.s.ramanujam@risoe.dk*

Recording of polarisation gratings has been realized in porous glass with pore diameter of 40 Å filled with nematic liquid crystal 4-methoxy-4'-butyl-azobenzene.[1] Such recording is possible due to the strong decrease in the rotational diffusion of the liquid crystal molecules and their photo-products in ores compared with the bulk. Reversible and irreversible

components in the grating formation were observed. These could be associated with different photochemical reactions of liquid crystal molecules.

1. O. Yaroshchuk, K. Otto, G. Pelzl, F. Janovski and P.S. Ramanujam, *Mol. Cryst. Liq. Cryst. Sci. Technol.*, Sect. A, 359, 315 (2001)

### 2.3.5 High diffraction efficiency polarisation gratings recorded by biphotonic holography in an azobenzene liquid crystalline polyester

*P.S. Ramanujam, C. Sanchez*, R. Alcala* (Departamento de Fisica de la Materia Condensada, Zaragoza, Spain) and S. Hvilsted (Technical University of Denmark)*
*p.s.ramanujam@risoe.dk*

We have achieved high diffraction efficiency of the order of 30% with polarisation gratings recorded in thin films of an azobenzene side-chain liquid crystalline polyester by means of biphotonic processes; see Figure 6. This value is at least two orders of magnitude higher than those previously reported for biphotonic recording. The gratings can be erased with unpolarised blue light, and partial recovery of the diffraction efficiency has been observed after the erasure process when the sample is kept in darkness. Red light illumination of the erased film increases the recovered efficiency value and the recovery rate.[1]

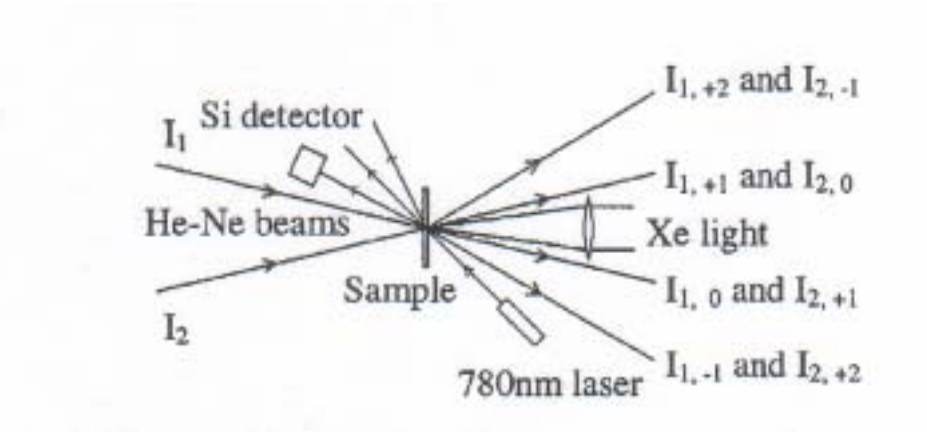


Figure 6. Biphotonic polarisation holographic set-up showing the recorded ($I_1$ and $I_2$) and diffracted beams ($I_{i,j}$) of the He-Ne laser.

1. C. Sanchez, R. Alcala, S. Hvilsted, P. S. Ramanujam, *Appl. Phys. Lett.* **78**, 3944 (2001).

## 2.4 New laser systems

### 2.4.1 A high-power diode laser system for the graphic industries

*B. Thestrup, P.M. Petersen, B. Sass, M. Chi and S. Juul Jensen*
*birgitte.thestrup@risoe.dk*

GaAs-based diode lasers are unique due to their small dimensions, low costs and high efficiency in comparison with, e.g., gas and solid-state lasers. Broad, single emitters can deliver up to several watts of output power and the diodes typically have long lifetimes in the order of 10,000 hours. However, the high output power of single emitters is achieved by increasing the width of the emitter aperture from a few microns to a few hundred microns.

This aperture increase gives rise to a multimode nondiffraction limited laser beam that cannot be focused properly.

In the present project, we are developing a new high-power diode laser system for the graphic industries in which we improve the spatial coherence of such high-power broad area lasers. The system will be implemented in an internal-drum image-setter machine developed by the Danish company Purup-Eskofot. By increasing the laser power it is possible to decrease the exposure time of the illuminated offset plates used in the machine, which is important for, e.g., the newspaper industry.

The laser system, developed at Risø, is based on external feedback of a broad area laser. By applying external feedback to the laser from an optical grating or a mirror, the $M^2$-value of the laser beam can be improved by more than one order of magnitude. Thereby, the beam can be focused down to a small spot size close to the diffraction limit.

Figure 7 shows a photo of the feedback system. The system contains several new designs developed at Risø, including the feedback unit.

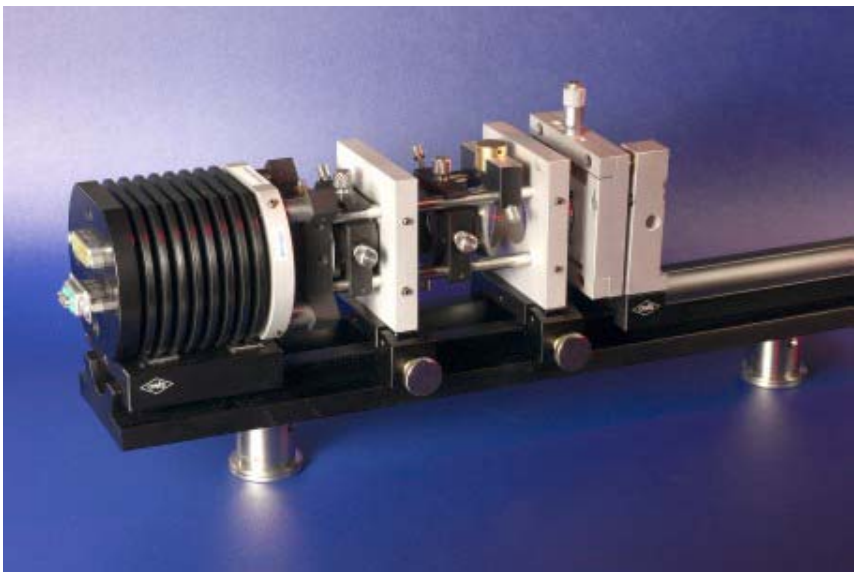

Figure 7. Photograph of a diode laser system including the newly designed feedback unit.

Figure 8 (a) shows a conventional diode laser in the internal-drum configuration.

Due to the poor $M^2$-value of a conventional high-power diode laser, a low-intensity nonfocused laser beam is produced at the offset plate. In Figure 8 (b) the new grating laser has been placed inside the internal drum. Due to the high spatial beam quality of this laser a high intensity focused laser beam with a small spot size is produced at the offset plate.

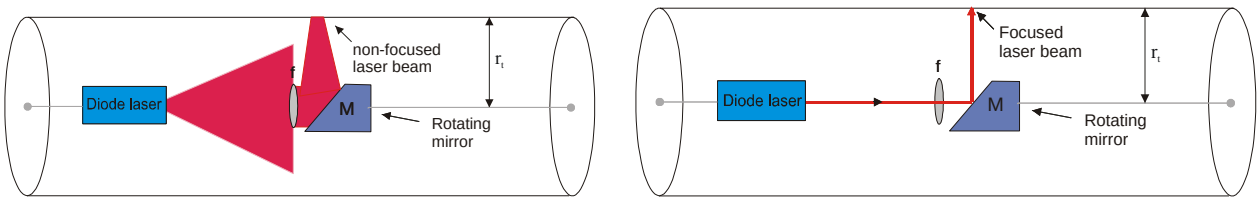


Figure 8. (a) A conventional diode laser in the internal-drum configuration (b) The new grating laser in the internal-drum configuration.

### 2.4.2 Diode laser systems for photodynamic therapy

*E. Samsøe (also at Physics Department, Lund Institute of Technology, Lund University, Lund, Sweden), P.M. Petersen, P.E. Andersen, P. Malm (Physics Department, Lund Institute of Technology, Lund University, Lund, Sweden), S. Andersson-Engels (Physics Department, Lund Institute of Technology, Lund University, Lund, Sweden.) and K. Svanberg (Department of Oncology, Lund University Hospital, Lund University, Lund, Sweden)*
*eva.samsøe@risoe.dk*

Photodynamic therapy (PDT)[1] is a rapidly evolving treatment modality that in many clinics has become routine treatment for precancerous and cancerous skin lesions. Although the procedure is registered in some countries, its general use is still in an early phase. The treatment relies on the coexistence of light, oxygen and a photosensitive component, a photosensitiser. The photosensitiser accumulates to a higher degree in the diseased tissue than in the surrounding healthy tissue, leading to noticeable treatment selectivity. When the laser light excites the photosensitiser, a photochemical process that kills the cancerous cells occurs.

At Lund University Hospital, PDT treatment of various skin lesions is regarded a standard procedure. However, it is desirable to widen the treatment to include solid, deeper lying tumors and lesions in body cavities as well. This requires the treatment light to be delivered through thin (e.g. 50 μm) optical fibres.

Today typical light sources for PDT are diode laser systems or filtered flash lamps. Both light sources suffer from poor beam quality and, thus, inferior coupling efficiency to optical fibres. These light sources are generally used in connection with superficial lesions since the treatment light is delivered through fibres with diameters as large as 400 μm or more.

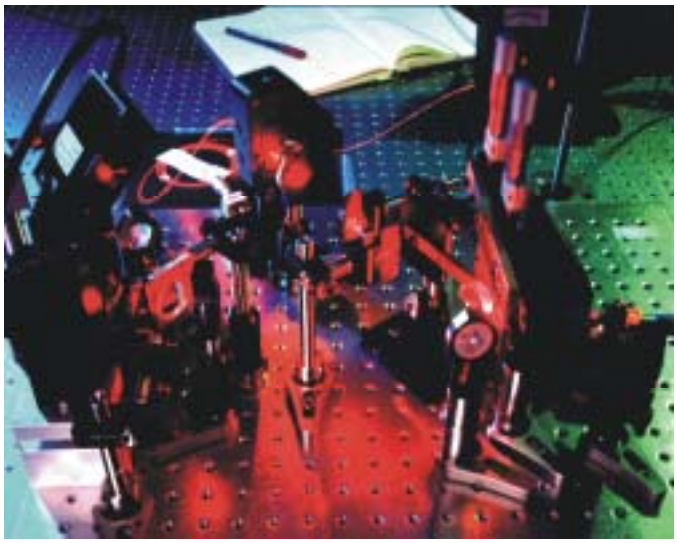

Figure 9. The PDT laser developed at Risø National Laboratory. The fibre has a core diameter of 50 μm.

At Risø, a novel high-power diode laser system with unique coherence properties has been invented.[2] The system is based on a high-power diode laser implemented in an external cavity which includes a spatial mode selection unit. The external feedback system forces the multimode diode laser to exhibit a highly improved output with large coupling efficiency to optical fibres. A similar system for PDT, delivering the treatment light through a 50 μm fibre has been constructed at Risø[3] (Figure 9) and tested in the clinic in Lund[4] (Figure 10).

Figure 10. Preliminary clinical trials (animal model) carried out at Lund University Hospital using the laser system developed at Risø National Laboratory.

To increase the power from the laser, two similar diode laser systems have recently been coupled by means of polarisation coupling. The new system, which delivers the treatment light through a 100 μm fibre, has just recently been tested in the clinic at Marselisborg Hospital, Århus.

This project is supported by the Danish Technical Research Council, grant no. 9901433.

1. J. C. Kennedy, R. H. Pottier and D. C. Pross, "Photodynamic therapy with endogenous protoporphyrin IX: Basic principles and present clinical experience", *J. Photochem. Photobiol.* **6**, 143-148 (1990).
2. M. Løbel, P. M. Petersen and P. M. Johansen, "Single-mode operation of a laser-diode array with frequency-selective phase conjugate feedback", *Opt. Lett.* **23**, p. 825 (1998).
3. E. Samsøe, "A new diode laser system for photodynamic therapy", M.Sc. Thesis, Risø-R-1285 (EN), ISBN 87-550-2921-3, 87-550-2922-1 (internet), ISSN 0106-2840 (2001).
4. M. Løbel, P. M. Petersen and P. M. Johansen, "Single-mode operation of a laser-diode array with frequency-selective phase conjugate feedback", *Opt. Lett.* **23**, p. 825 (1998).

### 2.4.3 VELI – Virtual European Laser Institute

*P.E. Andersen and P.M. Petersen*
peter.andersen@veli.net, paul.michael.petersen@veli.net; www.veli.net

In 2001, a multidisciplinary Virtual European Laser Institute (VELI) was formed with support from the European Commission in order to enhance and promote the available laser expertise in Europe. The Center for Biomedical Optics and New Laser Systems (BIOP) was invited to join VELI in order strongly to promote the use of lasers and optical methods in the field of bio-optics.

Laser laboratories and institutes all over the world perform research in many fields of expertise concerning laser and laser-based technologies. Currently, Europe holds a strong position as far as knowledge on laser and laser applications is concerned. Industry in general, but in particular small- and medium-sized enterprises may experience significant difficulties in reaching the enormous body of knowledge that exists at the various laser institutes across Europe. Moreover, from the point of view of industry, it is difficult to gain insight into the existing and available expertise in lasers and optical measurement technologies at the various dispersed laser centres.

A multidisciplinary Virtual European Laser Institute (VELI) has thus been formed. The purposes of VELI are:

- to increase the transparency and knowledge of available laser expertise in Europe,
- to remove the current inefficiency (or lack) of exploitation of new laser knowledge and techniques,
- to create common agreements and procedures for knowledge transfer.

This European effort will achieve the critical mass in human and technological terms bringing together the expertise and resources needed and will consequently enhance the competitiveness of European industry. Furthermore, the wide variety of competencies of the participating scientists representing different disciplines supports the creation of an outstanding state-of-the-art knowledge base at a European level.

In the VELI network, BIOP collaborates with 15 leading research institutions that specialise in laser physics and applications of lasers. The wide variety of competencies of the participating scientists representing different disciplines supports the creation of an outstanding state-of-the-art knowledge base on a European level, including advanced applications of lasers in bio-optics.

The major outputs of the VELI project are:

- A fully operational core network consisting of 15 leading professional laser institutes in Europe possessing core competencies in the fields of laser technology.
- A database containing state-of-the-art expertise, experience and knowledge formerly dispersed at various laser institutes. Moreover, the database also contains the gathered knowledge that has been generated from the extensive list of industrial needs of small- and medium-sized enterprises.
- A virtual surrounding, i.e. a site where the requests coming from the small- and medium-sized enterprises (industrial needs/demand) meets the available expertise and the wide array of possible applications of laser and laser technology (laser institute supply) speeding up the realisation of potentially new and highly competitive applications.
- A framework or structure for knowledge and technology transfer and mutual assistance in fulfilling the local needs for laser and laser-based technologies at a European level prohibiting the duplication of efforts and reaching an effective and efficient provision of user demands.


Figure 11. Logo for the VELI project. Visit www.veli.net and read more about VELI.

### 2.4.4 The Center for Biomedical Optics and New Laser Systems

*P.M. Petersen, P.E. Andersen and E. Samsø (also at Physics Department, Lund Institute of Technology, Lund University, Lund, Sweden)*
paul.michael.petersen@risoe.dk

The research programme on Laser Systems and Optical Materials is a part of the activities in the Center for Biomedical Optics and New Laser Systems (BIOP). The BIOP centre is a Danish initiative where engineers, physicists, chemists and physicians collaborate on the development of new biomedical applications based on the most recent progress in lasers and optical measurement techniques. The aim is to conduct research in advanced laser systems and optical measurement technologies and to apply these systems in dermatology, ophthalmology and biosensing.

The main purposes of BIOP are to demonstrate and develop state-of-the-art diagnostic procedures and to improve therapeutic facilities at Danish hospitals. The collaboration will result in the development of novel biomedical applications of modern laser technology, including three-dimensional imaging in human tissue, blood flow visualisation, non-invasive spectroscopy and fluorescence measurements for diagnostics and biosensors for measurements of concentrations of, e.g., glucose and protein.

In the BIOP centre four focus areas have been selected:

- biomedical imaging systems
- new laser systems for diagnostic and therapeutic applications
- biomedical bio-sensing
- biomedical image and data processing

The BIOP centre creates a strong Danish research activity within biomedical optics by gathering scientists from areas where Danish universities, Danish hospitals and Danish industry have already demonstrated results at a high scientific and international level. The BIOP centre collaboration coordinates these activities and, furthermore, establishes the foundation for education of young scientists specialised in a combination of the fields of physics, optics, biology and medicine.

The following departments from the Technical University of Denmark and Risø National Laboratory participate in the BIOP centre:

- Research Center COM, Technical University of Denmark
- Department of Mathematical Modelling, Technical University of Denmark
- Department of Physics, Technical University of Denmark
- Optics and Fluid Dynamics Department, Risø National Laboratory

## 2.5 Laser ablation

### 2.5.1 Production of tin-doped zinc oxide films

*E. Holmelund, J. Schou, A. Nordskov, S. Tougaard (Institute of Physics, University of Southern Denmark, Odense, Denmark) and N.B. Larsen (Danish Polymer Centre)*
j.schou@risoe.dk

The demand for transparent, conductive materials for thin films is strongly increasing. An alternative to ITO (indium tin oxide) is ZnO (zinc oxide), but it has turned out that doped ZnO can be superior to pure ZnO with respect to high conductivity, stability and hardness. Typically, the specific resistivity of pure ZnO films is between $3\times10^{-3}$ Ωcm and 0.01 Ωcm.

We have produced tin-doped films of ZnO in our set-up for pulsed laser deposition (PLD). As usual, the intense laser irradiation of a ZnO target leads to ejection of target particles, where a plume of ionised and neutral particles is formed. By collecting the plume particles on a suitable substrate, thin films can be produced. During this deposition procedure a thin rod of tin is moved periodically into and out of the laser beam like a metronome. The laser ablated material from the rod is deposited as well on the substrate during the deposition. We have achieved concentrations of up to 15% tin in the ZnO film. The concentration of tin was determined with X-ray photoelectron spectroscopy.[1]

The specific resistivity as a function of the tin concentration for two typical values of the fluence is shown in Figure 12. Obviously, the doping leads to enhanced resistivity of the zinc oxide. Therefore, tin does not seem to be an appropriate candidate for improving the electrical properties of ZnO films.

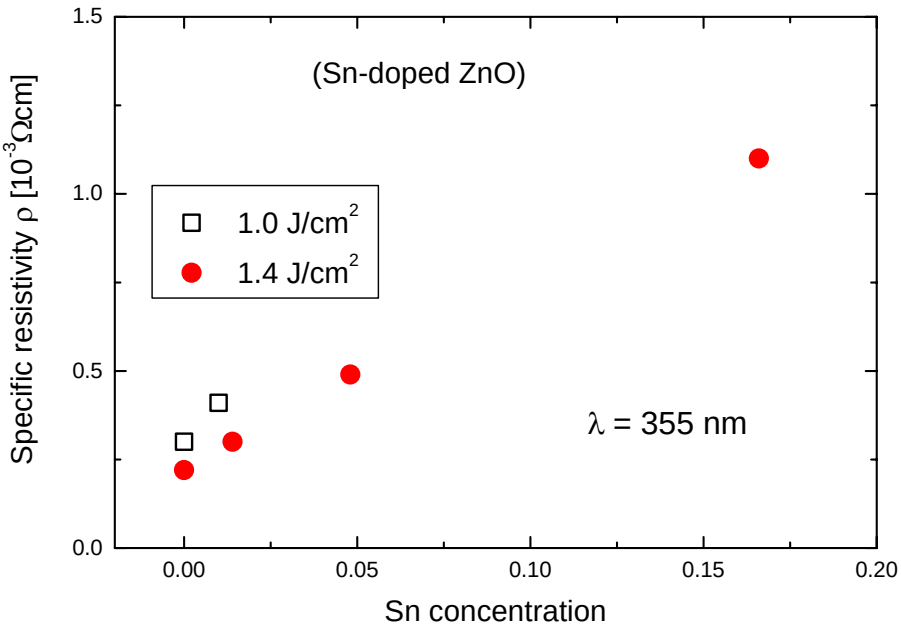


Figure 12. The specific resistivity as a function of tin concentration for films produced at the wavelength 355 mn.

1. “Pure and Sn-doped ZnO films produced by pulsed laser deposition”, E. Holmelund, J. Schou, S. Tougaard and N.B. Larsen, presented at the COLA conference 2001 (to be published in Appl. Surf. Sci.).

### 2.5.2 Ion dynamics in laser ablation plumes from metals

*B. Thestrup, B. Toftmann, J. Schou, A. Nordskov, B. Doggett* and J. Lunney**
*(*Trinity College, Dublin, Ireland)*
*j.schou@risoe.dk*

Ion production during laser irradiation of solids is important for studies of pulsed laser deposition (PLD) and for more fundamental processes of laser ablation. Even though the plume of ablated material may contain both neutrals and ions, the ions may comprise a

considerable fraction at high fluences. In contrast to neutrals, the ions can be studied relatively easily with Langmuir probes.

We have used a probe array to obtain measurements of the ion current in laser plasmas from selected metals. The cylindrical probes are placed in a semicircular ring 80 mm from the target in the horizontal plane. The current signal from all probes can be integrated in time to give the total current of ions arriving at a specific probe.

The distribution of ions as a function of angle for Cu, Zn, Ni and Ag for two fluences is shown in Figure 13. For all metals the distribution shows a pronounced peak along the normal of the target surface ($\theta = 0^o$). Close to the threshold, at the fluence of 0.8 J/cm$^2$, the curve for Zn is significantly higher than those for the other metals. This trend is also seen at the high fluence 2.5 J/cm$^2$, but the behaviour is not so distinct. Figure 13 shows that the volatile materials have the highest ablation yield.[1]

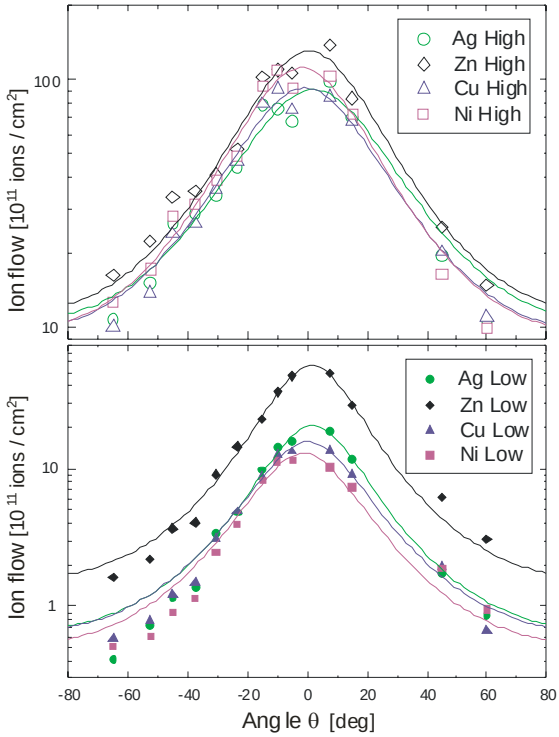


Figure 13. The angular distribution of the ablated ions in units of $10^{11}$/cm$^2$ for four metals at high (2.5 J/cm$^2$) and low fluence (0.8 J/cm$^2$).

1. “Ion dynamics in laser ablation plumes from selected metals at 355 nm”, B. Thestrup, B. Toftmann, J. Schou, B. Doggett and J.G. Lunney (presented at the COLA conference 2001 (to be published in *Appl. Surf. Sci.*).

# 3. Optical diagnostics and information processing

## 3.1 Introduction

*S.G. Hanson*
steen.hanson@risoe.dk

During the past year the research programme on Optical Diagnostics and Information Processing has been heavily involved in two so-called talent projects funded by the Danish Technical Research Council. Both projects have aspects related to bio-optical applications, which is a joint theme for most of the work carried out in the research programme. One project aims at further development of systems for non-invasive tomography by light making use of the so-called optical coherence tomography (OCT) effect. The objective of the second talent project is to exploit the phase contrast method in various fields, one of which is the use of the technique for optical tweezers. Both of these projects heavily rely on intensive programming, on the one hand for controlling the tweezers, and on the other - to a larger extent - for signal processing in the case of OCT measurements. The expertise in bio-optics is increasing in good accordance with the interest from industry and society within this field.

The ongoing work on miniaturisation of optically based sensor systems has been carried on primarily within the framework of a centre contract named MINOS (MINiaturised Optical Sensors) funded by the Danish Agency for Trade and Industry. A primary objective of this work is the hunt for ways to miniaturise optically based sensors in order to penetrate new markets for the participating companies. In addition to the industrial partners, this work is performed in collaboration with (1) the Technical University of Denmark, (2) DELTA, Danish Electronics, Light and Acoustics and (3) the Danish Technological Institute. At present one separate product has been released based on the concept of optical miniaturisation.

Basic investigations into light scattering from various surfaces have been conducted and new methods based on the analysis of the dynamics of speckles from moving objects have been developed. Of special interest has been the analysis of speckle statistics arising from scattering off surfaces giving rise to partially developed speckle. Furthermore, scattering from surfaces having a fractal-like height distribution is becoming of increasing interest.

A second centre contract has been negotiated successfully in 2001. Our contribution to the project is to implement advanced exploitation of the technique of Fourier Transform Infrared Spectroscopy for biological objects. Furthermore, infrared technology is the key point for our participation in a programme named MENELAS (Minority effluent measurements of aircraft ENgine Emissions by infrared LAser Spectroscopy) funded by the EU.

The accredited work on temperature calibration has been supplemented with accredited infrared calibration, i.e. non-contact measurement, sometimes named IR-calibration, in the temperature range from –80 $^0$C to 1600 $^0$C.

# 3.2 Medical optics

### 3.2.1 Fast scanning OCT system and image processing

*L. Thrane, F. Pedersen, T.M. Jørgensen, H. Larsen and P.E. Andersen*
peter.andersen@risoe.dk

Optical coherence tomography (OCT) has developed rapidly since its potential for applications in clinical medicine was first demonstrated in 1991.[1] OCT performs high-resolution, cross-sectional tomographic imaging of the internal microstructure in materials and biological systems by measuring backscattered or backreflected light. The origin of OCT lies in the early work on white-light interferometry that led to the development of optical coherence-domain reflectometry (OCDR), a one-dimensional optical ranging technique.[2] OCDR uses short coherence length light and interferometric detection techniques to obtain high-sensitivity, high-resolution range information. OCDR was originally developed for locating faults in fibre-optic cables and network components.[2] However, its capability of performing ranging measurements in the retina and other eye structures was soon recognised. Currently, new areas of applications emerge and, in particular, in the field of cardiology OCT is demonstrating its potential as a diagnostic tool, see e.g. Ref. 3.

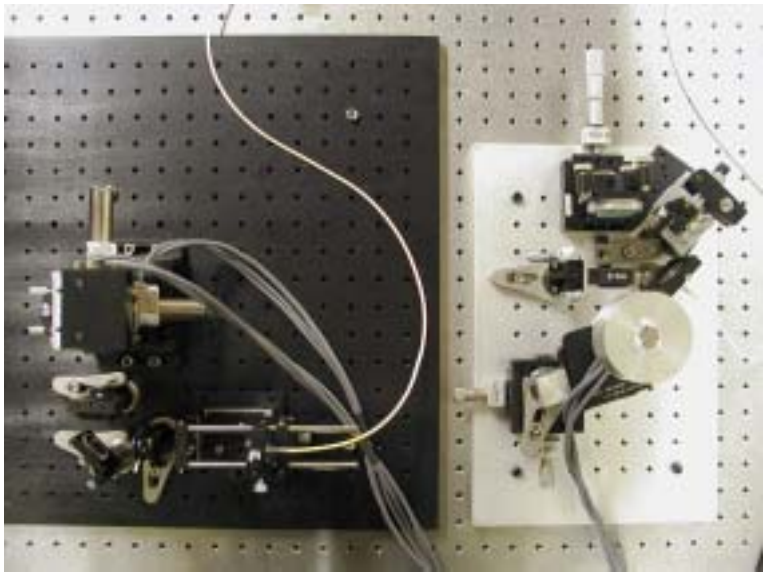

Figure 14. Scanners in the OCT system. Left: the XY sample beam scanner. Right: The reference beam delay line.

In these new endoscopic applications, the scan rate of each so-called A-scan and the data acquisition rate should be optimised in order to provide fast OCT imaging or what is often referred to as 'real-time imaging'. An OCT set-up based on a broadband source at 1330 nm for 3D imaging of tissue has been constructed at Risø.[4] The resolution of the system, both laterally and longitudinally, is 10-15 mm. The configuration is centred on a Fourier domain rapid scanning optical delay line[5] in combination with fast scanning of the sample. A LabVIEW program for data acquisition providing a user-friendly interface to the measuring configuration is also a part of the system. In order to speed up the data processing, an electronic envelope detector has been built and integrated into the electronic postprocessing of the detector signal. A picture of the system is shown in Figure 14. The system incorporates the possibility of repeated measurements during the scan cycle, i.e. spatial averaging of single

scans. Hereby, it is possible to increase the signal-to-noise ratio, with the price paid being an increased recording time.

Speckle noise may degrade the OCT images to a smaller or larger degree dependent on the characteristics of the source and the geometrical set-up. Repeated scans will normally not reduce this type of noise unless small perturbations in the measuring process do occur naturally or are being introduced during the measurements. One possibility[6] is to produce averages over neighbouring B-scans as illustrated in Figure 15. An alternative is to apply a denoising wavelet filter.

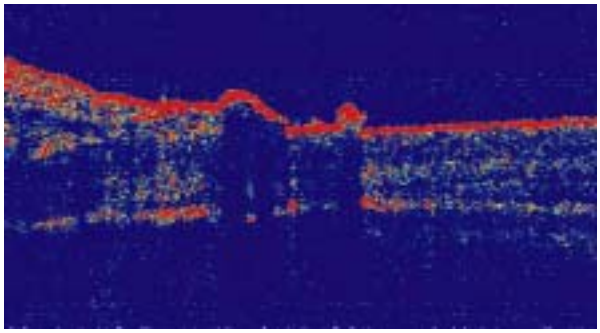

a)

Figure 15a. Single B-scan.

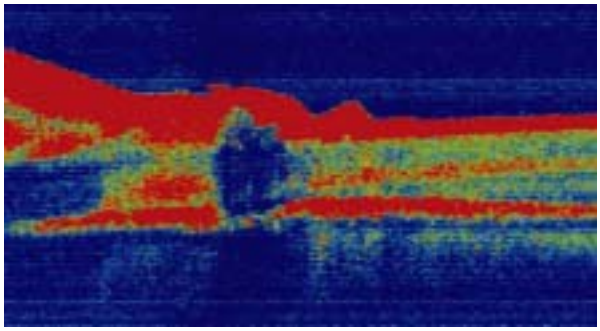

b)

Figure 15b. Average over neighbouring B-scans.

For adequate visualisation of the recorded image data, we apply different types of volume rendering. An example of a 3D OCT image of a biopsy of a heavily calcified aortic plaque is shown in Figure 16.

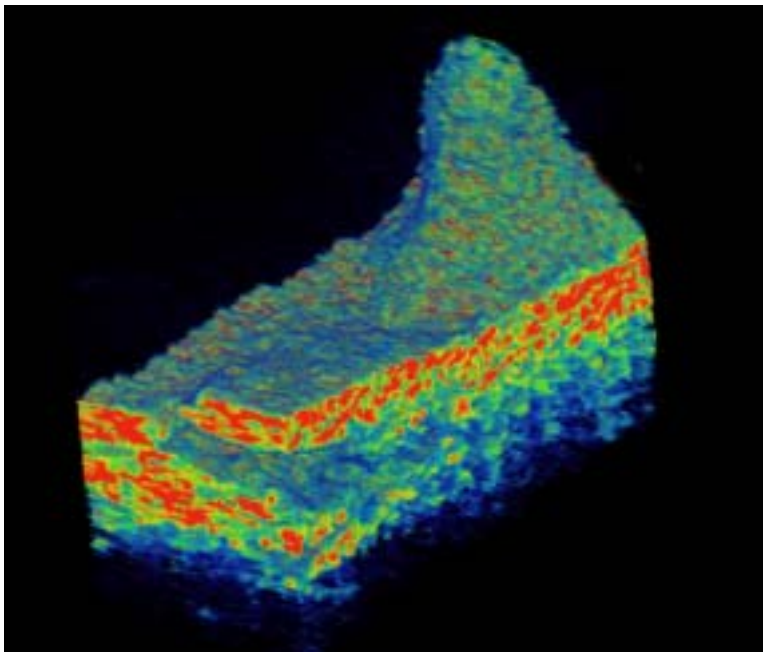

Figure 16. 3D OCT image of a biopsy of heavily calcified aortic plaque.

1. D. Huang, E.A. Swanson, C.P. Lin, J.S. Schuman, W.G. Stinson, W. Chang, M.R. Hee, T. Flotte, K. Gregory, C.A. Puliafito and J. G. Fujimoto, "Optical coherence tomography", *Science* **254**, 1178-1181 (1991).
2. R.C. Youngquist, S. Carr and D.E.N. Davies, "Optical coherence-domain reflectometry: A new optical evaluation technique", *Opt. Lett.* **12**, 158-160 (1987).
3. B.E. Bouma and G.J. Tearney (eds.), *Handbook of optical coherence tomography*, M. Dekker Inc., New York, NY, USA, 2002.
4. L. Thrane, P.E. Andersen, T.M. Jørgensen, A. Tycho, D. Levitz, H.T. Yura and F. Pedersen, "Optical coherence tomography", *DOPS-NYT* **16** (4), 13-18 (2001).
5. G.J. Tearney, B.E. Bouma and J.G. Fujimoto, "High speed phase- and group-delay scanning with a grating-based phase control delay line", *Opt. Lett.* **22**, 1811-1813 (1997).
6. T.M. Jørgensen, L. Thrane and B. Ersbøll, "Assessment of the intrinsic noise in optical coherence tomography images", (oral presentation) 2. International workshop on computer assisted fundus image analysis (CAFIA-2), Copenhagen (DK), 5-7 Oct 2001. Unpublished. Abstract available.

### 3.2.2 Optical coherence tomography for intracoronary diagnostics

*D. Levitz (also at Institute of Optics, University of Rochester, NY, USA), P. Riis Hansen (Department of Cardiology, Gentofte University Hospital, Denmark), L. Thrane, P.E. Andersen, T.M. Jørgensen, C. Andersen (Department of Pathology, University Hospital Copenhagen, Denmark) and F. Pedersen*
peter.andersen@risoe.dk

Optical coherence tomography (OCT) is an imaging technique based on low-coherence interferometry.[1] OCT can provide microscopic, cross-sectional, tomographic imaging by measuring backscattering properties of the scanned tissue. Aside from histology, no conventional imaging modality, e.g. ultrasound-based techniques, can achieve sufficient spatial resolution and contrast to analyse the microstructure of atherosclerotic plaques and hereby provide information on their stability and propensity to rupture.

We have therefore developed an OCT system with the aim of assessing and classifying atherosclerotic plaques in human arteries.[2] Our OCT system utilised a Fourier-domain rapid scanning optical delay line (see, e.g., Ref. 3) and is capable of scanning both two-dimensional cross-sections and three-dimensional volumes. The recorded backscattering intensities from different axial and transverse positions were plotted as grey-scale or false-colour maps. The system achieved lateral and longitudinal resolutions of 10-15 μm and a penetration depth of 0.4-1 mm, which is satisfactory for plaque classification.

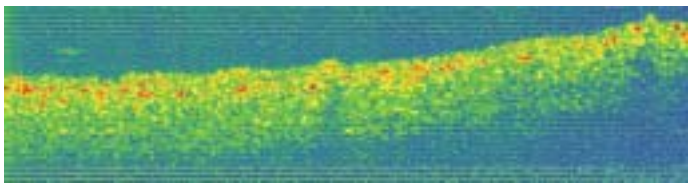

Figure 17. Two-dimensional OCT image of normal aortic tissue (3 mm wide).

In this preliminary study, aortic tissue samples at different stages of plaque development were obtained at necropsy and scanned using the OCT system. An example of normal aortic tissue is shown in Figure 17. The image shows a two-dimensional section of the artery wall (the blood flow would be above the scanned sample from left to right). Figure 18 shows an example of a heavily calcified lesion, which could lead to thrombosis. Areas of high

reflectance (red colour) correspond to highly calcified tissue as marked by (A), which correlates well with histology. Fissures, marked by (B), may cause the lipid content from inside the lesion to enter into the blood stream. This may cause onset of a series of biochemical events leading to thrombosis and occlusion of aorta. The lipid pool of the lesion is marked by (C).

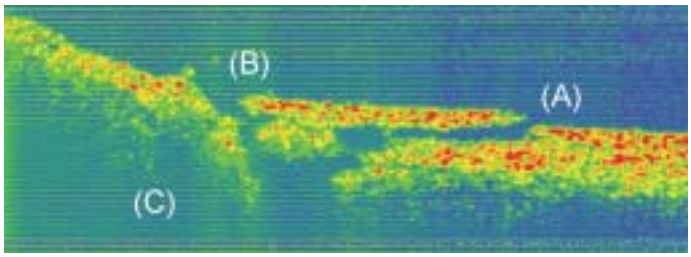


Figure 18. Two-dimensional OCT image of atherosclerotic plaque at a late stage of development; (A) highly calcified tissue, (B) fissures, and (C) large lipid pool below calcified tissue.

The scanned biopsies subsequently underwent routine histological processing and classification, and the histological images were compared with those obtained with OCT. From these two sets of independent images, a classification was carried out, and the preliminary results showed a correlation of 75%. The encouraging results lead us to conclude that OCT is capable of delineating the microstructure of human atherosclerotic plaques. Furthermore, future intravascular applications of this new imaging modality represent promising avenues of research, which are currently pursued in the research group.

The present research project is supported financially by the Danish Technical Research Council under grant no. 9901433, and by the Graduate School in Nonlinear Science.

1. D. Huang, E.A. Swanson, C.P. Lin, J.S. Schuman, W.G. Stinson, W. Chang, M.R. Hee, T. Flotte, K. Gregory, C.A. Puliafito and J.G. Fujimoto, "Optical coherence tomography", *Science* **254**, 1178-1181 (1991).
2. L. Thrane, P.E. Andersen, T.M. Jørgensen, A. Tycho, D. Levitz, H.T. Yura and F. Pedersen, "Optical coherence tomography", *DOPS-NYT* **16** (4), 13-18 (2001).
3. G.J. Tearney, B.E. Bouma and J.G. Fujimoto, "High speed phase- and group-delay scanning with a grating-based phase control delay line", *Opt. Lett.* **22**, 1811-1813 (1997).

### 3.2.3 Optical coherence tomography for industrial process monitoring

*A. Tycho (also with COM, Technical University of Denmark, Building 349, 2800 Kgs. Lyngby, Denmark), A-M. Thommesen (FORCE Technology, Park Allé 345, DK-2605 Brøndby, Denmark), L. Thrane, P.E. Andersen, T.M. Jørgensen, S. Arnfred Nielsen (FORCE Technology, Park Allé 345, DK-2605 Brøndby, Denmark) and S. Rahbæk (Coloplast A/S, Ostomy Products Division, Bronzevej 2-8, DK-3060 Espergærde, Denmark)*
peter.andersen@risoe.dk

The origin of optical coherence tomography[1] (OCT) stems from white-light interferometry for optical ranging.[2] Disregarding the imaging capabilities of the technique, a single longitudinal scan performed with an OCT system represents optical ranging of the internal layers of an opaque object. Notice that the object may be multilayered, and the system will then produce a scan from which the optical thickness of each layer may be determined. This property may be utilised for on-line industrial process monitoring and (or) quality control.

In collaboration[3] with Coloplast A/S and FORCE Technology, we have investigated the possibility of on-line monitoring of the thickness of a polymer film while this is being extruded. The film itself is non-transparent and has a thickness in the range 1-1.5 mm. The thickness must be controlled and measured with a resolution of approximately 15 μm, a number which has been fixed by Coloplast A/S. Preliminary investigations carried out at Risø demonstrated that this technology is a viable solution to such on-line process monitoring. Figure 19 shows the OCT envelope signal for a moving polymer film at a single point: the surface reflection and the back-reflection. Note that the back-reflection is lower due to the attenuation from the scattering in the bulk polymer. Moreover, the polymer is stuck on special paper, and the resolution of the system is capable of resolving the fine structures of this paper. By measuring the thickness at several positions, the quality of the polymer film may be monitored on-line and, furthermore, these signals may be used in a feedback loop to control the fabrication process dynamically. FORCE Technology and Coloplast A/S are now collaboratively developing the technique into a monitoring prototype device.

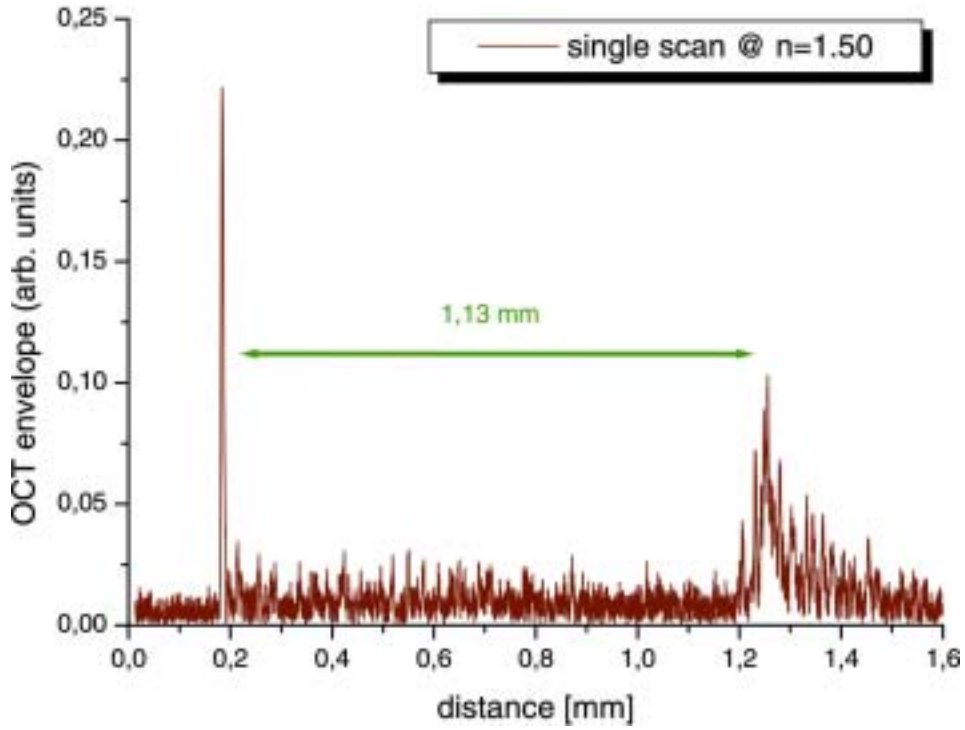


Figure 19. Single longitudinal scan of polymer film (courtesy of Risø, FORCE Technology and Coloplast A/S).

1. D. Huang, E.A. Swanson, C.P. Lin, J.S. Schuman, W.G. Stinson, W. Chang, M.R. Hee, T. Flotte, K. Gregory, C.A. Puliafito and J.G. Fujimoto, "Optical coherence tomography", *Science* **254**, 1178-1181 (1991).
2. R.C. Youngquist, S. Carr and D.E.N. Davies, "Optical coherence-domain reflectometry: A new optical evaluation technique", *Opt. Lett.* **12**, 158-160 (1987).
3. Carried out as part of "Centre for On-Line, Non-Contact Sensing, Monitoring, and Control of Industrial Processes and Systems (BIPS)", under grant 1999-603/4001-35.

### 3.2.4 Machine learning for classification

*T. Martini Jørgensen and C. Linneberg (Intellix A/S, H.C. Ørsteds Vej 4, Frederiksberg C, Denmark)*
*thomas.martini@risoe.dk*

Over the past years there has been close collaboration between Risø and Intellix A/S within the area of machine learning. Intellix A/S delivers solutions in decision support systems based on artificial intelligence. The collaboration has been focused on an industrial Ph.D. project, which was successfully finished this year.[1] As a result of this work an improved theoretical understanding of the mechanism in the so-called n-tuple classification scheme has been obtained which in turn has led to a number of improved schemes for training n-tuple classifiers.[2] A recent result of the research efforts has been to relate the impact of the improved schemes to the more general problem of ensemble-based classifiers. Ensemble-based classifiers exploit the fact that a combination of many weak and possible simple classifiers will often be capable of outperforming even the strongest complex classifier. The challenge is to combine and pick the individual classifiers in an optimum way corresponding to creating classifiers with low inter-correlation and moderate individual strengths.

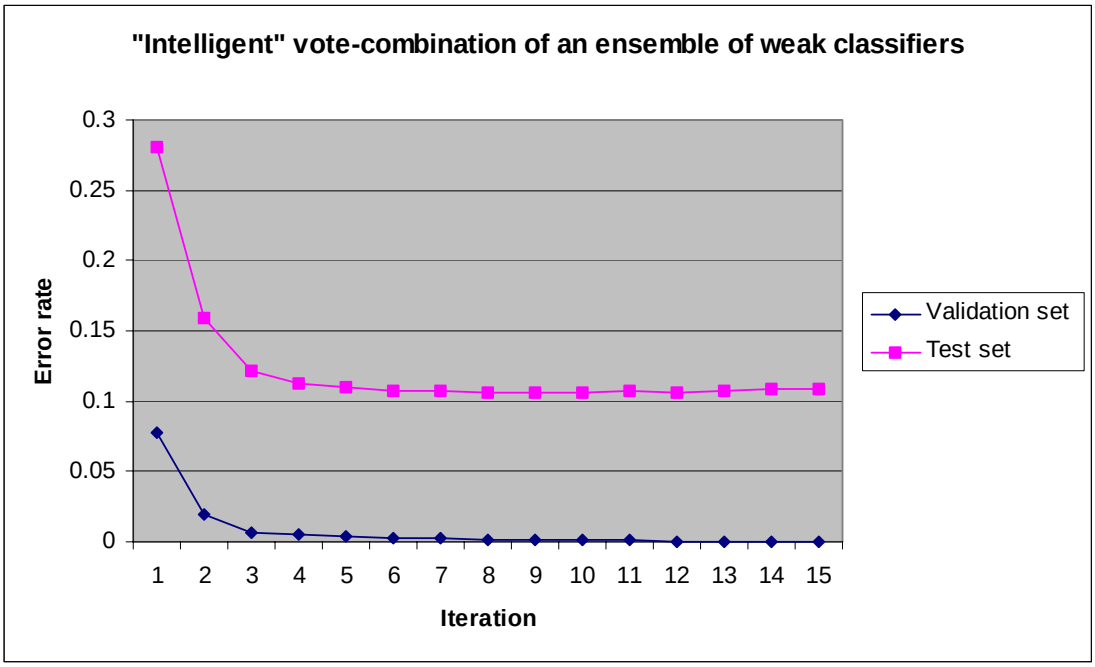


Figure 20. The two graphs illustrate how the performance of an ensemble of 100 weak classifiers (PERT decision trees) can be improved by applying an iterative scheme for adjusting the contribution of the different branches of the decision trees to the overall decision. The validation set and test set error rates are obtained on the so-called DNA data set from the Statlog repository (see http://www.niaad.liacc.up.pt/statlog/datasets/dna/dna.doc.html).

So-called boosting and bagging are principles often used to create ensembles of weak classifiers. Another approach is to incorporate randomisation in the process of generating the individual classifiers. This is the mechanism applied for training n-tuple networks. However, no matter how the members of the ensembles are created, it may still be an open question how one should optimally weight the members in order to form a competitive committee decision and it may not even be so that the individual members always contribute with the same weight. We have shown that for ensembles of decision trees as well as for the n-tuple classifier it may actually be beneficial to apply a training scheme for setting such weights,[3]

although the training phase gets longer and more complex. Specifically we have shown that if a simple majority voting procedure fails, the very same individual members may very well be useful if one allows the weights to be dependent on the estimated output class for a given individual member, see Figure 20.

1. C. Linneberg, Analysis and Extensions of the n-Tuple Classifier with Implications for Ensembles, Ph.D.-Thesis, Technical University of Denmark, 2001.
2. C. Linneberg and T.M. Jørgensen, "The n-tuple classifier with arbitrary threshold levels - theory and implications", *Recent Res. Dev. Pattern Rec.* (2000) **1 Part 2**, 219-236.
3. T.M. Jørgensen and C. Linneberg, "Feature weighted ensemble classifiers - a modified decision scheme" In: Proceedings. 2. International workshop on multiple classifier systems (MCS 2001), Cambridge (GB), 2-4 Jul 2001. Kittler, J.; Roli, F. (eds.), (Springer, Berlin, 2001) (Lecture Notes in *Computer Science*, 2096) p. 218-227.

### 3.2.5 Interferometric backscatter detection of small concentrations in microfluid systems

*H. Schiøtt Sørensen, H. Pranov, D.J. Bornhop (Department of Chemistry and Biochemistry, Texas Tech University, Lubbock, USA), N.B. Larsen (Danish Polymer Centre, Risø National Laboratory, Denmark), P.E. Andersen and H.K. Rasmussen (Danish Polymer Centre, Technical University of Denmark, Denmark)*
peter.andersen@risoe.dk

In this project, we aim at measuring small concentrations of substances, e.g. glucose, in a small-volume solution. This is done using the micro-interferometric backscatter detection (MIBD) scheme,[1] which is based on a simple optical system shown in Figure 21. The optical system itself comprises a laser, a capillary tube (serving as both the micro-fluidic system and the interferometer) and detecting means. The alignment of the laser beam incidence with respect to the flow channel is non-critical with regard to producing interference fringes from which the concentration of substance may be inferred.

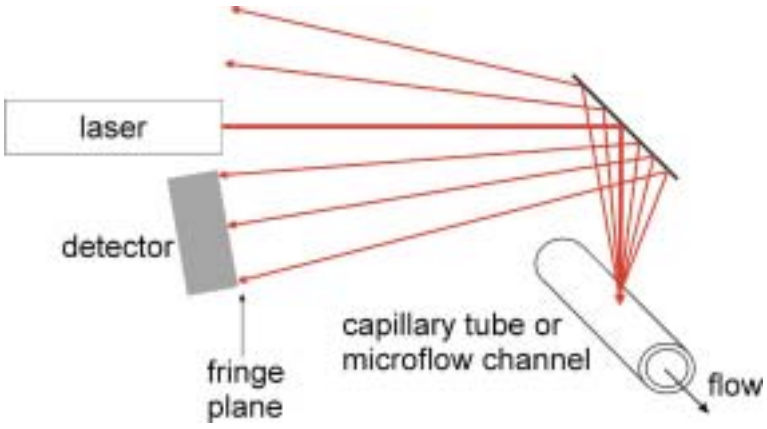


Figure 21. Sketch of MIBD system: The laser illuminates the flow channel (here a capillary tube), and an interferometric signal may be detected in the backscatter plane.

MIBD is universal since the refractive index varies with a wide range of parameters. Changes in temperature, concentration and pressure may thus be detected inside a small volume of the liquid by using this method. Previously, it has been used for measuring small changes in the refractive index in fluids, and it was demonstrated that this simple optical system detects $\Delta n$ at least at the $10^{-6}$ level.[1]

The on-going project focuses on the general behaviour of the MIBD system. The side illumination of the capillary by a laser produces a 360 degrees fan of scattered light that contains several sets of high-contrast interference fringes (only part of the scattered light is depicted in Figure 21). For this part of the project, the objective is to gain further insight into the mechanism responsible for the observed fringe patterns and to optimise the configuration further leading to improvement of the device sensitivity. To do this, the interference pattern is examined, i.e. the change in the different sets of fringes with various changing physical parameters, such as refractive index and optical activity, is investigated theoretically and experimentally. We have extended the four-beam ray-tracing model originally proposed by Tarigan *et al*.[2] to include polarisation and an additional thin layer, which may be on the inner or outer surface, respectively. Such a thin layer could be an affinity layer (inside) or the polymer coating of the capillary (outside). The new model is compared with experimental results. Figure 22 shows the behaviour of the fringes with changing refractive index caused by a temperature change obtained with our experimental set-up.

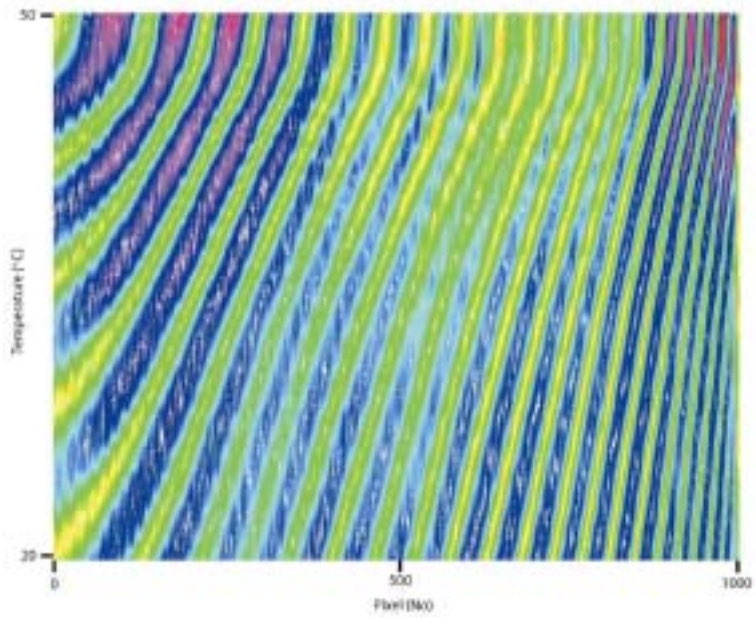


Figure 22. The interference pattern from pure water in the capillary tube at varying temperature. From these measurements, a refractive index sensitivity of 5 x $10^{-6}$ may be inferred.

The long-term goal of this project is to implement a MIBD system using a plastic chip with microflow channels, and to demonstrate that extremely high sensitivity, as seen in other realizations,[1] is still attainable. Fabrication of such a chip has been achieved by hot embossing in thermoplast using a photoresist master. However, this technique needs further refinement before channels of adequate quality may be produced.

1. K. Swinney and D. Bornhop, ”Chip-scale universal detector for electrophoresis based on backscattering interferometry”, *The Analyst* **125**, 1713-1717 (2000).
2. H.J. Tarigan, P. Neill, C.K. Kenmore and D.J. Bornhorp, ”Capillary-scale refractive index detection by interferometric backscatter”, *Anal. Chem.* **68**, 1762-1770 (1996).

## 3.3 Phase contrast techniques

### 3.3.1 Programmable optical tweezers based on generalised phase contrast

*R.L. Eriksen, J. Glückstad and P.C. Mogensen*
jesper.gluckstad@risoe.dk

Optical tweezers use the radiation pressure effect from a highly focused laser beam to trap and manipulate objects with forces in the order of piconewton. The use of single-beam optical tweezers, originally demonstrated by Ashkin *et al.* in 1986, is now widespread as a tool for manipulation of cells, subcellular structures and individual DNA-molecules as well as for assembly of microstructures and measurement of interaction forces on the micronscale. In a broader perspective, simultaneous trapping of irregular particles or more than one particle would require more than one tweezer beam. There is thus a demand for a multiple optical tweezer system that is capable of generating a number of independently steerable beams where both the beam shape and the intensity can be controlled.

There have been a number of approaches proposed for multiple-beam tweezer systems. The simplest approach is to increase the number of light sources, and independent manipulation of the trapping beams is implemented using high-speed scanning mirrors. This has been shown to work well for the trapping of multiple polystyrene particles in various patterns. All of the multiple-tweezer approaches are based on either refractive optics with multiple-beam paths or raster-type mechanical beam steering resulting in systems that are either component intensive or mechanically complex. Diffractive optics with computer-generated holograms (CGHs) has also been proposed and demonstrated as a non-mechanical alternative to producing multiple-beam optical tweezer systems. However, this approach is currently limited by the restrictive space-bandwidth product of commercially available spatial light modulators (SLMs) and diffraction losses from pixelated structures.

The generalised phase contrast (GPC) approach has previously been proposed by our group for dynamic array generation and pattern formation for optical tweezers using SLMs.[1,2] The advantage of this approach is the direct correspondence between phase in the input plane and intensity at the output plane, in contrast to the CGH approach. This also implies that the space-bandwidth product requirements and the number of phase levels for the SLM approach are substantially lower than what is required for the equivalent CGH approach. Another advantage of using the GPC approach is that the computation time required to produce the desired intensity pattern is very short when compared with the iterative computer algorithms frequently required to optimise dynamic CGH-based methods.

In the February 2002 issue of *Optics Letters*,[3] we describe what is believed to be the first experimental demonstration of the GPC method applied to the trapping of multiple particles in an optical tweezer system. Figure 23 shows a schematic diagram of the implementation of an optical tweezer system based on phase contrast. The purpose of this demonstration system was to create a 2×2 square array of tweezer beams using a fixed binary phase mask as the input for a GPC system. The laser source used is a 200 mW diode laser operating at 830 nm. This wavelength was chosen since it lies centrally in a low absorption window for both water and biological objects. The filtered, expanded and collimated laser beam is incident on a binary π-phase mask (PM) with a 2 mm aperture defined by the iris (Ir1) that is matched to the diameter of the phase contrast filter (PCF). The phase-modulated light is passed into the 4-f filtering system formed by the lenses L1 (f = 100 mm) and L2 (f = 50 mm) containing the PCF that is placed in the Fourier plane. The binary π-phase mask and the PCF are made by depositing photoresist on a glass that is optically flat. The dimensions of the circular phase

dots forming the 2×2 input phase pattern are 0.5 mm with a spacing 0.71 mm and the phase contrast filter has a diameter of 80 μm.

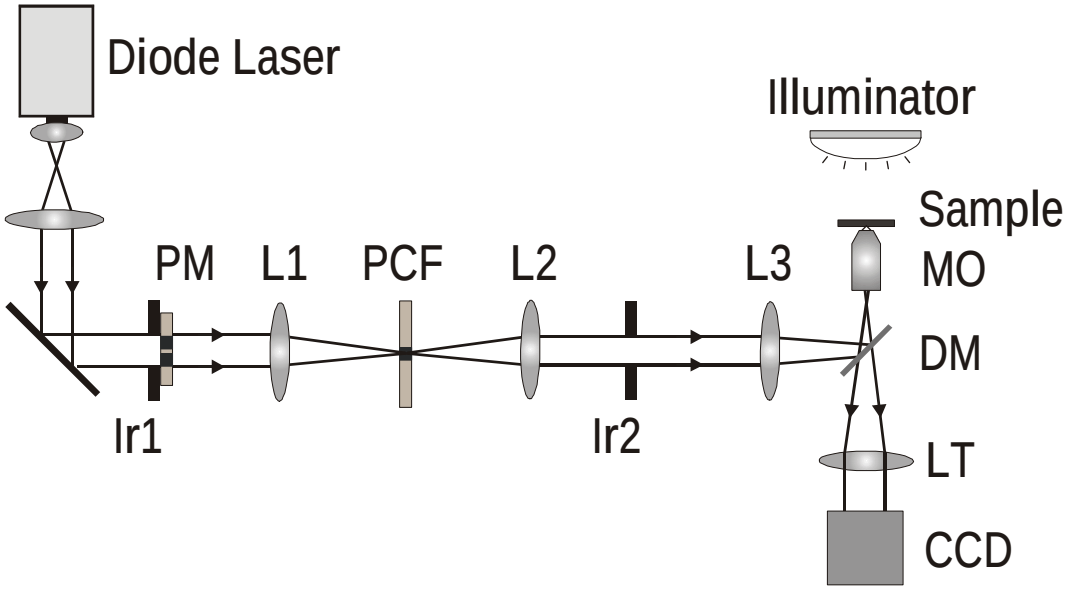


Figure 23. A schematic diagram showing the experimental set-up for an optical tweezer system based on multiple-beam phase contrast.

A high-contrast binary intensity distribution, which is directly related to the phase pattern on the fixed phase mask, is generated at the back focal plane of L2 (the intermediate image plane). The lens L3 (f = 300 mm) and the microscope objective MO (Leica PL-APO, x100, NA = 1.4) form a second 4-f system that scales the intensity distribution and brings it to a focus in the tweezer plane. The EPI-fluorescence port of an inverted microscope (Leica DM-IRB) is used to couple the infrared laser light into the back-focal plane of the microscope objective via a dichroic mirror (DM). The sample plane is imaged with a CCD camera (Hitachi KP-M3).

The functionality of this optical tweezer system was tested using a suspension of 1 μm polystyrene microspheres in de-ionised water. A 30 μm thick test cell was produced, using a microscope slide and a cover slip separated by sticky tape in which the microsphere solution was placed.

In Figure 24, an image sequence showing the simultaneous trapping of four polystyrene microspheres in the 2×2 tweezer array is presented. The field of view of each image is 14 μm × 12 μm. The first image (a) in Figure 24 shows five particles moving freely around in the water solution just before the laser beam is switched on. As can be seen on all four images, the particle on the left-hand side of the image moves freely due to Brownian motion and is not influenced by the radiation pressure effects when the trapping beams are introduced. Figure 24 shows four particles being trapped by the generated intensity distribution. The time between each image frame is 0.3 second. When the laser was switched off, the particles rapidly diffused away from the trapped positions. It was found that a total laser power of approximately 3 mW in the tweezer plane was sufficient to trap all four particles effectively.

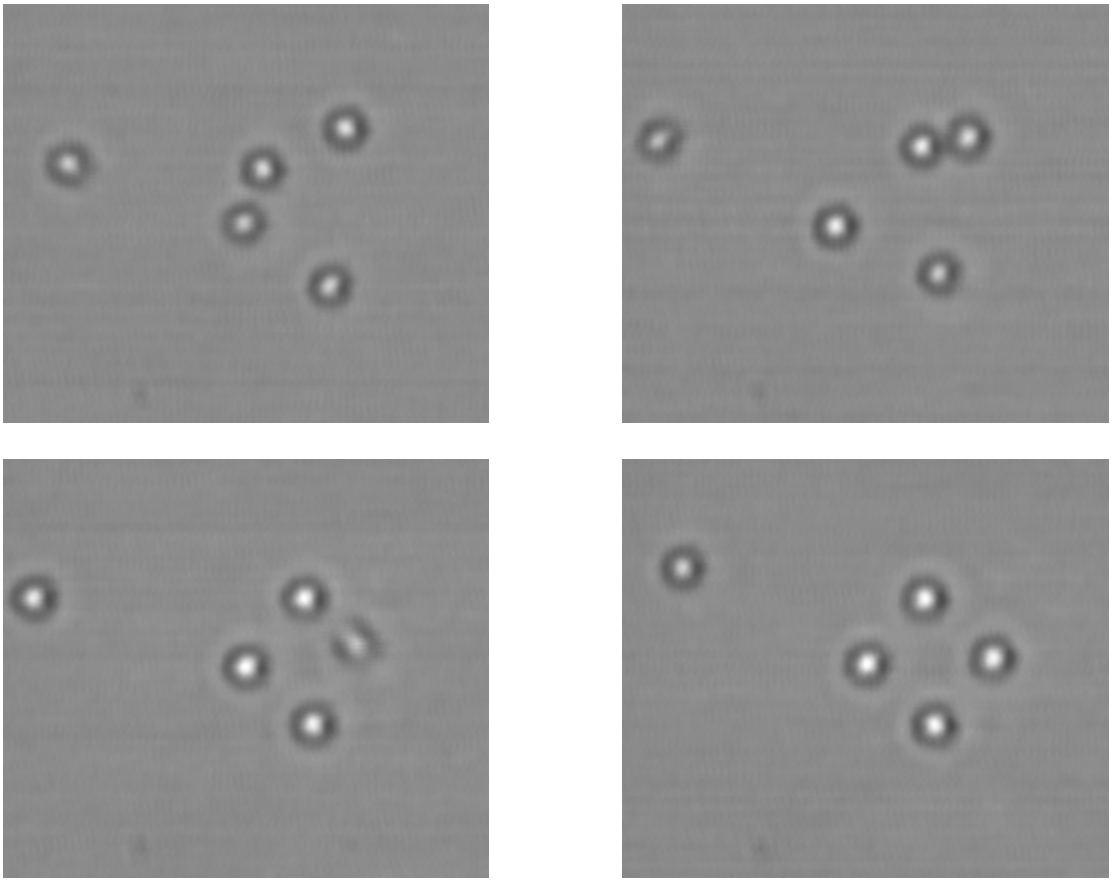

Figure 24. An image sequence showing the trapping of four one micron sized polystyrene beads in a structured four-beam optical trap. The field of view of each frame is 14 μm ×12 μm.

1. J. Glückstad, "Phase contrast imaging", U.S. Patent No. 6,011,874 (2000).
2. J. Glückstad and P. C. Mogensen "Optimal phase contrast in common path interferometry" *Appl. Opt.* **40**, 268-282, (2001)
3. R.L. Eriksen, P.C. Mogensen and J. Glückstad "Multiple beam optical tweezers generated by the generalised phase contrast method", *Opt. Lett*. 15. Feb. issue (2002).

### 3.3.2 Reverse phase contrast generating spatial phase modulation

*J. Glückstad, R.L. Eriksen and P.C. Mogensen*
jesper.gluckstad@risoe.dk

The generation of a well-controlled phase distribution has a number of applications in contemporary applied optics and there currently exist several techniques for producing such phase modulation of an optical wave front. These include, for example, electrically or optically addressed phase-only spatial light modulators (SLMs) that modulate the phase of a wave front by a spatial variation in the optical path length of transmitted or reflected light. Accurate phase-only SLMs are rather complicated and expensive items, and we are thus interested in a simple practical technique for producing reconfigurable two-dimensional phase modulation.

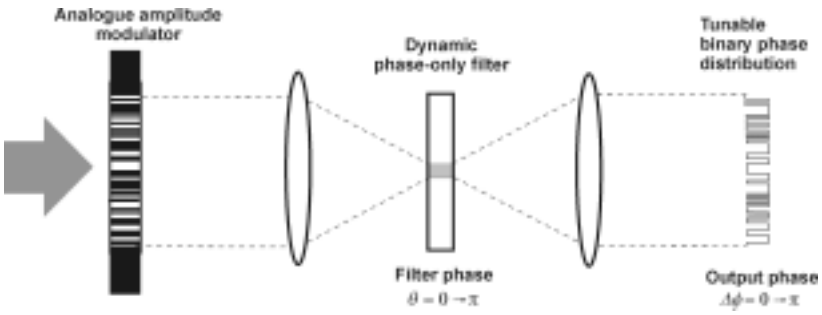


Figure 25. Generic RPC-based phase-only spatial light modulator.

We propose a technique for the conversion of a given amplitude pattern to a phase distribution by a technique which we refer to as the reverse phase contrast (RPC) method.[1] In this method, a high contrast amplitude mask is applied to generate a phase-encoded version of the amplitude pattern using the basic 4-f filtering set up as shown in Figure 25. The spatial filter determines the resultant phase shift between the elements of the output wave front. Using a liquid crystal based phase-contrast filter the dynamic range of the phase modulation can be adjusted arbitrarily within the interval $]0;\pi]$. Thus, combining an amplitude modulator with a tunable phase filter would result in a high performance phase-only SLM in which the spatial light modulation and the phase shift are effectively decoupled.

Reconfigurable spatial phase modulation of a light field is required in a number of areas in optics, including phase modulation for holographic multiplexing, storage and encoding, phase-only encryption and decryption and the testing of focus in optical apparatus. In addition, the RPC technique can be used with a binary amplitude mask acting as the input information to create interchangeable, but static phase distributions. In the case of a fixed phase distribution, a major advantage of the use of amplitude masks to define the required phase pattern is the relative simplicity with which they can be manufactured when compared with phase-only elements. The use of standard chrome on glass mask technology would make it possible to achieve high-resolution phase patterns, the phase shift of which would be controlled by the filtering system. In fact, it is possible to tune the output phase shift via the contrast ratio of the mask or by tuning the filter parameters. If a dynamic phase modulator is required, then an amplitude modulator, in the form of a commercially available liquid crystal display (LCD) projector element, or possibly a MEMS (micro electronic mechanical system) type device, can be used.

We have undertaken experiments to characterise the performance of the RPC technique using both fixed amplitude masks and SMLs for the input amplitude modulation. We have used a Hamamatsu parallel-aligned liquid crystal modulator in conjunction with polarisors to generate a binary on/off modulation of the amplitude of the input wave front. In general, such an SLM will have a lower contrast than a fixed mask, and the resolution of the resulting phase distribution will be limited to that of the modulator.

In Figure 26(a), we show the input image without the Fourier plane filter in place. The image consists of a number of circular and ellipsoidal dark regions on a light background. The 4 mm iris is slightly out of focus due to axial displacement between the SLM and iris, and some slight interference fringes are visible due to stray light scattered off the beam-splitter placed in front of the SLM. The interferometric measurement of the phase is shown in Figure 26(b) and it can clearly be seen that there is a binary phase modulation imposed on a uniform amplitude wave front. The fringe spacing indicates that we have a phase shift of approximately $\pi$ in the output modulation and we have consequently successfully converted our input amplitude distribution into a spatially identical phase distribution. The fringes in the

region outside the aperture are due to the small fraction of light scattered by the filtering operation.

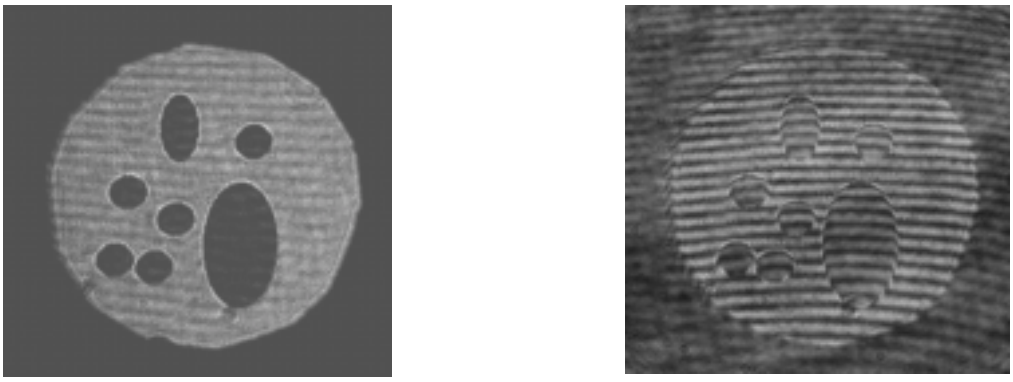

(a) (b)

Figure 26. Experimental results for the generation of phase modulation using an SLM operating as the input amplitude modulator. (a) An image of the input amplitude distribution without the filter in place; (b) interference fringe measurement of the output phase modulation.

1. J. Glückstad and P. C. Mogensen, "Reverse phase contrast for the generation of phase-only spatial light modulation", *Opt. Comm.* **197**, 261-266 (2001).

### 3.3.3 The generalised phase contrast method in a planar, integrated micro-optics platform

*V. Daria, J. Glückstad, P.C. Mogensen, R.L. Eriksen, S. Sinzinger* and J. Jahns**
*(*Fernuniversität Hagen, Germany)*
jesper.gluckstad@risoe.dk

The generalised phase contrast (GPC) method[1] is a useful technique for imaging and visualisation of optical phase, and its applications span from optical data encryption and decryption, multiple-beam optical tweezers, wave front sensing and generation of spatial phase modulation.[2-5] The GPC method is an enhanced approach primarily because it is not limited to small phase disturbances that are characterised by the first order approximation of the Zernike technique. It enables analytic determination of the exact working parameters where any disturbance in the phase of an incident wave would yield significant information that is visualised by a high-contrast intensity distribution at the output. The GPC method also allows the analytic design of the filter to yield maximum transmission and phase-only filtering through the optical system.

In most applications, the GPC method has been implemented in macro-optical systems. In these systems, however, the optical components are well defined and the effect of the phase contrast filter as well as the imaging response could be efficiently analysed based on the paraxial approximation. To realise the applications of the GPC method to current technologies in electro-optical data transport, it is important to carry out the method in a scaled-down optical system such as its implementation using planar, integrated micro-optical components. Integration of free-space micro-optics in a surface of a thick transparent substrate has attracted much attention because its concept mutually complies with the requirements in the development of integrated electronic circuits. Its implementation thereby expands to "real world" applications such as, e.g., in the fields of micro-optical, electro-mechanical systems (MOEMs), opto-electronics, optical computing, optical communications.[6]

However, optical systems that work perfectly in macro-optical set-ups remain to be uncertain to function properly in a scaled-down environment. The quality of the fabricated lenses having a finite aperture affects the resolution as well as the size of the image field in an imaging system. Moreover, fabrication of diffractive optical elements (DOEs), although favoured for practical reasons, influences the imaging behaviour and the spatial resolution because of discrete phase quantisation of the incident wave front. On the other hand, refractive optical elements are impractical to fabricate due to the need for thick deposition of phase structures in order to achieve the necessary optical function. Another issue is the aberration caused by the oblique orientation of the optical axis. This comes as a result of the arrangement of the planar, integrated components, where the beam propagates at a certain angle in the optical system that is folded into a two-dimensional layout. Although the microlenses can be optimised to compensate for beam propagation along a tilted optical axis, slight distortion in the focal spot may influence the on-axis filtering that is applied in the GPC method. Furthermore, in applications where high throughput is required, the diffraction efficiency of the fabricated devices will pose as a problem. The finite number of quantisation steps results in the distribution of the input light to undesired higher-order diffraction beams.

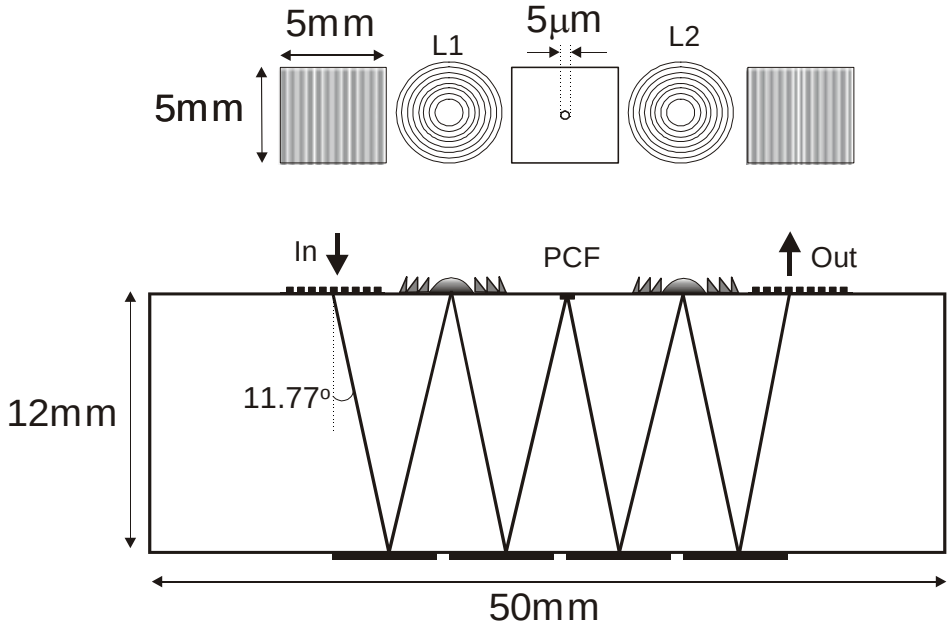


Figure 27. Implementation of the generalised phase contrast method in a planar, integrated micro-optics platform. Diffractive optical elements form the 4-f optical system that is fabricated on top of a 12 mm thick quartz glass substrate. The 5 μm diameter phase contrast filter is etched at the Fourier plane.

We have recently demonstrated the feasibility of implementing the GPC method in a planar, integrated micro-optics platform. The folded version of a 4-f lens configuration is implemented in a planar, integrated micro-optics platform as shown in Figure 27. Using multimask lithography, the multiple-phase level diffractive micro-optical elements were fabricated on the topside of the substrate while the base contains reflection-coated surfaces. An incident wave front, which is normal to the planar set-up, is coupled into the substrate through a binary diffraction grating with period 2.13 μm. The beam is deflected inside the 12 mm thick fused silica substrate with a propagation angle of 11.77$^{o}$. After reflection from the base, the beam is focused by the 5 mm diameter diffractive microlens (L1). The microlenses are reflection coated and are fabricated using two binary lithographic steps that make up a 4-phase level element. The focal length and the f-number of the microlenses are f = 24.5 mm

and f /#~ 5, respectively. The distance from the coupling grating to L1 is equivalent to the focal length which indicates that the object plane is located at the surface of the input grating. L1 focuses the beam to the Fourier plane where a reflection coated phase contrast filter (PCF) is fabricated on the substrate to perform a π–phase shift of the on-axis region of the focused light. The PCF is designed for operation at $\lambda = 0.633$ μm and is etched as a 5 μm diameter hole on the substrate. An anisotropic etching process is used to form a steep-edged cylindrical hole. The reverse Fourier transform is performed in the second half of the symmetric system. Both micro-lenses are slightly elliptical in order to compensate for the astigmatism due to the oblique optical axis.

We used a US Airforce resolution target phase mask as the input phase object. Figure 28(a) shows a low-contrast image where the angle of the collimated beam is set so that the focus is slightly off the PCF at the Fourier plane. This also represents the intensity distribution of the phase object. Setting the proper angle of the input beam so that the focus is directly phase shifted by the PCF yields a high contrast image as shown in Figure 286(c). The images are viewed using an input aperture with a diameter of 5 mm that corresponds to $D_{aperture} = 2.5$ mm at the surface of the planar optics. This aperture results in an Airy function at the Fourier plane with radius, $R2 = 1.22\lambda f/D_{aperture} = 7.6$ μm, of the mainlobe. With the radius of the PCF, R1 = 5 μm, the value of R2 corresponds to $\eta = 0.33$. This value of η, however, is not the desired setting that provides optimum contrast at the output interference pattern.[2] Setting η to further optimise the output would incur interference fringes that would alter the quality of the output image. This effect is also illustrated in Figure 28(c), which shows the onset of interference fringes at the sides. These fringes are the higher-order diffracted beams that come from the input DOE. Figure 28(b) shows the photograph of the planar, integrated micro-optics on a 12 mm thick fused silicon substrate.

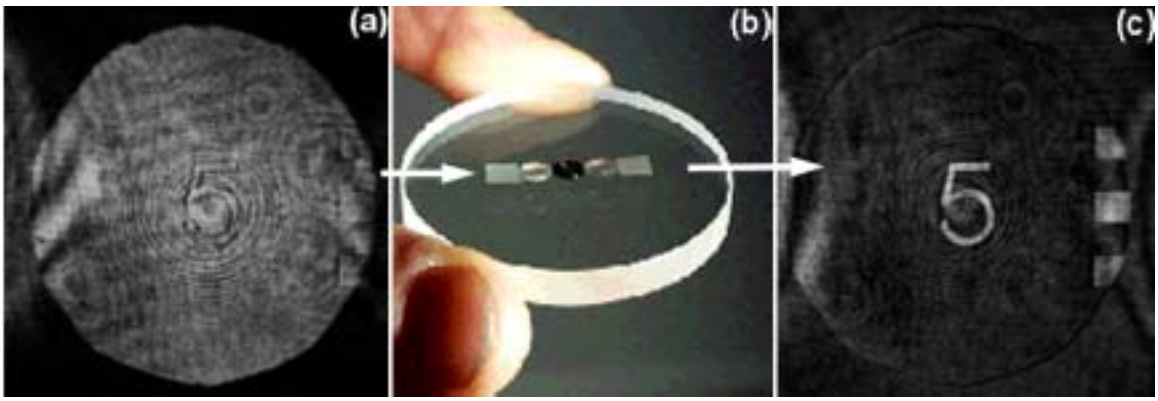


Figure 28. Intensity distribution of the (a) phase object and (c) the high contrast image at the output. Higher-order diffracted beams induce interference fringes at the sides of the image, which alters the output image when the input aperture is increased. (b) Shows the photograph of the planar, integrated micro-optics on a 12 mm thick fused silica substrate.

1. J. Glückstad, “Phase contrast imaging”, U.S. Patent No. 6,011,874 (2000).
2. J. Glückstad and P. C. Mogensen "Optimal phase contrast in common path interferometry" *Appl. Opt.* **40**, 268-282, (2001).
3. R. L. Eriksen, P.C. Mogensen and J. Glückstad ”Multiple beam optical tweezers generated by the generalised phase contrast method”, *Opt. Lett.* 15. Feb. issue (2002).
4. P.C. Mogensen and J. Glückstad “Phase-only optical decryption of a fixed mask”, *Appl. Opt.* **40**, 1226–1235 (2001).

5. J. Glückstad and P. C. Mogensen, “Reverse phase contrast for the generation of phase-only spatial light modulation”, *Opt. Comm.* **197**, 261-266 (2001).
6. S. Sinzinger and J. Jahns, Microoptics, Wiley-VCH Verlag GmbH, Germany (1999).

# 3.4 Optical measurement techniques

### 3.4.1 Miniaturising of optical sensors

*M.L. Jakobsen, F. Pedersen, H.E. Larsen, R.S. Hansen and S.G. Hanson*
michael.linde.jakobsen@risoe.dk

As a part of the Centre for Miniaturizing of Optical Sensors (MINOS) (http://www.sensortec.dk/stc.htm), we have investigated the potential for using miniature and low-cost light sources in the next generation of optical sensors. The need for sensors and particularly for non-contact optical sensors is increasing rapidly these years as conditional monitoring in more traditional manufacturing processes becomes important and, further, as the end products themselves are expected by the consumers to be more intelligent and automated. Thus, low costs, miniaturisation and high reliability are necessary demands for the future sensor technology. Within the MINOS project the concept of micro-optical sensor systems is studied, including miniature light sources, detectors, diffractive gratings, refractive miniature structures and their replication in plastic, as well as technologies for packing these micro-optical components.

MINOS has interest in incoherent light sources for illumination of spectroscopic samples. The demand for this type of light source is a stable spectrum within the maximally rated operating temperature range and within a given time interval during pulsed operation. Coherence and stability of the optical parameters are important for all the other types of micro-optical sensors developed in MINOS.

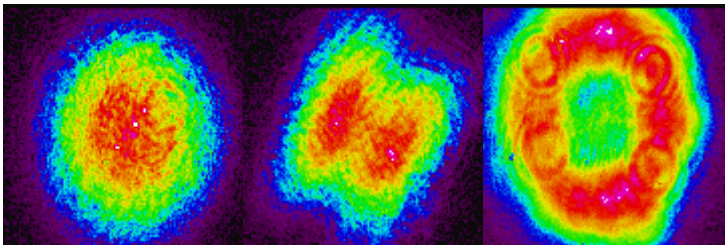

Figure 29. The figure illustrates the radiation diagram of three VCSELs with different configurations of single (most left) and multiple transversal laser modes.

This year one of our main contributions has been a market analysis of commercially available semiconductor-based light sources and a detailed characteristic of a minor selection of some of these that are particularly interesting for MINOS. The light sources, which have been selected for characterisation, range from near UV to near infrared wavelengths and include both incoherent and coherent devices such as light-emitting diodes (LEDs), edge-emitting laser diodes (EELs) and vertical-cavity-surface-emitting laser diodes (VCSELs). VCSELs are especially attractive due to their low power consumption, low costs, extreme compactness and low sensitivity to temperature and handling. On the other hand its special polarisation characteristics and multiple transversal laser modes must be dealt with (see Figure 29). Two databases have been established, one for laser diodes and one for light

emitting diodes with more than 400 and 100 different components, respectively. Two reports have been prepared: one report describes the potential of using today's commercially available semiconductor-based light sources for the relevant miniaturised optical sensors; the other summarises the measurements we have carried out on selected laser diodes.

Other main contributions have been the development of three different miniaturised optical sensor concepts for non-intrusive measurements of surface velocity and fluid flow velocity. These concepts are based on low-cost laser sources, such as EELs and VCSELs, and diffractive and refractive optics that can be replicated on, e.g., the surface of plastics. For the same reasons, the sensor designs must passively compensate for the influence of environmental effects such as, e.g., the temperature dependence on the emitted wavelength from a laser diode. Three corresponding patents will be filed around these sensor concepts.

Moreover, theoretical work has been carried out and published on partially developed speckles statistics and optical speckle formation from fractal structures, described separately in this report.

### 3.4.2 Common-path interferometers with Fourier plane filters for measuring various types of surface deflections

*S.R. Kitchen, S.G. Hanson and R.S. Hansen*
steven.kitchen@risoe.dk

Common-path interferometers are less sensitive to temperature fluctuations and common vibrations than many other types of interferometers. Additionally, the demands for the coherence length of the light source are considerably reduced.

We have proposed a common-path interferometer that can be used to probe various types of surface deflections, tilt or vibration. The system is a 4-*f* optical set-up with a holographic optical element (HOE) placed in the Fourier plane of the system (see Figure 30). This so-called Fourier plane filter splits the incoming light into a diffracted and an undiffracted field that interfere in the detector plane. The system can be designed to probe a desired type of deflection by proper choice of HOE.

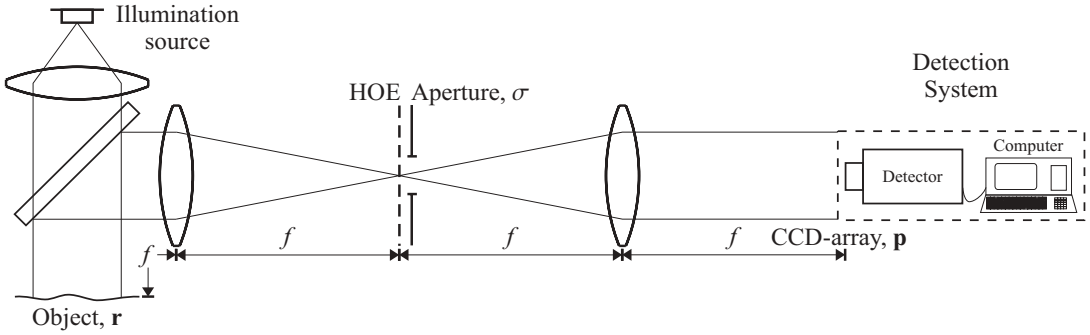


Figure 30. The 4-*f* set-up for measuring dedicated surface deflections, tilt or vibration.

With this system, we have presented a new type of common-path interferometer for measuring dedicated changes in curvature, e.g. the deflection of a circular diaphragm. We have designed the HOE in such a way that light from the centre of the diaphragm interferes with light collected from a circular ring on the edge (see Figure 31). The system is insensitive o a common translation of the object due to the common-path set-up and is also insensitive to rigid body tilt of the object due to the circular symmetry of the system.

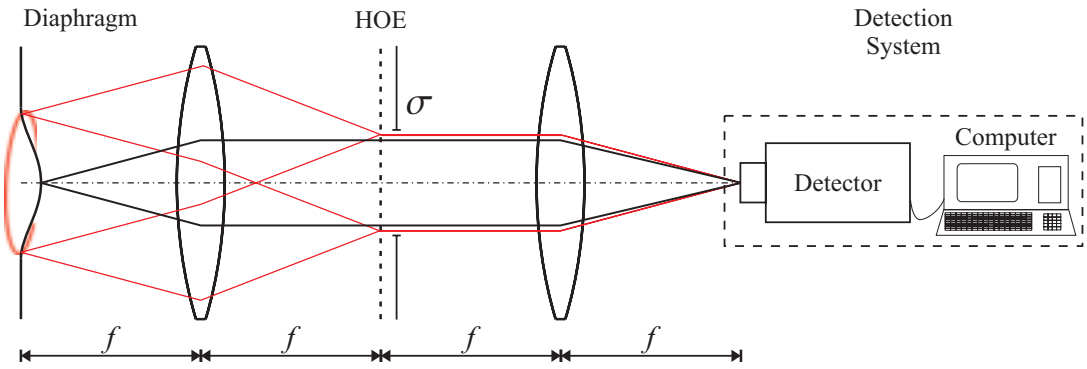


Figure 31. The receiver part of the interferometer for measuring changes in curvature.

A tool for depicting the effect of an arbitrary filter, called the impulse response function (IRF), has been presented and it has been shown how this tool can be used to design common-path interferometers for specific measurements. Fourier transforming the IRF will provide the phase function for the Fourier plane filter that subsequently can be implemented using, for instance, computer-generated holograms. If one has a desired impulse response function for the system such as the ones depicted in Figure 32, it is thus simple to design the dedicated HOE.

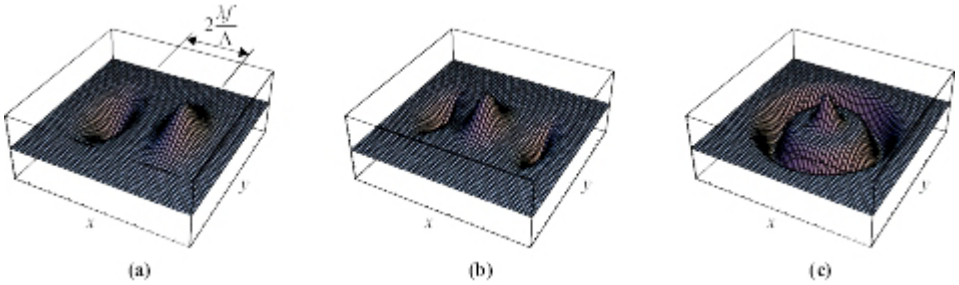


Figure 32. Impulse response for (a) shearing system (tilt sensor), (b) a one-dimensional, and (c) a two-dimensional curvature interferometer.

1. Kitchen, S.R.; Hanson, S.G.; Hansen, R.S., Fourier plane filters and common path interferometry in vibrometers and electronic speckle interferometers. In: Optical engineering for sensing and nanotechnology. 2001 International conference on optical engineering for sensing and nanotechnology (ICOSN 2001), Yokohama (JP), 6-8 Jun 2001. Iwata, K. (ed.), (The International Society for Optical Engineering, Bellingham, WA, 2001) (SPIE Proceedings Series, 4416) p. 108-111.
2. Kitchen, S.R.; Hanson, S.G.; Hansen, R.S., Introduction of the impulse response function in common-path interferometers with Fourier plane filters. *Opt. Rev.* (2001) **8** , 378-381.

### 3.4.3 Micro-optical system for mouse pen

*S.G. Hanson and R. Skov Hansen*
steen.hanson@risoe.dk, rene.skov.hanson@risoe.dk

A micro-optical system has been designed and has been implemented in the mouse pen, named *Zeptor* (www.kanitech.dk.), shown in Figure 33, intended for supplementing the well-known "mouse" as an input device for the personal computer. The rationale behind the alternative design of this input device is the increasing problem of repetitive strain injuries arising from the extensive use of the common mouse.

A steel ball with a diameter of 4 mm has been placed in the pen tip and rotates as the pen moves across the surface.[1] At the optical unit, shown in Figure 34, placed at a distance of 7 mm from the ball, a vertical surface emitting laser (VCSEL) facilitates the coherent illumination of the ball. The speckles arising from scattering off the surface are recorded by two pairs of adjacent detectors providing the necessary signals for depicting the direction and the amount of rotation of the steel ball. This information is repeatedly transmitted by a radio link from the pen to a receiver connected to the USB port of the PC. The received raw *x*- and *y*-counts are further processed in the PC to facilitate smoothing of the perceived movement and, moreover, to control speed and acceleration.

Figure 33. Side view of the Zeptor pen. The pen tip consists of a rotating steel ball, the rotation of which is recorded by an imbedded laser-based system.

The verification that a VCSEL-based system can be used in speckle-based schemes has paved the way for various low-cost and compact systems for probing speed, displacement, vibration and rotation.

1. Hanson, S.G., Miniaturized optical sensors for industrial use. In: New perspectives for optical metrology. International Balatonfüred workshop (HoloMet workshop), Balatonfüred (HU), 24-27 Jun 2001. Osten, W.; Jüptner, W. (eds.), (Bremer Institut für Angewandte Strahltechnik, Bremen, 2001) p. 87-93.

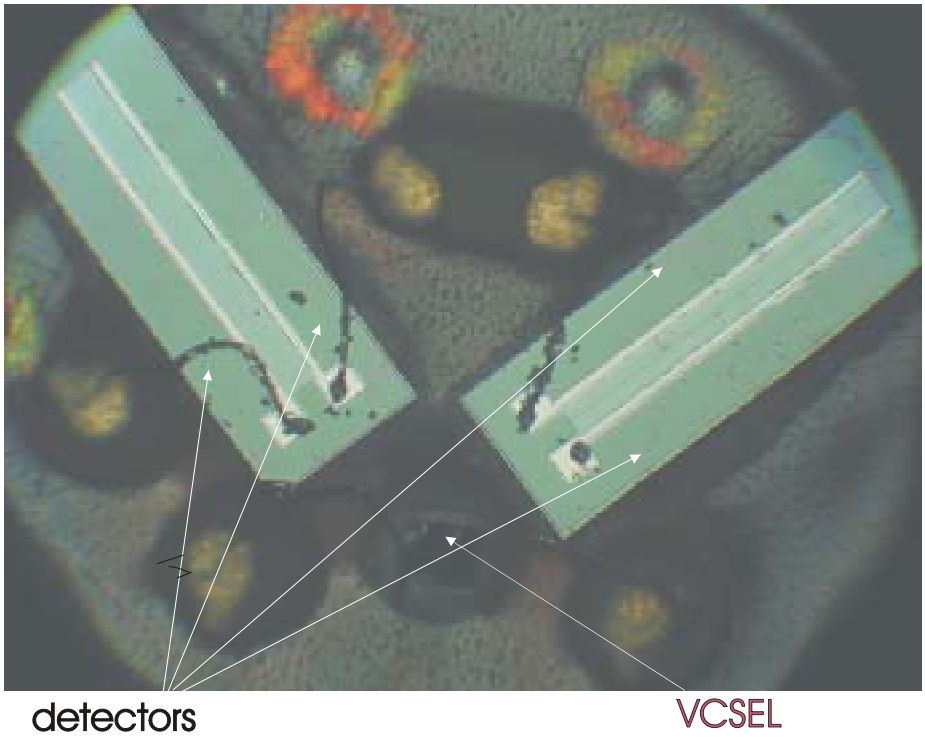


Figure 34. The optical unit placed in the tip of the pen has a diameter of 7 mm and includes four detectors and one VCSEL, sized 300 µm by 300 µm.

### 3.4.4 Laser anemometry for performance testing of wind turbines

*R. Skov Hansen*
*rene.skov.hansen@risoe.dk*

The general objective of the project is to improve the market position of wind power by enhancing the credibility by more accurate performance assessment of wind turbines.

The project carried out in the Optics and Fluid Dynamics Department deals with the construction of an anemometer to measure wind velocities in front of a wind turbine. Instead of using a cup anemometer mounted on a tower, a laser anemometer is found to constitute a more flexible instrument for performing remote measurements of wind velocities.

The laser anemometer is intended to be mounted on top of the nacelle and focuses a single laser beam in front of the wind turbine. The velocity of the wind is determined by measuring the introduced Doppler shift of the laser light, scattered backwards from the airborne aerosols in the focused laser beam. The measurement should be done so far away that the measured wind is unobstructed by the turbine. Based on the properties of the available lasers, a $CO_2$ laser with an optical wavelength of 10.6 µm has been selected. The laser is a sealed waveguide laser and has been specially designed for the laser anemometer in cooperation with Ferranti Photonics, Scotland.

The Doppler shift is measured by using a heterodyne principle, where the collected backscattered light interferes with a local oscillator. In order to reduce the costs of the instrument, a special design with a limited number of optical components has been developed and implemented.

Figure 35. An artistic impression of the otherwise invisible laser beam, emitted from the laser anemometer.

An important issue of the laser anemometer is the minimally required back-scattering coefficient of the aerosols in the measuring volume. Saturation phenomena of the detector establish an upper limit on the instrument sensitivity with respect to the back-scattered light. For the present detector, the lowest acceptable backscattering coefficient is approximately $\beta = 1*10^{-6}$ $m^{-1}sr^{-1}$, which gives a total reflection coefficient of the aerosols in the measuring volume of $1*10^{-11}$. This sensitivity, together with comprehensive digital signal processing of the detector signal, enables remote measurements of the wind velocity. The whole instrument is controlled from and transmits the measurements through the Internet.

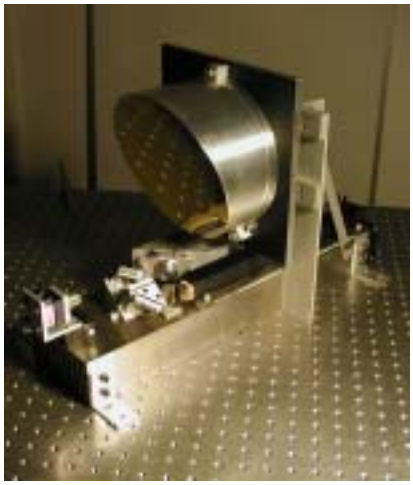

Figure 36. The whole optical assembly for the laser anemometer. The long black rod is the waveguide laser. The unit with the detector and amplifiers is seen mounted on the rear side of the laser heat sink underneath the large telescope mirror.

Figure 37. The final demonstration instrument mounted on a test platform on a mast in front of the large wind turbine at the Risø test site. The anemometer measures the wind velocity coming from Roskilde Fjord.

At present, comparative test measurements are performed at the Risø turbine test site. Velocity measurements are compared with measurements from a conventional cup anemometer.

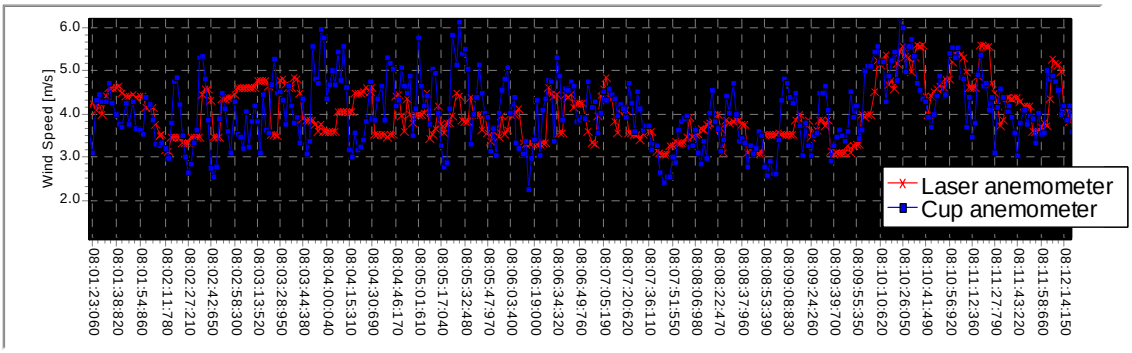


Figure 38. Comparison between the wind velocities measured by the cup anemometer (squares) and by the laser anemometer (cross).

The research is funded in part by The European Commission in the framework of the Non-Nuclear Energy Programme JOULE III.

### 3.4.5 On the fractal description of rough surfaces

*O.V. Angelsky*[*], *D.N. Burkovets**, *P.P. Maksimyak**, *V.V Ryukhtin**, *A.V. Kovalchuk**
*(*Department of Correlation Optics, Chernivtsy University, 2 Kotsyubinsky Street, 274012 Chernivtsy, Ukraine) and S.G. Hanson*
steen.hanson@risoe.dk

New feasibilities have been considered for optical correlation diagnostics of rough surfaces with different distributions of irregularities. The influence of deviations of the height surface roughness distribution from a Gaussian probability distribution on the accuracy of optical analysis is discussed. The possibilities of optical diagnostics of fractal surface structures are shown, and the set of statistical and dimensional parameters of the scattered fields for surface

roughness diagnostics is determined. Finally, a multifunctional measuring device for estimation of these parameters is proposed.[1]

Optical correlation techniques based on the random phase screen model (RPS) have been applied extensively during the last two decades. This method relies on having a surface with a characteristic length scale for the surface height distribution. During the last decade, some articles were published which confirmed that the structures of most surfaces are fractal or possess fractal-like structures. This fact can be explained as a consequence of the surface structure self-similarity, when the part of the surface of greater scale is of identical statistical structure as the parts of surface with smaller scales. In this case, the statistical approach based on the RPS model becomes insufficient. Fractals or self-similar objects must be considered within the framework of the theory of stochastic and chaotic oscillations. Such objects are characterised by unconventional parameters such as fractal, correlation, mass, volume and other dimensions. One of the possibilities of determining the dimensional parameters is to characterise them based on the slope of the power spectrum of the scattered radiation represented in a logarithm scale. But the techniques for measuring the dimensional parameters developed up to now also have some limitations. Thus, the development of new approaches for diagnostics of fractal surfaces is urgent.

Figure 39 shows the power spectrum for a random and a fractal surface height distribution, respectively. The investigation has shown that it is feasible to deduce the type of surface under study, i.e. if it is a fractal or a random one, by estimating the amplitude dispersion and the phase variance of the scattered radiation field.

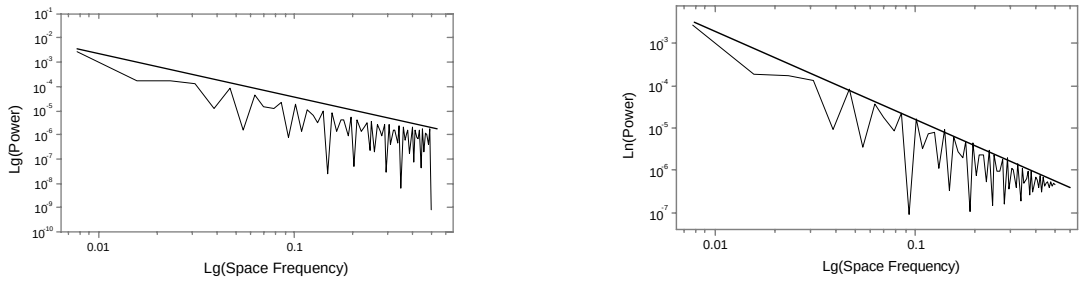


Figure 39. The experimentally found power spectra for random (a) and fractal (b) surfaces.

It has further been established that the kurtosis coefficient and the correlation exponent of the field are highly sensitive to changes of the surface irregularities. Thus, the kurtosis coefficient can be used as the diagnostic parameter within the height span from 0.1 to 20 $\mu m$, while the correlation exponent can be used as the diagnostic parameter within the height span from 0.8 to 20 $\mu m$.

1. Angelsky, O.V.; Maksimyak, P.P.; Ryukhtin, V.V.; Hanson, S.G., New feasibilities for characterizing rough surfaces by optical-correlation techniques. *Appl. Opt.* (2001) **40**, 5693-5707.

# 3.5 Infrared technology

### 3.5.1 Fourier transform infrared spectroscopy of aqueous solutions using optical subtraction

*P. Snoer Jensen and J. Bak*
peter.snoer.jensen@risoe.dk

The non-invasive measurement of trace organic components in aqueous solutions has a large number of important applications in such diverse areas as the dairy industry, wastewater analysis and medical diagnostics. Fourier transform infrared (FT-IR) spectroscopy has a great potential for such applications, but the demand for measurement of very small concentrations of organic substances is limited by the performance of the FT-IR spectrometer and by the strong absorption of water. The principal disadvantages may be summarized as follows: a) Sample and reference measurement are separated in time, meaning that stability is a problem. b) The measured signal is a sum of a large undesired background caused by water and the small signal from the trace component. c) The measured signal, which is the intensity as a function of the optical path length difference in a Michelson interferometer, has a large dynamic range so that digitisation by the 16-bit analog-to-digital converter in the spectrometer creates digitisation noise. The large dynamic range also limits the usable source intensity, since one must be able to measure the largest signal, which occurs at zero path length difference.

Optical subtraction is a method designed to eliminate the above weaknesses of the standard FT-IR spectrometer by measuring the difference between sample and reference directly. It provides a simultaneous measurement of sample and reference and reduces the dynamic range of the measured signal. This results in increased stability, elimination of digitisation noise and potentially introduces the ability to use more powerful light sources, thereby increasing the signal-to-noise ratio.

In our department, an accessory for a standard FT-IR spectrometer that facilitates optical subtraction has been developed.[1] The accessory, shown schematically in Figure 40 (left), sends light simultaneously through a reference cell containing pure water and through a sample cell containing the sample under investigation. The light is sent through two input ports into a standard FT-IR spectrometer where the light interferes destructively on the detector, so that a null signal is measured when sample and reference are identical. This is shown in Figure 40 (right).

The optical subtraction mode of operation has been found to provide increased stability and sensitivity compared with the standard mode of operation. To illustrate this, Figure 41 shows the second derivative of combination band urea signals, in the concentration range from 0 to 1 g/dl, for traditional absorbance measurements (left) and for optical subtraction measurements (right). The noise present in the traditional measurements is seen to disappear in the optical subtraction measurement scheme. This advantage translates into an improvement in detection limit for urea by more than a factor of 10. The present detection limits are better than 0.5 mg/dl.

1. Proc. SPIE, Vol. 4624, 2002. To be published.

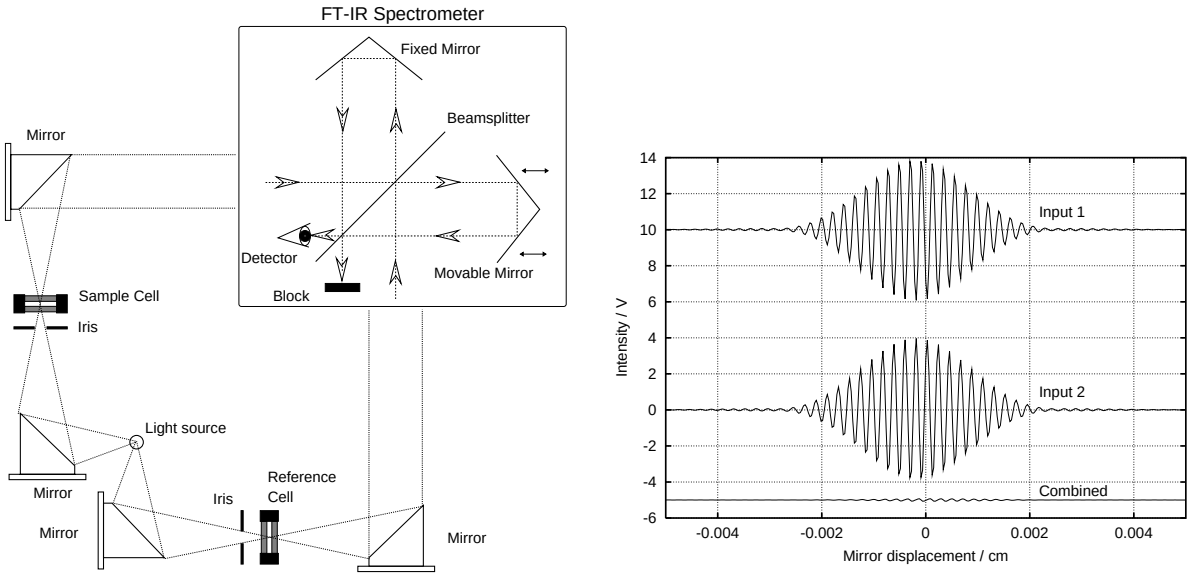


Figure 40. Left: Schematic drawing of optical subtraction instrumentation. Right: Interferogram from inputs 1, 2, and optical subtraction.

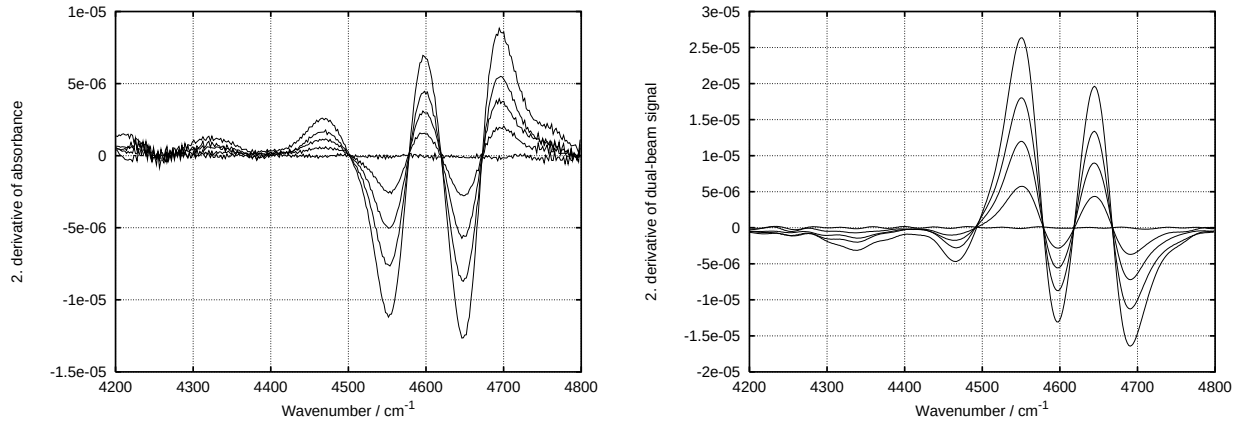


Figure 41. Second derivative of urea signals in concentration range 0-1 g/dl. Left: Traditional absorbance. Right: Optical subtraction.

### 3.5.2 Modelling of gas absorption cross sections using PCA model parameters

*J. Bak*
*jimmy.bak@risoe.dk*

The Aeroprofile project, which was partly funded by the European Commission Brite Euram III programme (Contract No. BRPR-CT97-0509), was initiated in December 1997 and was after a short extension scheduled to be terminated at the end of March 2001. The scientific goal of the project was to develop software and an experimental set-up to be used for temperature and concentration profiling in aircraft exhaust gas.

Our contributions to the project have been (1) to develop a hot gas cell facility for reference measurements, (2) to check the quality of the developed software and methods by judging the results obtained by measurements carried out in the reference hot gas cell, (3) to develop software which could be used to compare the performance of procedures based on

high and low spectral resolution for the determination of concentration and temperatures, respectively and (4) to support the aircraft exhaust measurements by infrared camera recordings. In addition, as an outcome of the software development process, a data compression method based on multivariate calibration techniques for modelling of gas absorption cross sections has been developed by Risø.

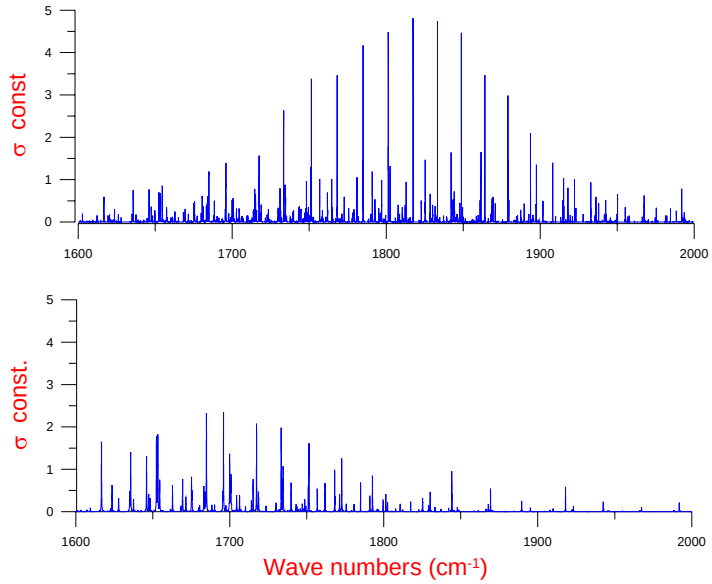


Figure 42. An example of the big difference in shape between the 300 K (lower spectrum) and 650 K (upper spectrum) $H_2O$ absorption cross sections. The described method based on PCA is capable of modelling this nonlinear relationship between absorption cross sections and temperatures.

Monitoring the amount of gaseous species in the atmosphere and exhaust gases by remote infrared spectroscopic methods calls for the use of a compilation of spectral data that can be used to match spectra measured in a practical application. Model spectra are based on time-consuming line-by-line calculations of absorption cross sections in databases using temperatures as input parameters combined with path length and partial and total pressure.

In this project it was demonstrated that PCA (principal component analysis) can be used to compress the spectrum of absorption cross sections, which depend strongly on temperature (see Figure 42), into a reduced representation of score values and loading vectors. The temperature range from [300-1000 K] is studied. This range is divided into two subranges, [300-650 K] and [650-1000 K], and separate PCA models are constructed for each of them. The relationship between the scores and the temperature values is highly nonlinear. It is shown, however, that since the score-temperature relationships are smooth and continuous, they can be modelled by polynomials of varying degrees. The accuracy of the data compression method is validated using line-by-line calculated absorption data of carbon monoxide and water vapour. Relative deviations from the absorption cross sections reconstructed from the PCA model parameters and the line-by-line calculated values are found to be smaller than 0.15 % for cross sections exceeding $1.27\times10^{-21}$ $cm^{-1}$ $atm^{-1}$ (CO) and 0.20 % for cross sections exceeding $4.03\times10^{-21}$ $cm^{-1}$ $atm^{-1}$ ($H_2O$). The computing time is reduced by a factor of $10^4$. A detailed description of the method and the achieved results can be found in reference 1.

1. Bak, J., Modelling of gas absorption cross sections using PCA model parameters. Accepted for publication in *Appl. Optics*, 2001.

### 3.5.3 Infrared temperature calibration and emissivity

*S. Clausen*
sonnik.clausen@risoe.dk

A reference laboratory for calibration of infrared instruments was established at Risø in 1996. Traceable calibration of infrared thermometers and blackbodies is offered in the temperature range -50 °C to 1600 °C. In 2001 the laboratory was approved by the Danish Accreditation Scheme, DANAK, to issue certificates for calibration of non-contact tempe-rature measuring equipment.

The work affects the following six main topics in reducing uncertainties of non-contact temperature measurements:

- Calibration service of infrared thermometers for customers
- Temperature measurements for customers
- Development of new and improved methods for infrared temperature measurements
- Measurement of spectral emissivity of samples and coatings
- Consultative service and information
- International comparisons of standards and procedures

Risø is involved in the EU project "TRIRAT" with participants from laboratories from most of Europe. The overall objective of the project is to provide improved, sub-Kelvin accuracy in infrared (IR) radiation thermometry at industrial levels in the range from –50 °C to 800 °C. The traceability is transferred from the highest metrological levels down to the industrial level. We work towards reaching sub-Kelvin accuracy of our calibration sources at temperatures in the range from –50 °C to 250 °C. The TRIRAT project ended in 2001 with the following results:

- Risø participated in two successful intercomparisons[1]
- A new method for emissivity measurements was developed, verified and applied for a number of different blackbody coatings[2]

With the combination of high-accuracy traceable blackbody sources and spectral measurements of infrared radiation with an FTIR spectrometer, Risø has state-of-the-art calibration capabilities in the spectral range from 1–25 μm. An example of results obtained for a customer is shown in Figure 43.

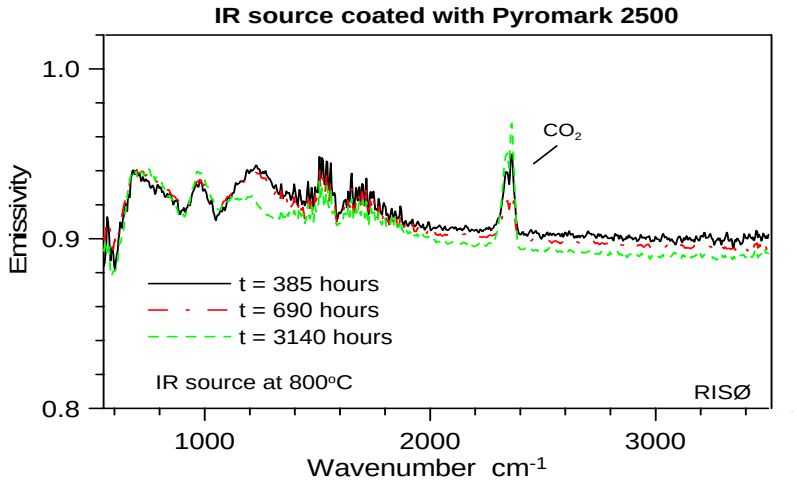


Figure 43. Example of repeated emissivity measurement of small IR source coated with Pyromark 2500. A minor change in emissivity is seen at 1050-1400 $cm^{-1}$ after 3140 hours due to reactions with the base material.

1. Clausen, S., Measurement of spectral emissivity by a FTIR spectrometer. In: Abstracts. 8. International symposium on temperature and thermal measurements in industry and science (TEMPMEKO 2001), Berlin (DE), 19-21 Jun 2001. (Physikalisch-Technische Bundesanstalt, Berlin, 2001) p. 45.
2. Ham, E.W.M. van der; Battuello, M.; Bosma, R.; Clausen, S.; Enouf, O.; Filipe, E.; Fischer, J.; Gutschwager, B.; Hirvonen, T.; Holtoug, J.U.; Ivarsson, J.; Machin, G.; McEvoy, H.; Pérez, J.; Ricolfi, T.; Ridoux, P.; Sadli, M.; Schmidt, V.; Staniewicz, C.; Struss, O.; Weckström, T., Intercomparison of local temperature scales with transfer radiation thermometers between -50 deg. C and 800 deg. C. In: Abstracts. 8. International symposium on temperature and thermal measurements in industry and science (TEMPMEKO 2001), Berlin (DE), 19-21 Jun 2001. (Physikalisch-Technische Bundesanstalt, Berlin, 2001) p. 77.

### 3.5.4 Hysteresis, hysteria or history for type K thermocouples

*F. Andersen*
*finn.andersen@risoe.dk; http://www.termometerkalibrering.dk or: http://www.risoe.dk*

The use of type K thermocouples has always been influenced by the negative effect of hysteresis. The Thermometry Laboratory at Risø National Laboratory has for many years calibrated thermometers for Danish industry. During these calibrations, especially for customers in the heat treatment industry and power plants, the Thermometry Laboratory has in the latest years seen better and better type K thermocouples without the former hysteresis problems. Risø therefore set up a programme for detecting this hysteresis in new thermocouples. About 30 years ago the hysteresis was told to be as big as 7-8°C in the range from 250 to 550°C. At Risø hysteresis has never been measured to more than 4°C.

Some manufacturers have since the beginning of the 1980's improved their type K thermocouples by different annealing processes before the thermocouples leave the factories. Risø has observed this annealing process as a way to minimise hysteresis and to get a better product.

During normal calibration work in the Thermometry Laboratory we have discovered that some thermocouples can still be improved in their uncertaincy of calibration if they are annealed before calibration. At the annealing procedure the hot junction and the "working length" of the wires are heated in a furnace to a temperature just above the maximum working temperature. The annealing not only reduces the hysteresis, it also stabilises the output of the thermocouple and changes it by 1 – 2 °C.[1]

This test has included new thermocouples from four different manufacturers in the United Kingdom and Germany and also some 25-year-old thermocouples from two of the same manufacturers from the laboratory stock. The old thermocouples were measured together with the new ones to see the differences in hysteresis after the annealing procedure had been started.

The results show that the present industrial standard type K thermocouples are better than the 25-year-old type K thermocouples, but it is still possible for some of the manufacturers to improve their thermocouples. The hysteresis is still a problem for some of the manufacturers, but it is smaller than before and there is no reason for hysteria.

As a critical user of thermocouples in the range 300-600°C it is recommended to anneal the thermocouples to a temperature above 700°C to stabilise the electromotoric force and eliminate hysteresis before calibration. If exact measurements have to be done by a thermocouple due to its small size of diameter or measuring point, it is sometimes better to use another type, i.e. type N, or in the lower temperature range type T.

Hysteresis still exists; it is not history, but it has been minimised for new type K thermocouples and can nearly be eliminated by extra annealing before calibration. No reason for hysteria. Former hysteresis up to 8°C in the 400-500°C temperature range has now been reduced for some manufacturers to be at the same level as the normal uncertainty for measurements for the best product. The test set up at Risø contains both bare wire and mineral-insulated thermocouples from several manufacturers.

1. Andersen, F., Hysteresis, hysteria or history for type K thermocouples. In: Abstracts. 8. International symposium on temperature and thermal measurements in industry and science (TEMPMEKO 2001), Berlin (DE), 19-21 Jun 2001. (Physikalisch-Technische Bundesanstalt, Berlin, 2001) p. 14.

# 4. Plasma and fluid dynamics

## 4.1 Introduction

*H. Bindslev*
henrik.bindslev@risoe.dk

A unifying theme of the research performed in the Plasma and Fluid Dynamics programme is the dynamic behaviour of continuum systems. The continuum systems under investigation cover fluids, plasmas and solids. In the case of solids, the research is carried out in the fields of optics and acoutics as well as in their borderland called opto-acoutics. Both linear and nonlinear problems are addressed in a combination of experimental, numerical and theoretical studies. Scientific computing in a broad sense plays a major part in these investigations and includes theoretical modelling of the physical phenomena, development of numerical algorithms, visualisation of the computed results and last, but not least, validation of the numerical results by detailed comparisons with carefully conducted experiments.

Due to the broad approach to the problems, the various projects are scientifically overlapping, not only inside the programme, but to a large extent also with projects in the rest of the department as well as in other departments at Risø. This overlap is considered an expression of strength since it gives rise to considerable synergy between different parts of the laboratory.

The goals of the scientific studies are two-fold: on the one hand the investigations aim at achieving a deeper understanding of the fundamental behaviour of complex physical and technical systems; on the other the acquired knowledge is sought utilised in the definition and design of solutions to specific technological problems. In the following three subsections, descriptions of the scientific projects carried out during 2001 have been collected under the headings: *fusion plasma physics*, *fluid dynamics* and *optics and acoustics*.

## 4.2 Fusion plasma physics

### 4.2.1 Scrape off layer simulations and comparison with experiment

*V. Naulin, A.H. Nielsen, M. Endler*, Th. Klinger* and H. Thomsen**
*(*IPP Greifswald, Greifswald, Germany)*
volker.naulin@risoe.dk

Many features of magnetically confined plasmas are crucially determined by their interaction with material boundaries or, in other words, by the physics of the edge and the scrape off layer plasma. In the past, turbulence simulations looked at very simple models to get a grip on the basic behaviour of the fluctuations while, on the other hand, detailed plasma wall interactions were modelled in 2D transport codes that basically eliminate the dynamics of turbulence, using parameterisations to include the effects of turbulence and the associated transport in the modelling. Many effects like pedestal formation, LH transition and ELM generation cannot, however, be treated in such a manner as they are based on the interplay between fluctuations and profile variations. We have therefore upgraded the TYR drift Alfvén turbulence code to include sheath boundary conditions in limiter geometry for parts of the

domain. An extension to incorporate the more complex divertor geometry is on its way. The numerical results will be compared with probe measurements from the Wendelstein 7AS devices and JET. The influence of active probes will be modelled additionally and will be used to assess the possibilities of actively influencing the edge turbulence. Figure 44 shows the flux surface averaged plasma potential developing self-consistently in a 3D turbulence simulation.

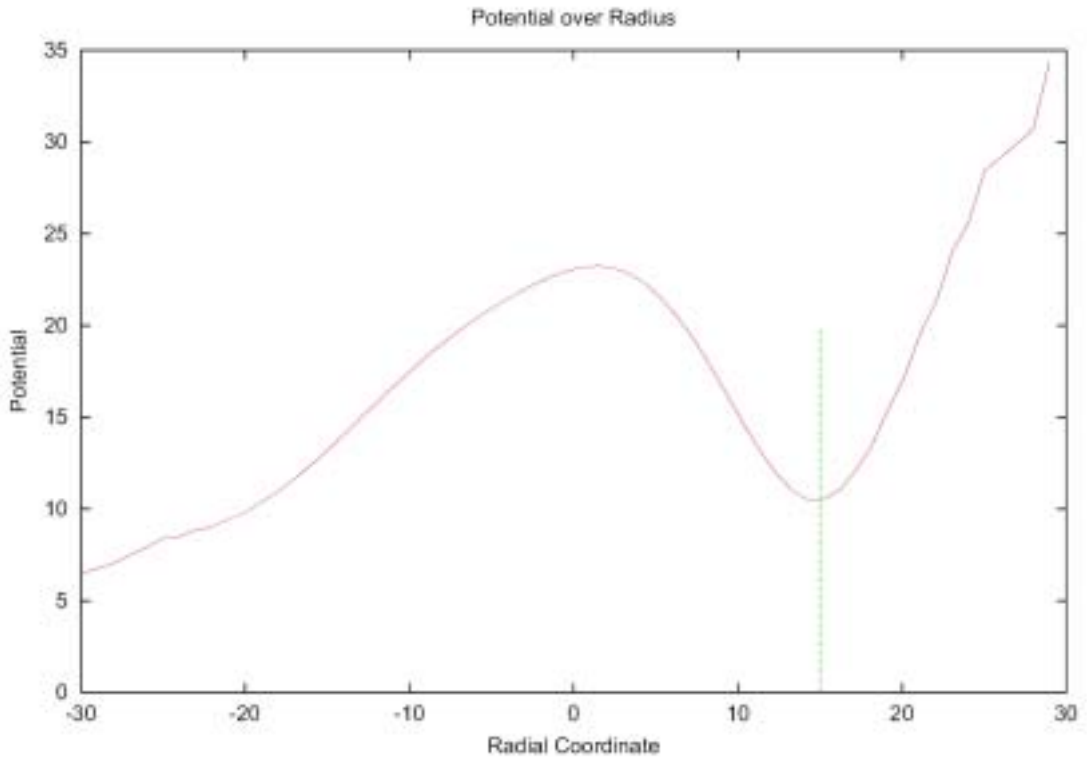


Figure 44. Flux surface averaged plasma potential from a three-dimensional turbulence simulation. Limiter sheath boundary conditions are active outwards from the green line.

### 4.2.2 Global dynamics of plasmas

*V. Naulin, G. Bonhomme (Laboratoire de Physique des Millieux Ionisés, Université Henri Poincaré Nancy, France), D. Block*, F. Greiner*, A. Piel* (*Christian Albrechts Universität Kiel, Germany) and Th. Klinger (IPP Greifswald, Greifswald, Germany)*
volker.naulin@risoe.dk

The complete self-consistent description of even a simple linear plasma is challenging and has as yet not been successfully achieved. Here we try to model the dynamics of a bounded plasma with sources and sinks. The goal is to compare the results with detailed measurements available for these classes of devices like, e.g., the KIWI (Kiel, Germany), the Mirabelle (Nancy, France) and the Vineta (Greifswald, Germany). The results will be used to validate the numerical models used for sheath boundary conditions and for global plasma dynamics. Furthermore, this model will allow experimental and numerical investigations of wave and turbulence phenomena in parameter regimes relevant to the edge region of existing or upcoming major fusion plasma devices.

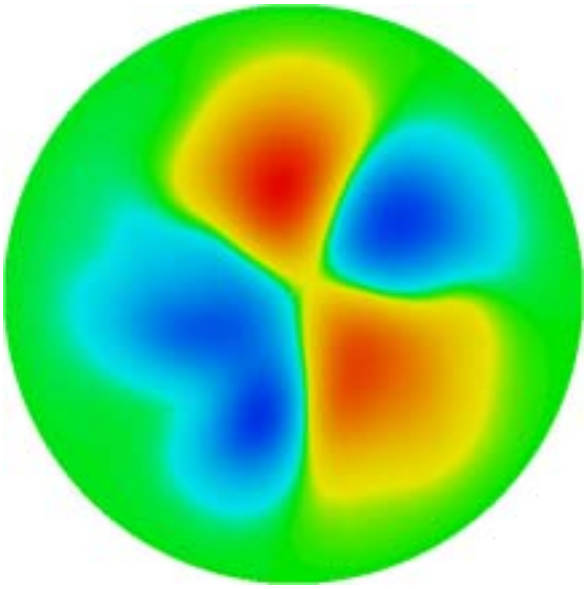

Figure 45. An m = 2 mode with about 3% fluctuation amplitude develops in these 3D simulations of a linear plasma device.

Figure 45 shows the fluctuating part of the density exhibiting an unstable m = 2 mode with a saturated fluctuation amplitude of about 3% of the background density. This numerical result is similar to what is observed in experiments.

### 4.2.3 Electromagnetic transport effects

*V. Naulin and J. Juul Rasmussen*
volker.naulin@risoe.dk

The paradigm for transport barriers is based on the simple argument that sheared flows suppress turbulence and transport via a decorrelation mechanism. Here we present simulation results from the stationary phase of drift-Alfvén turbulence in a sheared 3D geometry. The results show an intrinsic relationship between the shear flows and the magnetic field perturbations, leading to somewhat more complex behaviour, where for larger values of the plasma beta the transport might rise in the presence of shear flows.

The simulations show that the electro-magnetically induced component of the flux – although very small – is localised in just the regions where velocity shear reduces the ExB transport component. This leads to permeability of the transport barrier due to magnetic field line bending by the parallel current component. An ad hoc explanation of this phenomenon can be based on the fact that the ExB shear region is also a transport barrier for the nonlinearly convected parallel current component that thus reaches rather large values just close to the transport barrier. This results in relatively large perturbations of the magnetic field that allow for transport processes parallel to the field lines to somewhat mitigate the effect of the barrier. This is exemplified in Figure 46 that shows that the EM component of the transport is largest where the ExB flux is smallest. Note that in steady state the **total** flux has to be flat as any finite divergence of the flux corresponds to an ongoing profile modification.

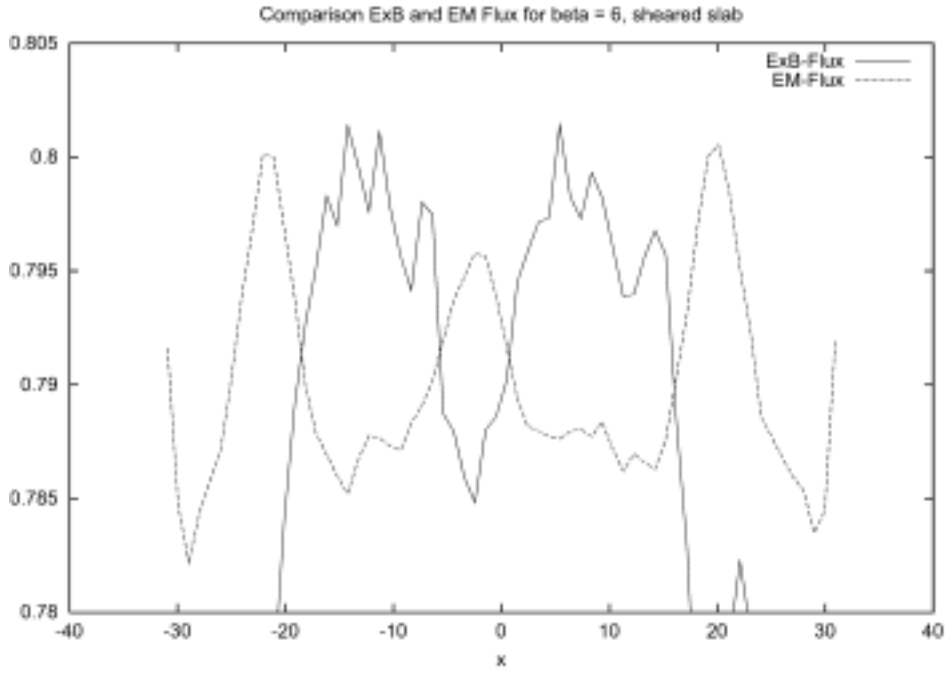


Figure 46. Radial flux surface and time averaged profile of the EXB and the electromagnetic component of the particle flux (note that a constant value of about 0.795 is added to the EM component), showing that the EM component is large where the ExB component is small, namely at the transport barrier.

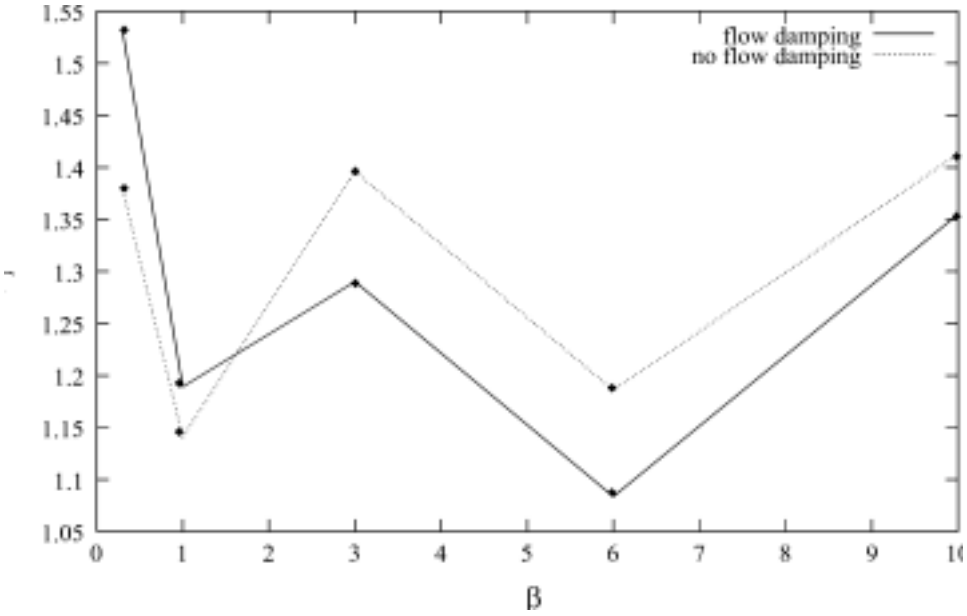


Figure 47. Flux versus normalized plasma beta for runs with and without zonal flow damping. A crossover in the flux scaling can be seen for beta larger then 1.5.

The resulting effect is that when we switch off flow damping in the simulations, the zonal flow level and the transport rise for a plasma beta larger than 1.5. This opposes the simple picture, where an increasing shear flow always leads to a diminished transport. This phenomenon has been depicted in Figure 47 where the flux is shown versus normalized plasma beta for cases with and without zonal flow damping. For a plasma beta larger than 1.5,

a crossover in the transport level scaling is visible, marking the onset of the mechanism described above.

### 4.2.4 Dispersion of heavy particles in developed drift wave turbulence

*R. Basu, V. Naulin and J. Juul Rasmussen*
jens.juul.rasmussen@risoe.dk

We have extended the investigation of particle dispersion in drift wave turbulence to account for the dispersion of "heavy" particles. While the dispersion of "plasma ions" is well described by employing the lowest order approximation for their velocity, $\mathbf{v}_{E\times B}$, the E×B velocity (see 4.2.2), we have to account for inertial effects in the drift velocity of heavier particles. This is incorporated by adding the polarisation velocity, $\mathbf{v}_{pol}$, to the E×B velocity. $\mathbf{v}_{pol}$ depends directly on the mass and the charge of the heavy ion.

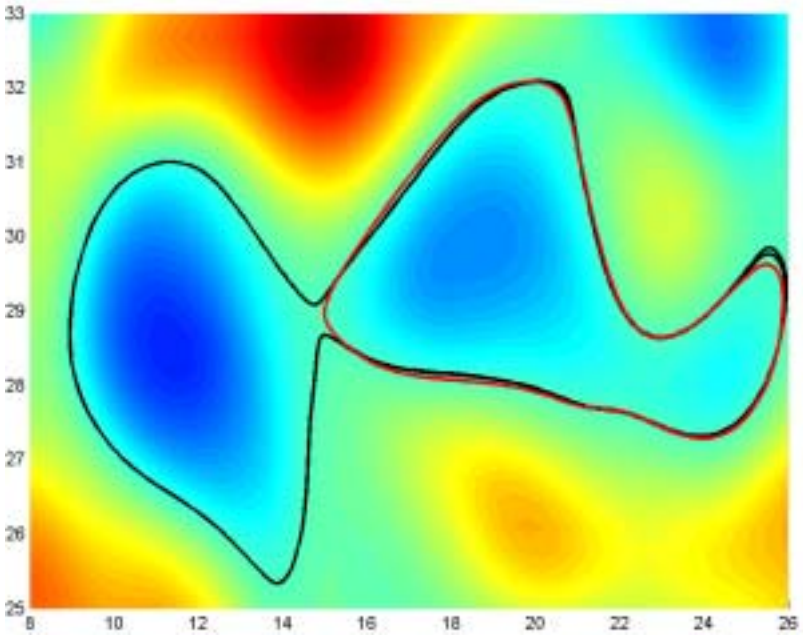


Figure 48. Contour plot of an electrostatic potential. The trajectories of "alpha particles" in a frozen field: red curve: E×B-velocity, only; black curve includes polarisation drift.

The initial results of these investigations are shown in Figure 48 and Figure 49. In Figure 48 we show typical trajectories of a "heavy" ion (parameters like an alpha particle in a hydrogen plasma) in a frozen potential. The red trajectory is the result obtained when using only the E×B velocity, and it is seen that the particle strictly follows the potential contours. The black trajectory is obtained by including $\mathbf{v}_{pol}$. We observe that the trajectory is now deviating from the potential contours and is not necessarily closed, i.e. vortical structures with closed potential contours will not be impermeable to heavy particles. We expect that the dispersion of the heavy particles will be different from the dispersion of the plasma particles. In Figure 49 we have depicted the running diffusion coefficients in the radial as well as in the poloidal direction for "alpha particles" with and without the polarisation drift. We observe an enhanced diffusion.

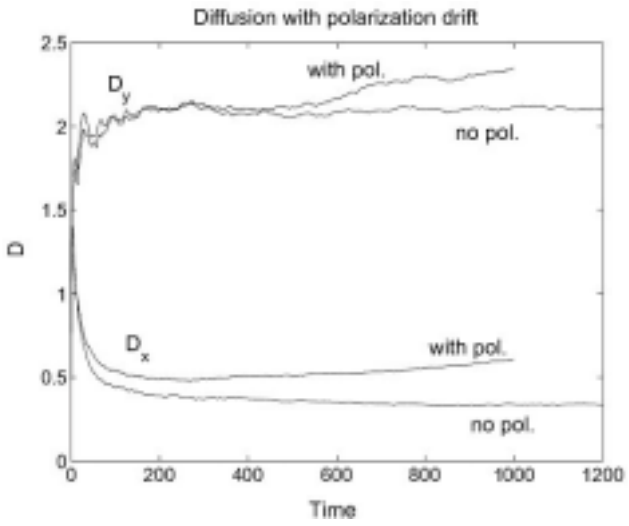


Figure 49. The diffusion coefficients for "alpha particles", with and without the polarisation drift.

### 4.2.5 Anomalous diffusion and particle flux

*R. Basu, T. Jessen, P.K. Michelsen. V. Naulin, A.H. Nielsen and J. Juul Rasmussen*
jens.juul.rasmussen@risoe.dk

The high levels of energy and particle transport across magnetic field lines, known as anomalous transport, are generally agreed to be due to low-frequency turbulence. A good candidate for understanding and explaining this phenomenon from first principles is drift-wave turbulence.

There are two approaches to describe transport in plasma turbulence. One is to look at the convected density, n, leading to an expression $\mathbf{\Gamma} = n\mathbf{v}_{\mathbf{E}\times\mathbf{B}}$ for the density flux, which is usually measured in experiments (here $\mathbf{v}_{\mathbf{E}\times\mathbf{B}}$ is the E×B velocity). The other is to determine a diffusion coefficient from the displacement of test particles. From the outset it is not evident that these two approaches should yield the same result. The flux is degrading the plasma confinement, while the charged particle diffusion reflects the mixing properties of the flow rather than giving information of the direct cross-field transport. A transport of mass is not connected to it, as the centre of mass of the considered test particles stays fixed. We have shown that for drift-wave turbulence the two transport predictions will yield the same result by employing the Langrangian invariance of the potential vorticity. This result is further verified by extensive numerical simulations of drift-wave turbulence based on the Hasegawa-Wakatani model for plasma edge turbulence driven by the resistive instability. That is, we have compared the averaged flux $\langle\mathbf{\Gamma}\rangle$ in the radial direction with the flux obtained from the particle diffusion coefficient via Fick's law.

The trajectories of particles inserted in the turbulent plasma are found by using the first-order drift velocity, $\mathbf{v}_{\mathbf{E}\times\mathbf{B}}$, and the running diffusion coefficient in the radial ($x$) direction is defined as $D_x(t) = \langle(x - x_0)^2\rangle/2t$, and likewise for the diffusion coefficient in the poloidal ($y$) direction. We found that the diffusion in the poloidal ($y$-) direction is significantly larger then the diffusion in the radial ($x$) direction.[1]

Figure 50 shows the running diffusion coefficient in the radial direction, $D_x(t)$, compared with the diffusion coefficient obtained from the flux by means of Fick's law ($D_{flux} = \langle\mathbf{\Gamma}\rangle/\text{grad}\, n_0$ ; for the employed normalizations: $D_{flux} = \langle\mathbf{\Gamma}\rangle$). It is observed that after a transient initial period the two diffusion coefficients are in close agreement. This is observed for a wide range of parameters.

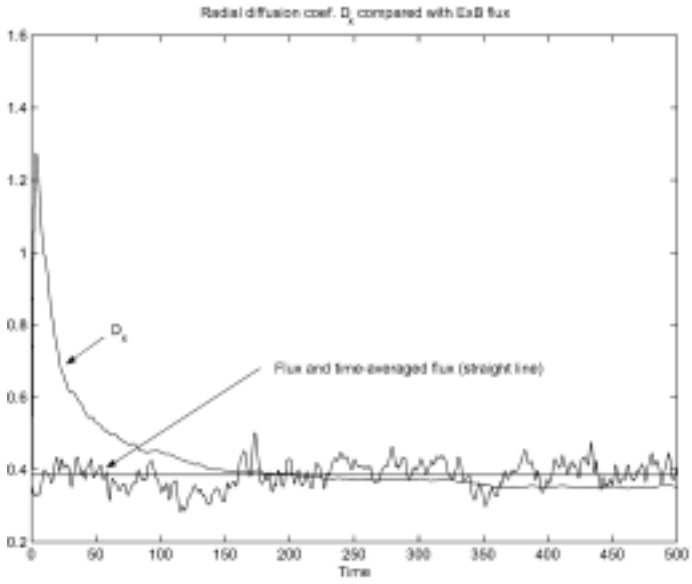


Figure 50. The running diffusion coefficient, $D_x$, obtained from following the trajectory of 5000 test particles, compared with the turbulent flux.

1. V. Naulin, A.H. Nielsen and J. Juul Rasmussen, *Phys. Plasma* **6**, 4575 (1999).

### 4.2.6 Dynamics of transport barriers and ELM-like behaviour in electrostatic turbulence

*V. Naulin, J. Nycander (FOA, Stockholm, Sweden) and J. Juul Rasmussen*
volker.naulin@risoe.dk

It is generally recognized that self-consistently developing large-scale poloidal - or zonal - flows strongly reduce the radial turbulent transport by "quenching" the turbulence in hot magnetised plasmas. This mechanism may be responsible for the transition to an enhanced confinement, e.g. the H-mode regime first observed in the ASDEX tokamak. The H-mode is often found to be accompanied by bursts in transport related to edge localised modes (ELMs), the so-called ELMy H-mode. If no such intermittent transport behaviour is present, the rising pressure gradients often violently terminate the H-mode plasma by disruptions. Since neither turbulence nor the associated bursty transport can - or should - be avoided, it is essential to understand the interplay between zonal flows (transport barriers) on the one side, and turbulence as well as transport on the other.

We have investigated the evolution and dynamics of transport barriers in the form of zonal flows in a self-consistent model for pressure driven electrostatic turbulence in a plasma in an inhomogeneous magnetic field. This is a simplified model of the outboard side of a toroidal confinement device. It captures the effects of unfavourable curvature in an energy-preserving manner and describes the evolution of profiles as well as fluctuations.

The model is solved numerically on a two-dimensional domain bounded in the radial ($x$) direction with length $L_x$ and periodic in the poloidal ($y$) direction with length $L_y$. The poloidal periodicity length may be interpreted as the recurrence length of a magnetic field line: Assuming an infinite correlation along magnetic field lines for a rational surface characterised by the safety factor q we would have $L_y = 2\pi r/q$.

We have performed numerical simulations for various values of the different parameters of the system: the imposed temperature difference, $T_0$, the aspect ratio, $a = L_y/L_x$, the size of the system, $L_x$, and the dissipation coefficients. The behaviour is found to be most sensitive to

variations in the aspect ratio, a, which is related to 1/q. When $T_0$ is sufficiently large to drive the instability, we observe the following general scenarios, depending on aspect ratio as can be seen in Figure 51.

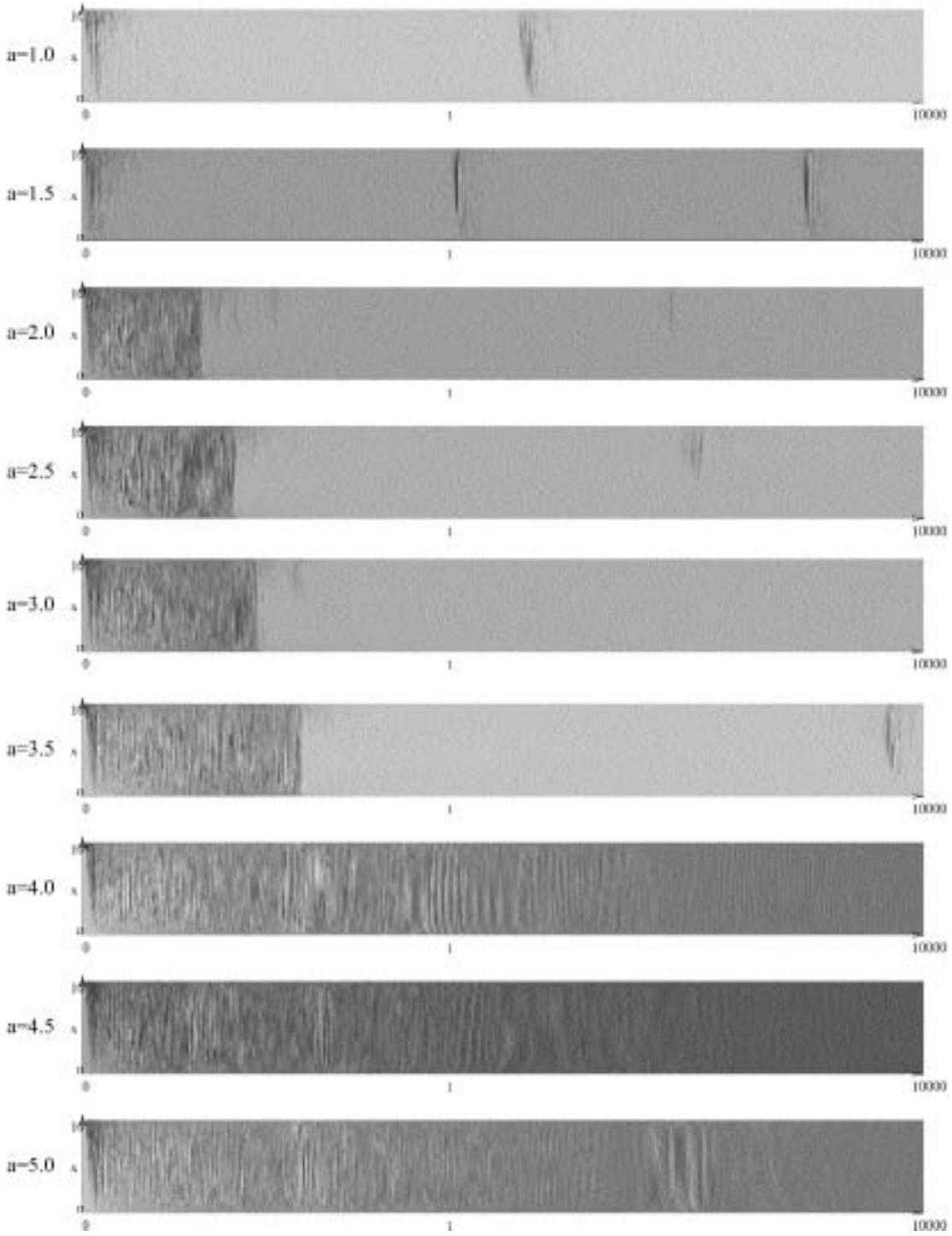


Figure 51. Poloidally averaged flux versus time and radial coordinate for different aspect ratios, a. For an aspect ratio larger than 3.8 no transport suppression is observed.

a) For sufficiently large a > $a_c$ ~ 3.8 the system develops into the state of turbulent equipartition (TEP) regardless of the value of $T_0$, demonstrating profile consistency.[1] This state is accompanied by a radial, turbulent heat flux that is persistent, but intermittent.

b) For smaller a, different behaviour is observed. In an initial phase the turbulence develops and establishes the TEP-profiles with a high flux level. Later on, the flux is interrupted - that is an H-mode-like state with steeper averaged gradients and where lower effective diffusion coefficients develop. For long periods of time the system is very quiescent, as can be seen in Figure 51. However, sporadic flux bursts of high amplitude - analogue to ELMs - are observed to occur at somewhat random intervals. The time scale of the quiescent periods between the bursts is, however, related to the viscous time scale.

The quiet periods are associated with the establishment of a strong poloidal mean flow - the zonal flow - that characterises the transport barrier. This flow, which is strongly sheared and often develops only in a part of the domain, quenches the turbulence and acts as an effective barrier for transport and mixing.

1. V. Naulin, J. Nycander and J. Juul Rasmussen, *Phys. Rev. Lett.* **81**, 4148 (1998).

### 4.2.7 Contour dynamics in 2D ideal electronmagnetohydrodynamic flows

*S. Senchenko (also at Department of Physics, Technical University of Denmark, Lyngby, Denmark) and V.P. Ruban (Landau Institute for Theoretical Physics, 2 Kosygin str., 117334 Moscow, Russia)*
senchen@fysik.dtu.dk

We have considered a special class of vortical flows in plasma that corresponds to the model of the ideal electron magnetohydrodynamics (EMHD). The EMHD model approximately describes the motion of the low-inertial electron component of a plasma on sufficiently short scales (below the ion inertial length). The much heavier ion component may be considered as motionless and is simply providing a static neutralizing background.

The dynamics of vortical structures are investigated by the Hamiltonian method. We follow the evolution of piecewise constant distributions of a conserved quantity related to the frozen-in canonical vorticity. The study includes the case of axisymmetric flows with zero azimuthal velocity component and also the case of flows with the helical symmetry of vortex lines. For an adequately large size of such a patch of the conserved quantity, a local approximation in the dynamics of the patch boundary is suggested. This is based on the possibility of representing the total energy as the sum of area and boundary terms. Only the boundary energy produces deformation of the shape with time. Stationary moving configurations are described.

### 4.2.8 Effect of shear flow on drift wave turbulence

*S.B. Korsholm, V. Naulin, J. Juul Rasmussen and P.K. Michelsen*
soeren.korsholm@risoe.dk

On the path towards future fusion reactors increased attention is given to the importance of turbulence for the efficiency of fusion devices. As a part of these investigations we have looked into the influence of self-generated and externally imposed poloidal shear flows on turbulence levels and turbulent transport. The model used in the numerical investigations is the three-dimensional drift wave Hasegawa-Wakatani model.[1] The simulations are performed in a slab geometry periodic in $y$ and $z$ (corresponding to the poloidal and toroidal directions, respectively), and in the radial direction we use non-permeable walls, $\phi(x=0)= \phi(x=L_x)=0$ and $n(x=0)=n(x=L_x)=0$, i.e. Dirichlet boundaries in $x$. $\phi$ is the electrostatic potential fluctuations, $n$

is the density fluctuations and $L_x$ is the domain length. The simulations are performed using pseudospectral methods.

The energy of the system is defined as $E = \frac{1}{2}\int\left[\left(\nabla_\perp\phi\right)^2 + n^2\right]d\bar{x}$. In Figure 52 the evolution of the energy of the background flow $E\left(k_y = 0, k_\parallel = 0\right)$ and the energy of the drift waves $E\left(k_\parallel \neq 0\right)$ is shown, and it is seen that the drift waves are suppressed as the poloidal flow builds up. One may alternatively say that the drift wave turbulence self-organizes into the poloidal shear flow. To illustrate that the sheared flow also reduces the turbulent transport, the maximum shearing rate $\max\left(\frac{\partial v_y}{\partial x}\right)$ and the radial turbulent flux $\Gamma_n = -\int n\frac{\partial\phi}{\partial y}d\bar{x}$ have been plotted in Figure 53. One may see that the turbulent flux has a local minimum when the maximum shearing rate has a local maximum.

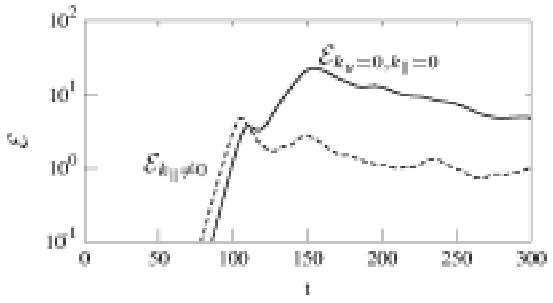


Figure 52. The temporal evolution of the background flow energy (full line) and the drift wave energy (dashed line).

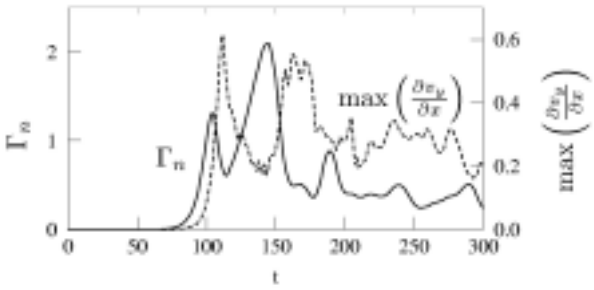


Figure 53. The temporal evolution of the turbulent flux (full line) and the maximum shearing rate (dashed line).

The fluctuations organize to flatten the background profile and this reduces the effective density gradient. Consequently, the drive of the drift wave turbulence is quenched by this backreaction of the density fluctuations. For situations close to adiabaticity $\left(\frac{n}{n_0} \approx \frac{e\phi}{T_e}\right)$ the density flux also arranges for a build-up of a potential profile. This in turn generates shear flow and ultimately suppression of the turbulence.

The shear flow described above is self-generated by the turbulence; however, other effects may lead to a shear flow that also affects the turbulence. We have investigated the effect of an externally imposed shear flow on the turbulence and the flow profiles. We applied a constant shear flow $\bar{v}_S = \bar{v}_S\left(x\right) = \Theta\tanh\left(2\pi(x - L_x/2)\right)\hat{y}$, where $\Theta$ is the amplitude of the shear flow.

The external shear flow was applied to the model in such a way that the fluctuations were not allowed to act back on $\bar{v}_S$. In Figure 54a)–c) profiles of the self-generated shear flow $\bar{v}_{E,y}$ as well as the total poloidal shear flow $\bar{v}_{E,y} + \bar{v}_S$ are shown for different values of $\Theta$. Note that for moderate amplitude $\left(\Theta = -1\right)$ the self-generated shear is affected, but maintains its amplitude, whereas for a strong external shear flow the fluctuations are suppressed resulting in low amplitude of the self-generated shear flow. Finally, in Figure 54d) we present the radial density profile in the case of a strong external shear flow, and it is seen that the shear flow causes a transport barrier to be formed.

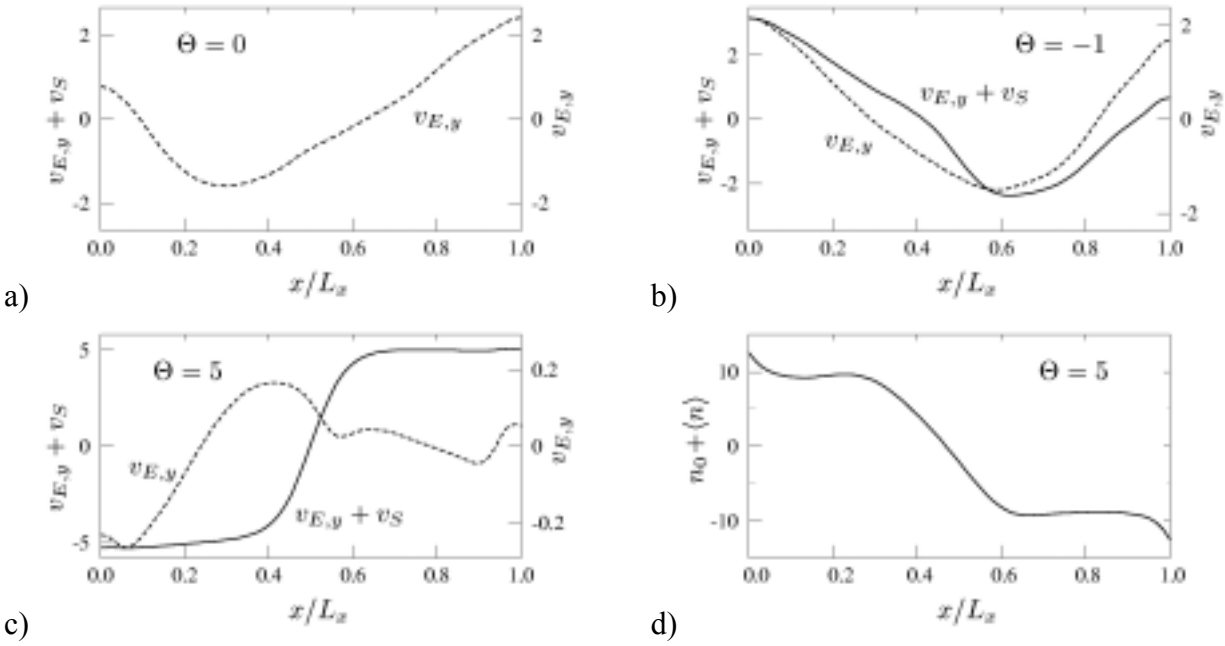


Figure 54. Self-generated shear flow $\overline{v}_{E,y}$ (dashed line) and total shear flow $\overline{v}_{E,y} + \overline{v}_S$ (full line) profiles for a) $(\Theta = 0)$, b) $(\Theta = -1)$ and c) $(\Theta = 5)$; d) the radial density profile for $(\Theta = 5)$. The scale for the full line is to the left.

1. A. Hasegawa and M. Wakatani, *Phys. Rev. Lett.* **50** (1983) 682-686.

### 4.2.9 Turbulence in high-density W7-AS divertor plasmas

N.P. Basse, S. Zoletnik (CAT-Science, Budapest, Hungary), M. Saffman (Department of Physics, University of Wisconsin, USA), M. Endler*, M. Hirsch* (*Max-Planck-Institut für Plasmaphysik, Garching, Germany), P.K. Michelsen, B.O. Sass, J.C. Thorsen and H.E. Larsen
nils.basse@risoe.dk

The localised turbulence scattering (LOTUS) density fluctuation diagnostic[1] installed on the Wendelstein 7-AS stellarator was operated routinely during the first six months of 2001. The discharges included partially detached plasmas and record-β shots.

We have here chosen to touch upon measurements in plasmas with extremely high densities and favourable confinement properties; the measurements were obtained using the recently installed divertor modules.[2] This discharge type has provisionally been identified as a high-density H-mode having central densities of up to $4 \times 10^{20}$ $m^{-3}$.[3] However, we will here call it improved confinement (IC), while normal confinement is denoted NC.

Two spectrograms are shown in Figure 55, illustrating the differences in density fluctuations between NC (left-hand plot) and IC (right-hand plot). The fluctuations measured in these discharges have a wave number of 20 $cm^{-1}$, corresponding to spatial scales of 3 mm. The spectra are shown up to frequencies of ± 2 MHz and from 0 to 900 ms; the discharges were steady state from 400 to 800 ms. It is immediately clear that the fluctuations below ± 1 MHz are larger in IC than NC. The reflectometry system observes the opposite, namely that fluctuations decrease in the NC → IC transition.[4] The difference is likely to be due to the scales observed; fluctuations having much longer wavelengths are observed using reflectometry. However, a reduction in high frequency (> 1.3 MHz) fluctuations is observed using LOTUS. This behaviour could be due to two distinguishable effects: An increase in

low-frequency edge fluctuations due to steepening density gradients and a decrease in high-frequency core turbulence. Each effect would be connected to the observed confinement transition.

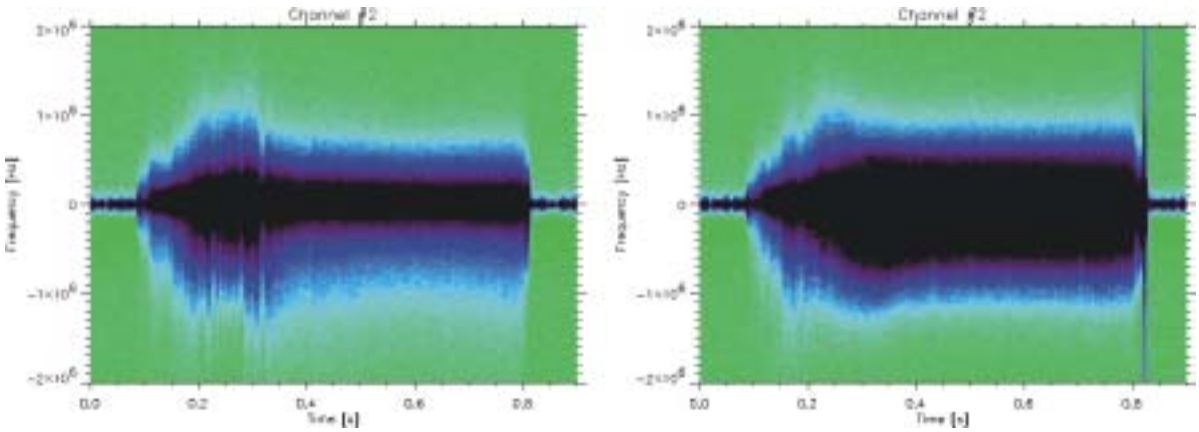

Figure 55. Spectrograms of density fluctuations at 20 $cm^{-1}$ for normal (left) and improved (right) confinement discharges. The colour scale is logarithmic (darker colour means larger amplitude) and identical for both discharges.


1. M. Saffman et al, *Rev. Sci. Instrum.* **72** (2001) 2579.
2. K. McCormick et al., *Plasma Phys. Control. Fusion* **41** (1999) B285.
3. P. Grigull et al., *Plasma Phys. Control. Fusion* **43** (2001) A175.
4. M.Hirsch, private communication (2002).


### 4.2.10 Fast ion dynamics measured by collective Thomson scattering


*H. Bindslev, P.K. Michelsen, M. Jessen, S. Nimb, J. Thorsen, P. Woskov (MIT, Cambridge, USA), TEC team (FZ-Jülich, Germany; FOM-Rijnhuizen, Netherlands; ERM/KMS, Belgium), ASDEX upgrade team (Max Planck Institute für Plasmaphysik, Garching, Germany)*
henrik.bindslev@risoe.dk; www.risoe.dk/euratom/cts


Magnetically confined fusion plasmas contain highly non-thermal populations of fast ions resulting from fusion reactions and plasma heating. With energies in the MeV range, two to three orders of magnitude above the bulk ion and electron energies, the fast ions typically carry one third of the plasma kinetic energy and even more of the free energy. It is essential that these energetic ions remain confined while they slow down and heat the thermal bulk plasma. The free energy associated with the fast ions is, however, also available for mischief. Non-linear wave particle interaction can drive waves and turbulence in the bulk plasma, significantly affecting both bulk and fast ion dynamics. In particular it can lead to catastrophic loss of fast ion confinement. The sawtooth instability, also affected by fast ions, appears to redistribute part of the ion population. If properly tailored, this can be an effective tool for removing helium ash from the core while leaving the valuable energetic alpha particles in place.

Wave particle interaction is also the basis of ion cyclotron resonance heating (ICRH); one of the main plasma heating schemes relying on the absorption of radio waves. Wave particle interaction depends critically on the phase space distribution of the energetic ions. The effect of waves and turbulence on the ion population manifests itself in the phase space distribution. So both to challenge and guide our understanding of dynamics involving fast ions, and to monitor our attempts at tailoring turbulence and instabilities affecting the ions, we need detailed measurements of the ion phase space distribution.

It has long been realized that collective Thomson scattering (CTS) has a unique capability for diagnosing the ion phase space distribution; that is, it can provide spatially resolved measurements of the velocity distribution. There are other techniques for diagnosing fast ions (charge exchange neutral particle spectroscopy and neutron spectroscopy), but no other diagnostic currently holds the potential for simultaneously resolving the distributions in time, space and velocity. Building on the experience gained with the fast ion CTS diagnostic at JET,[1] the technique had its breakthrough at TEXTOR, where a TEC-MIT team led by H. Bindslev built a proof-of-principle experiment.[2] This experiment demonstrated the feasibility of the measurements[3] and provided a wealth of new data on spatially localised ion velocity distributions at many time points in each plasma shot. These have, among others, permitted the investigation of fast ion dynamics at sawteeth. A sample measurement is shown in Figure 56, where both contours of the logarithm of the phase space density, and time traces for selected velocities have been plotted. The plots show the effects of the switch off of the ion heating at 2.2 s after which the velocity distribution contracts; the energetic ion population decaying in approximately 50 ms. Also evident is the effect of sawteeth. Comparing measurements from like discharges, in which the orientation of the resolved velocity component and the location of the measurement volume were varied independently, both inhomogeneity and anisotropy in the fast ion dynamics at sawteeth were observed.[3]

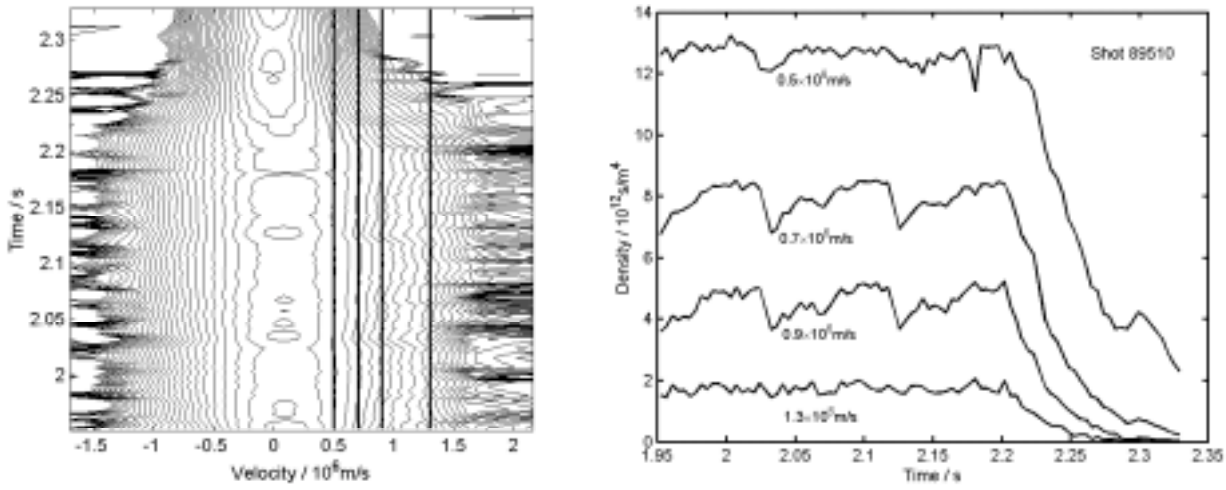


Figure 56. Both plots show the phase space density; number of ions per unit volume and unit velocity. In this shot (89510) the resolved velocity component makes an angle of 65.7° with the static magnetic field. The measurement volume is just to the high field side of the plasma centre, near the electron density inversion radius. Auxiliary heating (ICRH and NBI) is switched off at 2.2 seconds. Left: Contours of the logarithm of the ion phase space density. Right: Time traces of the phase space density for selected velocities.

The CTS effort at TEXTOR continues, now involving also Risø. Additionally, Risø, MIT and the ASDEX upgrade team have started the development of a fast ion CTS at ASDEX upgrade (AUG) tokamak at the Max Planck Institute für Plasmaphysik in Garching (Munich), Germany. This system will make use of the very substantial investments at AUG in fast ion sources (neutral beam injection and ICRH) and in new megawatt power level gyrotrons to be used as sources of the probing radiation in the CTS system. In addition to permitting fast ion dynamics to be studied in new and more ITER (reactor) relevant conditions, the proposed system for AUG will also provide experience with the use of high-power gyrotrons in a CTS system, as would be required in a fast ion CTS diagnostic for ITER.

1. H. Bindslev, J. A. Hoekzema, J. Egedal, J. A. Fessey, T. P. Hughes and J. S. Machuzak, *Phys. Rev. Lett.* **83**, 3206 (1999).

2. H. Bindslev, L. Porte, A. Hoekzema, J. Machuzak, P. Woskov, and D. van Eester, 26th EPS Conf. Contr. Fusion and Plasma Physics, Maastricht, Netherlands, Vol. 23J, part II, p765, EPS (1999) (http://epsppd.epfl.ch/Maas/web/pdf/p2049.pdf); H. Bindslev, L. Porte, A. Hoekzema, J. Machuzak, P. Woskov, D. van Eester, J. Egedal, J. Fessey and T. Hughes, *Fusion Engineering and Design*, **53**, 105 (2001); H. Bindslev, Journal of Plasma and Fusion Research. 76, 878 (2000); L. Porte, H. Bindslev, F. Hoekzema, J. Machuzak, P. Woskov and D. van Eester, *Rev. Sci. Instrum*. **72**, 1148 (2001); (http://www.risoe.dk/euratom/cts/TEXTOR).
3. H. Bindslev, L. Porte, J. A. Hoekzema, D. van Eester, A. Messiaen, G. van Wassenhove and P. Woskov, Proceedings of the 28th EPS conference on Controlled Fusion and Plasma Physics, Madeira, 18-22 June 2001. http://www.cfn.ist.utl.pt/EPS2001/fin/pdf/P3.077.pdf, (Or.09 & P3.077).

# 4.3 Fluid dynamics

### 4.3.1 Two-dimensional turbulence in bounded flows

*A.H. Nielsen, H.J.H. Clercx (University of Technology, Eindhoven, the Netherlands) and E.A. Coutsias (University of New Mexico, Albuquerque, USA)*
*anders.h.nielsen@risoe.dk*

During the last decades two-dimensional turbulence in unbounded domains (or more precisely in double periodic domains) in Navier-Stokes fluids has been investigated intensively by means of numerical simulations. The presence of an inertial range in the energy spectrum of these flows has been well documented. As two-dimensional flows exhibit an inverse cascade in the energy, coherent structures comparable with the size of the periodic domain will eventually emerge. Thus, the presence of boundaries and especially the conditions imposed on these will play a significant role in the evolution of the turbulence and the coherent structures.

In this contribution we perform numerical investigations of the evolution of a dipole that interacts with a curved wall with imposed no-slip constraint. The numerical scheme is a pseudospectral scheme based on Chebyshev polynomials and Fourier modes which solve the Navier-Stokes equations in the vorticity-stream function formulation. The computational domain is a periodic annulus.

In Figure 57 we display the time evolution of a bounded flow field where two shielded monopoles have been used as initial condition. During the simulations the shielding of the structures will be removed and a compact dipole will emerge and collide with the outer wall. During the collision a large boundary layer will form, will become unstable and will finally split the incoming dipole into two new asymmetric dipoles. We have investigated the amount of enstrophy generated at the no-slip wall as a function of the Reynolds number, Re. Before the incoming dipole is split up, the generated enstrophy scales like: $\Delta \approx (\mathrm{Re})^{0.5}$ as expected by boundary layer theory. After the dipole has been split up, we observed a more steep scaling of the form: $\Delta \approx (\mathrm{Re})^{0.75}$.

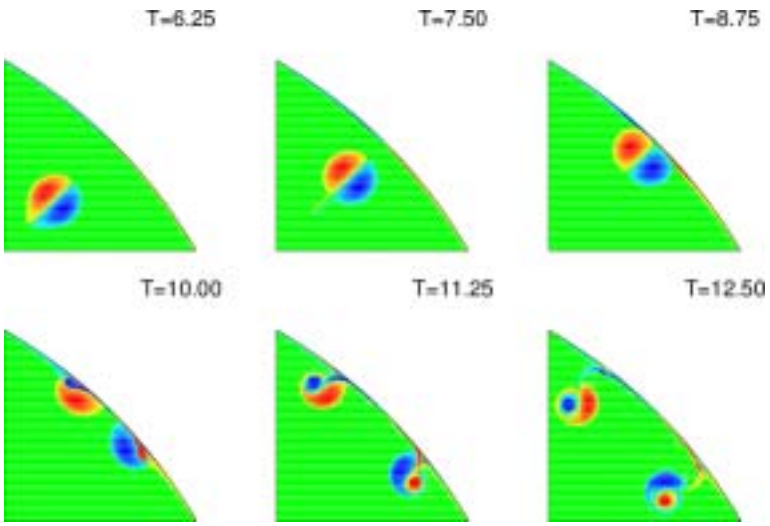


Figure 57. Time evolution of a dipole interacting with a curved wall. Red colours correspond to positive values, whereas blue colours correspond to negative values. Spectral evolution M = 1024 (radially), N = 1024 (azimuthally). The Reynolds number is Re = 10,000. Note that only a small part of the computational domain is displayed.

### 4.3.2 Vortex crystals

*V. Naulin, A.H. Nielsen and J. Juul Rasmussen*
anders.h.nielsen@risoe.dk

Numerical investigations of the interaction of turbulence and vortical structures with solid boundaries in a circular domain have been performed with both stress-free and no-slip conditions on the boundary. We mainly concentrated on the evolution of decaying turbulence for high Reynolds number flows, and considered a large variety of initial conditions. The characteristic tendency of two-dimensional turbulent flows to organise into domain filling structures is in general recovered in the presence of the boundaries.

For very high Reynolds numbers, $> 10^6$, we observed the tendency of formation of so-called vortex crystals. Vortex crystals were observed experimentally to form spontaneously from a particular initial condition consisting of a helical sheet or a ring of vorticity in a pure electron plasma column,[1] where the dynamics is essentially governed by the two-dimensional Navier-Stokes equations in the limit of vanishing viscosity. The initial configuration undergoes a rapid breakup due to Kelvin-Helmholz instability. This produces a quasirandom distribution of strong vortices that interact and thereby add to the small-scale background fluctuations. These large vortex structures either collapse to one strong central vortex or "freeze" into a regular pattern - a vortex crystal. A specific example is shown in Figure 58, where an initial ring of vorticity, which is perturbed by a mode 3 structure in addition to random noise, is observed to break up into three vortices that form a regular pattern of very long life time. Our aim is to investigate whether the generation of vortex crystals can be described within a fluid picture, or whether it is a specific feature of the pure electron plasma system.

1. K.S. Fine, A.C. Case, W.C. Flynn and C.F. Driscoll, *Phys. Rev. Lett.* **75,** 3277 (1995).

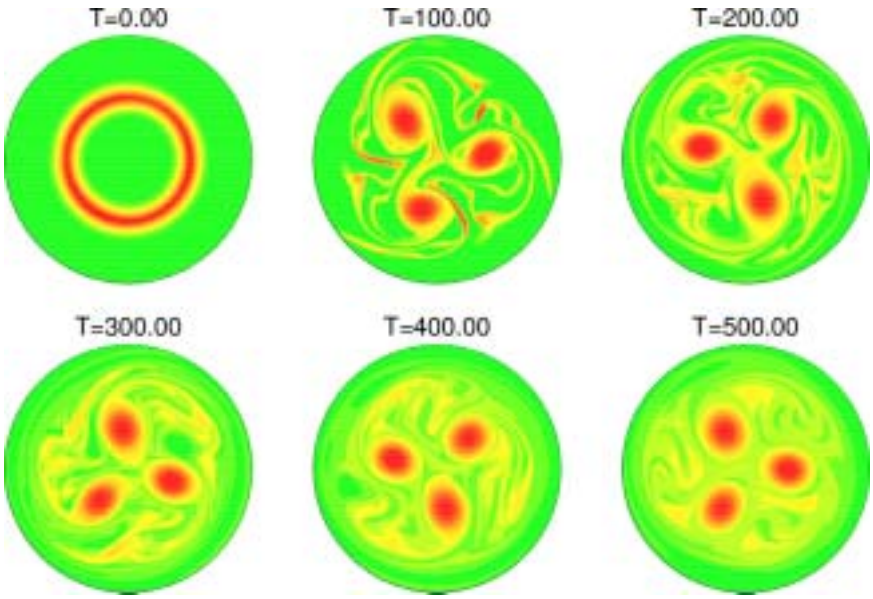


Figure 58. The evolution of a ring of vorticity with a dominant initial azimuthal mode perturbation of m = 3. Additionally a weak random perturbation has been added. The ring has a radius R = 0.5 and a width $\Delta = 0.03$, measured in units of the radius of the domain. The initial amplitude is vorticity = 0.5, and the viscosity = $10^6$ corresponding to a Reynolds number, Re = $3 \cdot 10^5$. A characteristic vortex turnover time is T = 10.0. Stress-free boundary condition has been used.

### 4.3.3 Bathtub vortex flows with a free surface

*A. Andersen (also at Department of Physics, Technical University of Denmark, Lyngby, Denmark), T. Bohr (Department of Physics, Technical University of Denmark, Lyngby, Denmark), B. Lautrup (The Niels Bohr Institute, University of Copenhagen, Denmark), J. Juul Rasmussen and B. Stenum*
aanders@fysik.dtu.dk

Bathtub vortex flows, i.e. swirling flows with a free surface, which may extend down to the drain hole of the fluid container, are abundant in nature. We investigate such source-sink flows in which an intense vortex is formed and the free surface is strongly perturbed and appears with a needle-like singular shape. To measure the free surface shape and the flow field we have constructed two experimental set-ups (one at the Technical University of Denmark and one at Risø), each consisting of a cylindrical container with a circular drain hole at the centre of the bottom. The cylinder is rotating about a vertical axis. Using a recirculation system, we obtain a steady bathtub vortex flow above the drain hole. By tuning the rotational frequency we control the length of the free surface dip. Flow visualisations and measurements of the free surface shape have been carried out at the Technical University of Denmark. Using the particle tracking system at Risø, we have measured velocity profiles.

At a distance away from the vortex centre the flow field is controlled by the bottom boundary layer, and in this region the measured velocity fields agree with the well-known linear theory for Ekman layers. We have extended the linear description of the bottom boundary layer to include non-linear terms. The non-linear terms are important close to the drain hole, and the extended theory allows us to describe the bottom boundary layer in this region. Currently we are working on the theoretical description of the vortex flow above the drain hole and on modelling the shape of the free surface dip.

### 4.3.4 Vortex dynamics around a solid ripple in an oscillatory flow

*A. Andersen (also at Department of Physics, Technical University of Denmark, Lyngby, Denmark), T. Bohr (Department of Physics, Technical University of Denmark, Lyngby, Denmark), T.S. Jespersen* and J.Q. Thomassen* (*The Niels Bohr Institute, University of Copenhagen, Denmark)*
aanders@fysik.dtu.dk

We have measured the time-dependent flow around a solid triangular profile that is oscillated back and forth horizontally in a narrow rectangular container. The flow around the triangle is approximately two-dimensional. Using particle image velocimetry we have measured the entire flow field at 20 different instances during a period of oscillation. Experimentally we are thus able to follow the temporal evolution of the vortices and to describe the vortex formation and interaction. We aim at formulating and solving a simple analytical model that captures essential features of the observed vortex formation and dynamics. The investigation is motivated by studies of sand ripples below an oscillatory flow of water made by C. Ellegaard and co-workers at the Niels Bohr Institute. Our experiment resembles the vortex flow around the ripple crests which play a crucial role in sand ripple formation and have features in common with other time-dependent vortex flows like, e.g., the flow around insect wings.

### 4.3.5 Stability of weak turbulence Kolmogorov spectra

*S. Senchenko (also at Department of Physics., Technical University of Denmark, Lyngby, Denmark) and V.P. Ruban (Landau Institute for Theoretical Physics, 2 Kosygin str., 117334 Moscow, Russia)*
senchen@fysik.dtu.dk

Five-wave interaction processes govern the one-dimensional, non-linear dynamics of deep-water surface gravity waves. In order to get the statistical description of a stochastic wave field one can use a pair correlation function.

The non-linear kinetic equation for the pair correlators has been derived and its stationary solutions have been found. These solutions turn out to be power-like, i.e. of a quasi-Kolmogorov type. We derive the linearised kinetic equation and investigate the stability of stationary solutions with respect to time-dependent one-dimensional perturbations. To perform this analysis we introduce the Melline functions, and the complex zeros of the latter define the stability of the stationary solutions. Particularly, we derive universal corrections for the Kolmogorov-type solutions.

## 4.4 Non-linear optics and acoustics

### 4.4.1 Hyperbolic shock waves of the optical self-focusing with normal group velocity dispersion

*L. Bergé (CEA/Bruyéres-le-Châtel, B.P. 12 Bruyéres-le-Châtel, France), K. Germashewski*, R. Grauer* (*Ruhr-Universität-Bochum, Germany) and J. Juul Rasmussen*
jens.juul.rasmussen@risoe.dk

The theory of focusing short light pulses in Kerr media with normal group velocity dispersion (GVD) in (2+1)- and (3+1)-dimensions is revisited. The investigations are based on the non-linear Schrödinger equation (NLS):

$$i\frac{\partial\psi}{\partial t}+\nabla_\perp^2\psi+s\frac{\partial^2\psi}{\partial z^2}+p|\psi|^2\psi=0\ ,\ \text{where}\ \nabla_\perp^2\psi\equiv\frac{\partial^2\psi}{\partial x^2}+\frac{\partial^2\psi}{\partial y^2}$$

that is a generic model for the non-linear evolution of the envelope of electromagnetic waves in Kerr-type media. These include various non-linear optical materials, plasmas and gases. Here $\psi$ is the complex envelope field and z is the direction of propagation. The second term models the diffraction in the transverse plane; the third term models the dispersion along the axis of propagation; here we consider the case of normal dispersion: $s < 0$. The last term on the left-hand side models the Kerr effect, and we consider the focusing, $p > 0$, case.

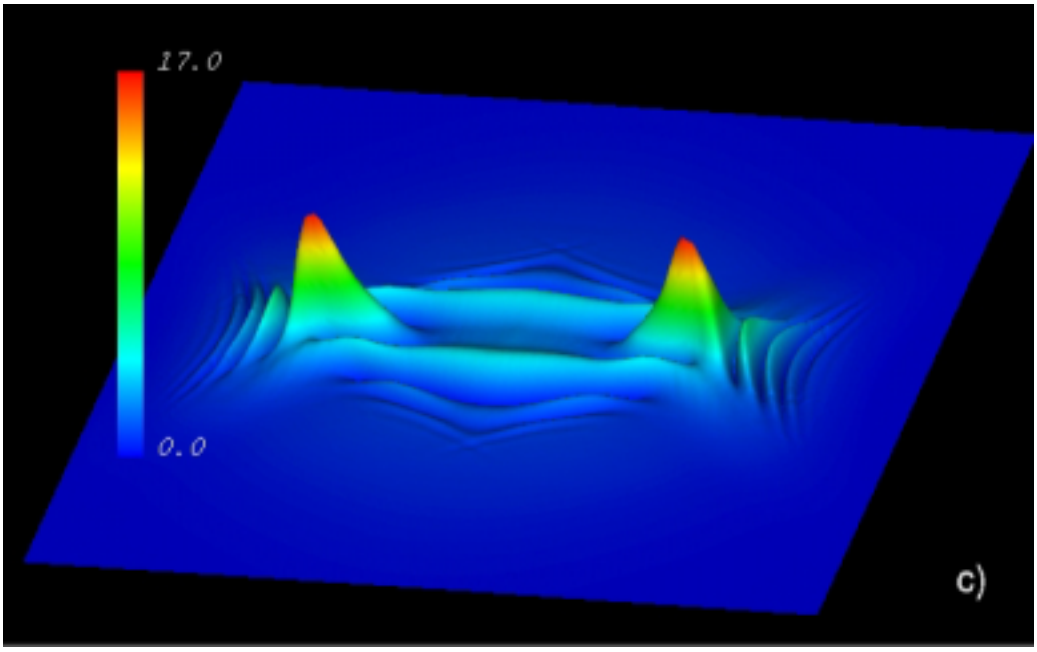


Figure 59. The evolution of a pulse in three dimensions. Shown is the amplitude of the envelope in the (x,z)-plane (y = 0) at a late time (t = 0.2735). The formation of ripple-like cells as the pulse spreads is clearly visible.

Numerical solutions of the NLS using an adaptive mesh refinement (AMR) code,[1] which accessed a remarkable resolution, showed that the interplay between self-focusing and GVD leads to the generic formation of temporal shocks at the peak edges. Beyond the shock, the two peaks disintegrate into ripple-like cells that, although they may partly self-focus, do not produce symmetric secondary peaks; this is illustrated in Figure 59 for the (3+1)-dimensional case. These observations are supported by analytical investigations. It is shown that pulse splitting introduced by GVD follows from shock fronts that develop along hyperbolas separating the region of transverse self-focusing from the domain of dispersion. The key idea is to reformulate the NLS in hyperbolic coordinates $\eta^2 = r^2 - z^2/|s|$ ($r^2 = x^2 + y^2$), in order to describe the shock fronts emerging between focusing ($\eta^2 > 0$) and defocusing ($\eta^2 < 0$) regions in the (r,z)-plane.

1. K. Germaschewski, R. Grauer, L. Bergé, V.K. Mezentsev and J. Juul Rasmussen, *Physica D* **151**, 175 (2001).

### 4.4.2 Quantum properties of spatial structures in cavity second-harmonic generation

*M. Bache (also at Informatics and Mathematical Modelling, Technical University of Denmark, Denmark), R. Zambrini*, P. Scotto* and M. San Miguel* (*Universitat de les Illes Baleares, Mallorca, Spain)*
morten.bache@risoe.dk

Cavity enhanced $\chi^{(2)}$ nonlinearities have recently drawn much attention on the formation of patterns in the intensity of the light beam. These patterns are observed in the transverse plane perpendicular to the propagation direction of the light beam and are a consequence of competition between the nonlinearity and the diffraction of the optical material. $\chi^{(2)}$ materials are interesting since they have a very fast response time giving them a potential application in information processing.

Another exciting feature of these materials is their inherent capability of producing highly non-classical light, being it squeezed states, sub-Poissonian statistics or entangled beams. This feature necessitates a quantum description of the system since a classical model cannot describe these states. The applications of the nonclassical light produced by $\chi^{(2)}$ materials are, e.g., ultraprecise measurements (of, e.g., gravitational waves), quantum computing and loss-less image amplification and duplication.

The manifestation of classical patterns such as hexagons and spiral waves in optics is merely a step in the right direction since the inherent quantum noise is not taken into account. We have investigated[1] the effect of this noise on a spatially unstable system that produces second-harmonic generation (SHG), where photons of frequency ω combine through nonlinear interactions in the material into photons of frequency 2ω. Interestingly, the spatial instability shows up in the spatial correlations even when the system is below the pump level for classical intensity patterns to occur. This phenomenon is called a *quantum image* since the correlations are exhibiting purely quantum behaviour. An example is shown in Figure 60 (left) where the normalised autocorrelation between intensity fluctuations in the far field, $C = \langle \delta I(+k)\delta I(-k)\rangle / \sqrt{\langle \delta I(+k)^2\rangle \langle \delta I(-k)^2\rangle}$, is calculated just below threshold. A clear structure around the critical pattern formation wave number $k_c \approx 2$ is seen even though this is below threshold where no classical image is observed.

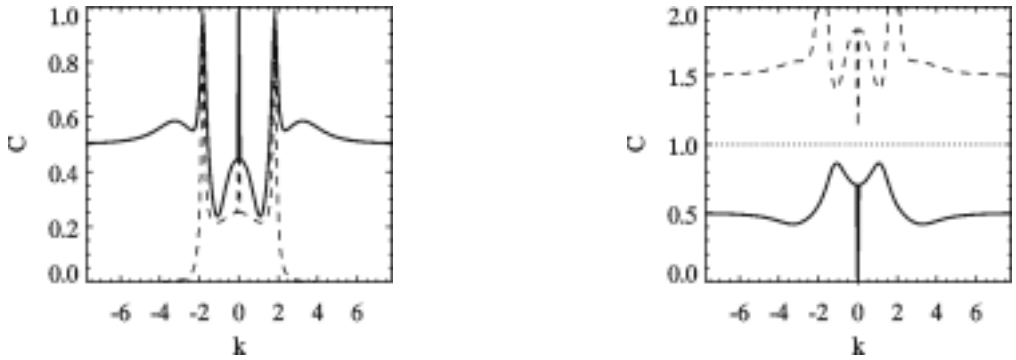


Figure 60. Left: Intensity correlation function in the far field, normalised so that $C = 1$ is the perfect correlation and $C = -1$ is the perfect anti-correlation. The full (dashed) line is the fundamental (second-harmonic) correlation between $+k$ and $-k$ calculated analytically just below threshold for pattern formation. Right: A plot in the far field showing the fundamental photon number variance of the sum (dashed line) and difference (full line) between intensities at $+k$ and $-k$, respectively. The dotted line shows the shot noise level, i.e. the limit between classical and quantum behaviour.

The complexity of SHG also allows us to speculate on the microscopic interaction in the system. Instead of thinking of the patterns as an intensity structure in the cross section of a beam, we now imagine what happens on a single photon level using the creation and the destruction operators of quantum mechanics and applying momentum and energy conservation. The fundamental photons of frequency ω are highly correlated, see Figure 60 (left) where near-perfect correlation at $k_c$ is observed. This is because they are destroyed in pairs to generate second-harmonic photons of frequency 2ω; they are therefore called twin photons. However strong correlations between second-harmonic photons are also observed as well as strong cross correlations between fundamental and second-harmonic photons. This fact is less intuitive and shows that the processes of creation and destruction of photons in the spatially unstable system must be thought of as transitive. Hence the strong twin-photon correlation spreads through other processes to generate strong correlations between the other modes of the system.

The photons of a coherent laser beam obey Poissonian counting statistics, while the nonlinear interaction in the $\chi^{(2)}$ material may produce sub-Poissonian statistics. This implies a less bunched appearance of the photons and is a manifest of the quantum fluctuations. The correlations were calculated as $C = \mathrm{Var}\left[I(+k) \pm I(-k)\right]$ and we were able to observe sub-Poissonian statistics in the intensity difference between the fundamental modes at $+k$ and $-k$, see Figure 60 (right). Here the dotted line denotes the classical limit of a coherent field and, clearly, the difference variance is below this level. On the other hand the sum variance of the modes displays super-Poissonian statistics, i.e. they are more bunched than a regular coherent beam.

In this work we include the spatial coupling through a diffractive Laplacian term, but the simplest coupling is through overlapping waves between two waveguides. We have proposed a model[2] investigating the quantum behaviour of such a simple spatial coupling, and expect to gain insight into the way the mode interaction takes place in the system.

1. M. Bache, R. Zambrini, P. Scotto, M. San Miguel and M. Saffman, "Quantum noise properties of spatial instabilities in second-harmonic generation", submitted to *Phys. Rev. A.*
2. M. Bache, Y.B. Gaididei and P.L. Christiansen, "Squeezing in intracavity coupled $\chi^{(2)}$ waveguides: the quantum optical dimer", in preparation.

### 4.4.3 Supercontinuum generation in photonic crystal fibres

*N. Nikolov (also at Informatics and Mathematical Modelling, Technical University of Denmark, Denmark) and O. Bang (Informatics and Mathematical Modelling, Technical University of Denmark, Denmark)*
nin@imm.dtu.dk

Since the first fabrication of a holey fibre in 1996,[1] many investigations on the remarkable properties of these fibres have been performed. Holey fibres are now used in many areas as, e.g., non-linear optics, quantum electrodynamics, fibre optics, spectroscopy, biomedical optics and metrology.[2]

Photonic –crystal fibres (PCFs) are holey fibres, where the cladding holes are arranged periodically. Due to the periodicity, a photonic bandgap effect in the transmission spectra perpendicular to the waveguide direction is formed. The photonic bandgap effect gives rise to an engineerable waveguide contribution of the group-velocity dispersion, and very unusual chromatic dispersion characteristics can be achieved using PCFs. Another important property of PCFs is the strong confinement of the light around the fibre core, a property that gives rise

to strong non-linear effects. Due to both the unusual dispersion and the enhanced non-linear properties, efficient supercontinuum generation is possible in PCFs.

We investigate the dispersion properties of PCFs, properties that were then used to model the propagation of ps and fs pulses by numerical integration of generalised coupled non-linear Schrödinger (GCNS) equations. The GCNS equations include terms describing the self- and cross-phase modulation, the four-wave mixing and the stimulated Raman scattering. According to our simulation results and to the experimental and numerical results of Ref. 3, the stimulated Raman scattering is the key for the formation of the supercontinuum through the generation of additional Stokes and anti-Stokes spectral components that are then broadened due to the other non-linear processes.

All this lets us conclude that PCFs are very promising tools for super-continuum generation.

1. J.C. Knight, T.A. Birks, P.St.J. Russell and D.M. Atkin, "All-silica single-mode optical fiber with photonic crysrtal cladding", *Opt. Lett.* **21**, 1547 (1996).
2. A. M. Zheltikov, "Holey fibers", *Physics-Uspekhi* **43**, 1125-1136 (2000).
3. S. Coen, A. Chao, R. Leonardt and J. Harvey, "White light supercontinuum generation with 60-ps pump pulses in a photonic crystal fiber", *J.Opt.Soc.Am. B* **26**, 1356 (2001).

### 4.4.4 Topological model for charge transport in disordered solids: ac universality and fracton superconductivity

*A.V. Milovanov (Department of Space Plasma Physics, Space Research Institute, 117810 Moscow, Russia) and J. Juul Rasmussen*
jens.juul.rasmussen@risoe.dk

Charge transport in structurally disordered solids reveals a number of unconventional features. Amongst them is the universality of the ac conduction recognized in materials as diverse as ion conducting glasses, amorphous and polycrystalline semiconductors, organic-inorganic composites, ion and electron conducting polymers, doped semiconductors at liquid helium temperatures, etc.[1] The defining feature of the ac universality is independence of the details of the disorder and of the nature of the conducting mechanism operating in the system (i.e. classical barrier crossing for ions and/or quantum-mechanical tunnelling for electrons). This makes it possible to rescale measurements of the frequency-dependent conductivity at different temperatures into a single master curve.

We advocate an unconventional description of charge transport processes in disordered solids, whereby the ideas of fractal geometry, percolation theory and topology of manifolds are brought together. We demonstrate that the marginal features of ac conductivity in disordered materials as seen in various experiments are reproduced with remarkable accuracy by the conduction properties of percolating fractal networks near the threshold of percolation. The universal character of ac conductivity in three embedding dimensions is given by the scaling law: $\sigma(\omega) \sim \omega^{\alpha}$ (where $\omega$ is the frequency). The value of $\alpha$ is between 0.6 and 1.0, which is typically observed in experiments. An important prediction of the present model is the 'hyperuniversal' scaling with $\alpha = 1/3$ for ac conduction in two dimensions.

In addition, we have considered an alternative explanation for the effective electron pairing mechanism in superconducting organic polymers. The key problem is that the electronic properties of polymers are dominated by the intrinsic structural disorder, which does not comply with the conventional Bardeen, Cooper and Schieffer (BCS) picture of superconductivity in regular crystal lattices. We argue that electron-electron interaction in self-assembling organic polymers is mediated by *fractons*, (quasi)acoustic excitations of fractal networks that mimic the complex microscopic organisation of the polymer systems.

The mechanism of the fracton superconductivity is discussed in connection with recent experimental observations.

1. J. C. Dyre and T. B. Schrøder, *Rev. Mod. Phys.* **72**, 873 (2000).

### 4.4.5 Random matrix theory and acoustic resonances

*A. Andersen (also at Department of Physics, Technical University of Denmark, Lyngby, Denmark), C. Ellegaard*, A.D. Jackson* and K. Schaadt* (*The Niels Bohr Institute, University of Copenhagen, Denmark)*
aanders@fysik.dtu.dk

Random matrix theory describes universal quantities determined by symmetries and has proved to be useful in many areas of physics in the description of correlations in energy level spectra. Random matrices do not only deal with level correlations, but are also applicable in the description of wave function properties. Motivated by experiments on acoustic resonances in plates of aluminium we have worked on the random matrix description of distributions of resonance widths. Acoustic resonances in a plate can be divided in different mode classes of which some are uncoupled and others mix to some extent. The effect of mixing of resonances on the width distribution has been described in terms of the change in wave function characteristics introduced by the mixing. The model motivated a new series of acoustic experiments in which a slit of increasing depth was cut on one face of a plate. Thereby the mirror symmetry through the middle plane of the plate was gradually broken and the otherwise uncoupled in-plane and bending modes mixed. The experiments turned out to confirm the theoretical predictions on the level correlations and the width distribution as discussed in Ref. 1.

1. A. Andersen, C. Ellegaard, A.D. Jackson and K. Schaadt, Random Matrix Theory and Acoustic Resonances in Plates with an Approximate Symmetry, *Physical Review E* **63**, 066204 (2001).

### 4.4.6 Re-orientation of optically active polymers

*P.M. Johansen, J. Juul Rasmussen, T.G. Pedersen (Aalborg University, Denmark), K. Jespersen, J. Wyller (Dept. of Mathematical Science, Agricultural University of Norway, Aas, Norway) and V. Naulin*
volker.naulin@risoe.dk

Understanding the relaxation processes in non-linear optical polymers is of critical importance to the development of materials for potential opto-electronic applications. We consider the relaxation behaviour of an active polymer with a finite electric dipole moment embedded in a polymer matrix without an electric far field.

The frictional backreaction of the matrix material onto the rotating polymer chain leads to a kind of behaviour that is often characterised by a phenomenological diffusion time. However, this approach only accounts for the influence of the polymer matrix in lowest order and the observed behaviour of the material is not well described by the assumption of a simple diffusion process. We have initialised analytical and numerical investigations of the statistical behaviour of the orientational dynamics of the active polymer in an external electric field. We incorporate the interaction of the active polymer with the matrix material in the form of a statistical molecular field that follows a separate evolution equation. Thereby we have a coupled non-linear model for the polymer–matrix interaction that will allow for a more precise and realistic description of the relaxation process.

Figure 61. Experimental set-up for investigating the reorientation effect.

### 4.4.7 Defect location with high-speed laser ultrasonics

*A. Bardenstein, B. Stenum and S. Arnfred Nielsen (also with FORCE Technology, Park Alle 345, DK-2605 Brøndby, Denmark)*
steen.arnfred.nielsen@risoe.dk

Laser ultrasound (LU) is a promising new technology for remote, non-contact inspection of material characteristics and defects in metals. In this technique, a pulsed laser is used to generate an ultrasonic pulse in the metal, and an interferometer or piezoelectric sensor is used to detect the ultrasonic pulse after it has propagated through the metal. LU has a number of unique applications: the high bandwidth of the laser-generated pulses enhances spatial resolution and provides more reliable defect detection compared with traditional ultrasonic techniques. The use of fibre optics allows new sensor configurations and inspection possibilities of complicatedly shaped metals. Inspection of metals in adverse manufacturing conditions, including vacuum or plasmas, is possible due to its remote, non-contact capability.

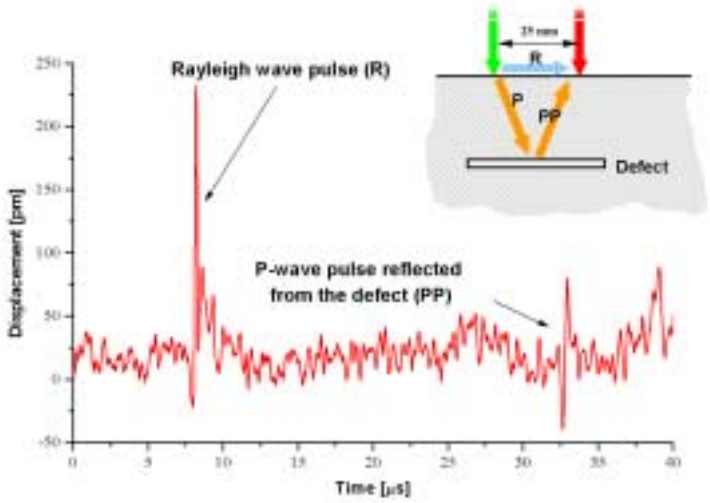


Figure 62. Defect location in a steel bar. The green laser generates an ultrasonic pulse into the material and the red laser is used for interferometric detection of the defect. The result: a received Rayleigh wave and a reflected P-wave. Notice that the reflected P-wave is only visible in the case of a defect.

In this project, we develop laser-optical, non-contact ultrasound methods for on-line process control. Figure 62 shows an example of defect location in a steel bar.

The aim is to apply LU to metal parts in industrial rough environments and to inspect metal parts during high speed. The project is a part of the Centre for On-Line, Non-Contact Sensing, Monitoring and Control of Industrial Processes and Systems (BIPS). The participants are FORCE Technology, Risø, Technical University of Denmark, Junckers Industrier A/S, Coloplast A/S, Danish National Railway Agency – Infrastructure Services Division, and SCITEQ-Hammel A/S.

# 5. Publications and educational activities

## 5.1 Laser systems and optical materials

### 5.1.1 International publications


*Bubb, D.M.; Horwitz, J.S.; McGill, R.A.; Chrisey, D.B.; Papantonakis, M.R.; Haglund Jr., R.F.; Toftmann, B.*, Resonant infrared pulsed-laser deposition of a sorbent chemoselective polymer. *Appl. Phys. Lett.* (2001) v. 79 p. 2847-2849

*Han, M.; Kidowaki, M.; Ichimura, K.; Ramanujam, P.S.; Hvilsted, S.*, Influence of structures of polymer backbones on cooperative photoreorientation behavior of p-cyanoazobenzene side chains. *Macromolecules* (2001) v. 34 p. 4256-4262

*Heisel, T.; Schou, J.; Christensen, S.; Andreasen, C.*, Cutting weeds with a $CO_2$ laser. *Weed Res.* (2001) v. 41 p. 19-29

*Helgert, M.; Wenke, L.; Hvilsted, S.; Ramanujam, P.S.*, Surface relief measurements in side-chain azobenzene polyesters with different substituents. *Appl. Phys. B* (2001) v. 72 p. 429-433

*Hvilsted, S.; Ramanujam, P.S.*, The azobenzene optical storage puzzle - Demands on the polymer scaffold?. *Monatsh. Chem.* (2001) v. 132 p. 43-51

*Hvilsted, S.; Ramanujam, P.S.*, Polymer scaffolds bearing azobenzene - Potential for optical information storage. *Chinese J. Polym. Sci.* (2001) v. 19 p. 147-153

*Juul Jensen, S.; Nicolaus, R.; Denz, C.*, Spatial-mode dynamics in a photorefractive ring oscillator with induced astigmatism. *J. Opt. Soc. Am. B* (2001) v. 18 p. 966-973

*Nedelchev, L.; Nikolova, L.; Todorov, T.; Petrova, T.; Tomova, N.; Dragostinova, V.; Ramanujam, P.S.; Hvilsted, S.*, Light propagation through photoinduced chiral structures in azobenzene-containing polymers. *J. Optics A* (2001) v. 3 p. 304-310

*Nikolajsen, T.; Johansen, P.M:; Sturman, B.I.; Podivilov, E.V.*, Modeling of photorefractive two-step gated recording by long-life-time intermediate levels. *J. Opt. Soc. Am. B* (2001) v. 18 p. 485-491

*Pedersen, H.C.; Johansen, P.M.; Pedersen, T.G.*, Analytical modeling of two beam coupling during grating translation in photorefractive media. *Opt. Commun.* (2001) v. 192 p. 377-385

*Pedersen, T.G.; Jespersen, K.; Johansen, P.M.*, Rotational diffusion model of orientational enhancement in AC field biased photorefractive polymers. *Opt. Mater.* (2001) v. 18 p. 95-98

*Podivilov, E.V.; Sturman, B.I.; Johansen, P.M.; Pedersen, T.G.*, Description of the photorefractive response in polymers. *Opt. Lett.* (2001) v. 26 p. 226-228

*Ramanujam, P.S.; Holme, N.C.R.; Pedersen, M.; Hvilsted, S.*, Fabrication of narrow surface relief features in a side-chain azobenzene polyester with a scanning near-field microscope. *J. Photochem. Photobiol. A* (2001) v. 145 p. 49-52

*Ramanujam, P.S.; Hvilsted, S.; Ujhelyi, F.; Koppa, P.; Lörincz, E.; Erdei, G.; Szarvas, G.*, Physics and technology of optical storage in polymer thin films. *Synth. Met.* (2001) v. 124 p. 145-150

*Sajti, S.; Kerekes, A.; Barabas, M.; Lörincz, E.; Hvilsted, S.; Ramanujam, P.S.*, Simulation of erasure of photoinduced anisotropy by circularly polarized light. *Optics Commun.* (2001) v. 194 p. 435-442

*Sanchez, C.; Alcala, R.; Hvilsted, S.; Ramanujam, P.S.*, High diffraction efficiency polarization gratings recorded by biphotonic holography in an azobenzene liquid crystalline polyester. *Appl. Phys. Lett.* (2001) v. 78 p. 3944-3946

*Schou, J.; Stenum, B.; Pedrys, R.*, Sputtering of solid deuterium by He-ions. *Nucl. Instrum. Methods Phys. Res. B* (2001) v. 182 p. 116-120

*Wyller, J.; Pedersen, T.G.; Johansen, P.M.*, Mathematical properties of the rotational diffusion equation. *J. Phys. A* (2001) v. 34 p. 6531-6542

*Yaroshchuk, O.; Otto, K.; Pelzl, G.; Janovski, F.; Ramanujam, P.S.*, Polarization holograms in a "liquid crystal-porous glass" system. *Mol. Cryst. Liquid. Cryst.* (2001) v. 359 p. 635-646

### 5.1.2 Danish publications

*Johansen, P.M.*, Linear and nonlinear space-charge field effects in photorefractive materials. Risø-R-1254(EN) (2001) 54 p. (dr.scient. thesis) www.risoe.dk/rispubl/ofd/ris-r-1254.htm

*Johansen, P.M.; Pedersen, H.C.; Petersen, P.M.*, Fotorefraktive materialer - et skoleeksempel inden for den ikke-lineære optik. *Nat. Verden* (2001) v. 84 (no.4) p. 10-17

*Samsøe, E.*, A new diode laser system for photodynamic therapy. Risø-R-1285(EN) (2001) 65 p. (master thesis) www.risoe.dk/rispubl/ofd/ris-r-1285.htm

### 5.1.3 Conference lectures

*Lörincz, E.; Ujhelyi, F.; Koppa, P.; Szarvas, G.; Erdei, G.; Fodor, J.; Sütö, A.; Várhegyi, P.; Ramanujam, P.S.; Hvilsted, S.*, Read/write demonstrator of rewritable holographic memory card system. In: Technical digest. Optical data storage topical meeting 2001, Sante Fe, NM (US), 22-25 Apr 2001. (International Society for Optical Engineering, Bellingham, WA, 2001) p. 166-168

*Ramanujam, P.S.; Hvilsted, S.*, Side-chain azobenzene polyesters for optical information storage. In: Extended abstracts. 4. NIMC international symposium on photoreaction control and photofunctional materials (PCPM 2001), Ibaraki (JP), 14-16 Mar 2001. (National Institute of Materials and Chemical Research, Ibaraki, 2001) p. 82-85

*Samsøe, E.; Petersen, P.M.; Andersen, P.E.; Andersson-Engels, S.; Svanberg, K.*, Novel diode laser system for photodynamic therapy. In: Laser-tissue interactions, therapeutic applications, and photodynamic therapy. International symposium, Munich (DE), 17-21 Jun 2001. Birngruber, R.; Bergh, H. van den (eds.), (International Society for Optical Engineering, Bellingham, WA, 2001) (SPIE Proceedings Series, v. 4433; Progress in Biomedical Optics and Imaging, v. 2, no. 33) p. 134-139

### 5.1.4 Publications for a broader readership

*Petersen, P.M.*, Center for Biomedical Optics and New Laser Systems. *DOPS-Nyt* (2001) v. 16 (no.4) p. 46

*Samsøe, E.; Andersen, P.E.; Petersen, P.M.; Andersson-Engels, S.; Svanberg, K.*, A novel diode laser system for photodynamic therapy. *DOPS-Nyt* (2001) v. 16 (no.4) p. 34-37

### 5.1.5 Unpublished Danish lectures

*Bubb, D.M.; Horwitz, J.S.; McGill, R.A.; Chrisey, D.B.; Haglund, R.H.; Papantonakis, M.R.; Toftmann, B.*, Resonant vs. non-resonant infrared pulsed laser deposition of polymer films (poster). DOPS annual meeting, Aarhus (DK), 22-23 Nov 2001. Unpublished. Abstract available

*Holmelund, E.; Schou, J.; Tougaard, S.; Larsen, N.B.*, Doping of thin films of optical materials by pulsed laser deposition (poster). DOPS annual meeting, Aarhus (DK), 22-23 Nov 2001. Unpublished. Abstract available

*Pedersen, H.C.*, Optiske anvendelser af polymerer. ATV SEMAPP topical meeting, Odense (DK), Nov 2001. Unpublished.

*Samsøe, E.; Malm, P.; Andersen, P.E.; Petersen, P.M.; Andersson-Engels, S.*, Development of diode laser systems for photodynamic therapy (poster). DOPS annual meeting, Aarhus (DK), 22-23 Nov 2001. Unpublished. Abstract available

*Schou, J.*, Sputtering of pure and doped ice by keV ions - does such an experiment work?. Workshop on surface physics in planetary and astrophysical environments, University of Southern Denmark, Odense (DK), 9 Aug 2001. Unpublished.

*Schou, J.; Thestrup, B.; Toftmann, B.; Doggett, B.; Hansen, T.N.; Lunney, J.G.*, Dynamics of the expansion plume from laser ablated silver. In: Programme. Abstracts. List of participants. Danish Physical Society annual meeting 2001, Nyborg (DK), 31 May - 1 Jun 2001. (HCØ Tryk, Copenhagen, 2001) AF03

*Toftmann, B.; Schou, J.; Hansen, T.N.; Lunney, J.G.*, Electron temperatures and densities from laser-ablated silver at 355 nm. In: Programme. Abstracts. List of participants. Danish Physical Society annual meeting 2001, Nyborg (DK), 31 May - 1 Jun 2001. (HCØ Tryk, Copenhagen, 2001) AF08

### 5.1.6 Unpublished international lectures

*Bubb, D.M.; McGrill, R.A.; Houser, E.J.; Horwitz, J.S.; Callahan, J.H.; Pique, A.; Chrisey, D.B.; Vertes, A.; Galicia, M.C.; Papantonakis, M.R.; Haglund Jr., R.F.; Toftmann, B.*, Laser-based processing of polymers for fabrication of chemical sensors. International workshop MATCHEMS (Materials and Technologies for Chemical Sensors), Brecia (IT), 13-14 Sep 2001. Unpublished.

*Ellegaard, O.; Nedelea, T.; Schou, J.; Urbassek, H.M.*, Plume expansion of a laser-induced plasma studied with the Particle in Cell (PIC) method. 6. International conference on laser ablation (COLA 01), Tsukuba (JP), 1-5 Oct 2001. Unpublished. Abstract available

*Holmelund, E.; Schou, J.; Tougaard, S.; Larsen, N.B.*, Pure and Sn-doped ZnO films produced by pulsed laser deposition. 6. International conference on laser ablation (COLA 01), Tsukuba (JP), 1-5 Oct 2001. Unpublished. Abstract available

*Ramanujam, P.S.*, Optical data storage in azobenzene containing polymers (invited talk). In: 9. International topical meeting on optics of liquid crystals (OLC 2001), Sorrento (IT), 1-6 Oct 2001. (Società Italiana Cristalli Liquidi, [s.l.], 2001) 1 p.

*Samsøe, E.*, A novel diode laser system for photodynamic therapy. IPA 8. World congress on photodynamic medicine, Vancouver (CA), 5-9 Jun 2001. Unpublished.

*Samsøe, E.*, A novel diode laser system for photodynamic therapy. European conference on biomedical optics 2001 (ECBO 01), München (DE), 17-21 Jun 2001. Unpublished.

*Schou, J.*, Sputtering of isotopes of the solid hydrogens by light ions. In: Extended abstracts. International symposium on isotope effects in physics, chemistry and engineering, Nagoya (JP), 22-24 Aug 2001. (Nagoya University, Department of Nuclear Engineering, Nagoya, 2001) p. 57-59

*Schou, J.; Thestrup, B.; Toftmann, B.; Hansen, T.N.; Doggett, B.; Lunney, J.G.*, Non-linear plume dynamics of a laser ablated plume in a background gas. Nonlinear science festival 3, Lyngby (DK), 12-15 Jun 2001. Unpublished. Abstract available

*Schou, J.; Toftmann, B.*, Laser and ion beam impact on solids. 19. International conference on atomic collisions in solids, Paris (FR), 29 Jul - 3 Aug 2001. Unpublished. Abstract available

*Thestrup, B.; Schou, J.; Hansen, T.N.; Lunney, J.G.*, Expansion dynamics of a laser ablation silver plasma in a background gas. E-MRS 2001 Spring meeting, Strasbourg (FR), 5-8 Jun 2001. Unpublished. Abstract available

*Thestrup, B.; Toftmann, B.; Schou, J.; Doggett, B.; Lunney, J.G.*, Ion dynamics in laser ablation plumes from selected metals at 355 nm. 6. International conference on laser ablation (COLA 01), Tsukuba (JP), 1-5 Oct 2001. Unpublished. Abstract available

*Toftmann, B.*, Laser ablation of silver: An experimental study of the ablation yield and plume expansion. Seminar at Naval Research Laboratory, Washington, DC, 4 May 2001. Unpublished.

*Toftmann, B.; Cheshire, R.*, Progress report from Risoe experiments, ion probes. 5. MPPP (midterm) meeting, Dublin (IE), 25-26 Jun 2001. Unpublished.

*Toftmann, B.; Schou, J.; Hansen, T.N.; Lunney, J.G.*, Electron temperatures and densities in a laser ablation plume. E-MRS 2001 Spring meeting, Strasbourg (FR), 5-8 Jun 2001. Unpublished. Abstract available

### 5.1.7 Internal publications

*Petersen, P.M.; Bøgh, N.S.; Nielsen, M.E.; Thestrup, B.*, GILAS. Statusrapport 5. Risø-Dok-683 (2001) vp.

*Petersen, P.M.; Chi, M.; Bøgh, N.S.; Thestrup, B.*, GILAS. Statusrapport 2. Risø-Dok-680 (2001) 16 p.

*Petersen, P.M.; Juul Jensen, S.; Chi, M.; Thestrup, B.*, GILAS. Statusrapport 1. Risø-Dok-679 (2001) 27 p.

*Petersen, P.M.; Paulig, T.; Bøgh, N.S.; Chi, M.; Nielsen, M.E.; Thestrup, B.*, GILAS. Statusrapport 3. Risø-Dok-681 (2001) 32 p.

*Petersen, P.M.; Thestrup, B.; Chi, M.; Bøgh, N.S.; Nielsen, M.E.*, GILAS. Statusrapport 4. Risø-Dok-682 (2001) 26 p.

*Ramanujam, P.S.; Hvilsted, S.; Koppa, P.; Lorincz, E.; Szarvas, G.; Richter, P.; Toth, P.*, Method and system for recording of information on a holographic medium. PTC patentansøgning PTC/HU/01/00016; WO 01/57602

*Schou, J.* (ed.), Monitoring for pulsed plasma processing - New plasma probes for advanced manufacturing. Mid-term report. Risø-Dok-677 (2001) 34 p.

*Schou, J.* (ed.), Monitoring for pulsed plasma processing - New plasma probes for advanced manufacturing. Progress report. Risø-Dok-678 (2001) 29 p.

## 5.2 Optical diagnostics and information processing

### 5.2.1 International publications


*Angelsky, O.V.; Maksimyak, P.P.; Ryukhtin, V.V.; Hanson, S.G.*, New feasibilities for characterizing rough surfaces by optical-correlation techniques. *Appl. Opt.* (2001) v. 40 p. 5693-5707

*Bak, J.*, Retrieving CO concentrations from FT-IR spectra with nonmodeled interferences and fluctuating baselines using PCR model parameters. *Appl. Spectrosc.* (2001) v. 55 p. 591-597

*Eriksen, R.L.; Mogensen, P.C.; Glückstad, J.*, Elliptical polarisation encoding in two dimensions using phase-only spatial light modulators. *Opt. Commun.* (2001) v. 187 p. 325-336

*Glückstad, J.; Mogensen, P.C.*, Optimal phase contrast in common-path interferometry. *Appl. Opt.* (2001) v. 40 p. 268-282

*Glückstad, J.; Mogensen, P.C.*, Reverse phase contrast for the generation of phase-only spatial light modulation. *Opt. Commun.* (2001) v. 197 p. 261-266

*Horvath, R.; Voros, J.; Graf, R.; Fricsovszky, G.; Textor, M.; Lindvold, L.R.; Spencer, N.D.; Papp, E.*, Effect of patterns and inhomogeneities on the surface of waveguides used for optical waveguide lightmode spectroscopy applications. *Appl. Phys. B* (2001) v. 72 p. 441-447

*Kitchen, S.R.; Hanson, S.G.; Hansen, R.S.*, Introduction of the impulse response function in common-path interferometers with Fourier plane filters. *Opt. Rev.* (2001) v. 8 p. 378-381

*Krebs, F.C.; Lindvold, L.R.; Jørgensen, M.*, Superradiant properties of 4,4'-bis(1*H*-phenanthro[9,10-*d*]imidazol-2-yl)biphenyl and how a laser dye with exceptional stability can be obtained in only one synthetic step. *Tetrahedron Lett.* (2001) v. 42 p. 6753-6757

*Linneberg, C.; Jørgensen, T.M.*, The n-tuple classifier with arbitrary threshold levels - theory and implications. *Recent Res. Dev. Pattern Rec.* (2000) v. 1 Part 2 p. 219-236

*Mogensen, P.C.; Eriksen, R.L.; Glückstad, J.*, High capacity optical encryption system using ferro-electric spatial light modulators. *J. Opt. A.* (2001) v. 3 p. 10-15

*Mogensen, P.C.; Glückstad, J.*, Phase-only optical decryption of a fixed mask. *Appl. Opt.* (2001) v. 40 p. 1226-1235


### 5.2.2 Danish publications


*Frandsen, S.; Kjær Hansen, J.; Hansen, R.S.; Hanson, S.G.; Kristensen, L.; Lading, P.; Miller, G.; Sangill, O.*, Laser anemometry for control and performance measurements on wind turbines. 6-monthly progress report for the period 1 July 2000 to 1 January 2001. (2001) 16 p.

*Frosz, M.H.; Juhl, M.; Lang, M.H.*, Optical coherence tomography: System design and noise analysis. Risø-R-1278(EN) (2001) 62 p. eksamensopgave (midtvejsprojekt) www.risoe.dk/rispubl/ofd/ris-r-1278.htm

*Hansen, R.S.; Frandsen, S.; Kristensen, L.; Sangill, O.; Lading, P.; Miller, G.*, Laser anemometry for control and performance measurements on wind turbines. Publishable final report 01.07.98 to 29.09.01. (2001) 26 p.

*Samsøe, E.*, A new diode laser system for photodynamic therapy. Risø-R-1285(EN) (2001) 65 p. (master thesis) www.risoe.dk/rispubl/ofd/ris-r-1285.htm

*Thrane, L.*, Optical coherence tomography: Modeling and applications. Risø-R-1217(EN) (2001) 76 p. (ph.d. thesis) www.risoe.dk/rispubl/ofd/ris-r-1217.htm

### 5.2.3 Conference lectures

*Eriksen, R.L.; Mogensen, P.C.; Glückstad, J.*, Generalized 2D polarization encoding using liquid-crystal spatial light modulators. In: Proceedings. Diffractive and holographic technologies for integrated photonic systems, San Jose, CA (US), 22-23 Jan 2001. Sutherland, R.L.; Prather, D.W.; Cindrich, I. (eds.), (International Society for Optical Engineering, Bellingham, WA, 2001) (SPIE Proceedings Series, 4291) p. 120-131

*Glückstad, J.; Sinzinger, S.; Mogensen, P.C.*, The generalized phase contrast method in a planar optics system implementation. In: Technical digest. 8. Microoptics conference (MOC '01), Osaka (JP), 24-26 Oct 2001. (Japan Society of Appied Physics (JP), Osaka (JP), 2001) p. 30-33

*Hansen, R.S.*, Laser anemometry for control and performance measurements on wind turbines. In: Proceedings. Contractors' meeting: Advances in wind energy RTD. From FP4 towards FP5 (on CD-ROM), Athens (GR), 3-5 May 2000. (Office for Official Publications of the European Communities, Luxembourg (LU), 2001) 8 p.

*Hansen, R.S.; Lading, L.; Miller, G.*, Optical Mixing in coherent LIDARs: Comparing three schemes. In: Applications of photonic technology 4. Closing the gap between theory, development, and application. 4. International conference on applications of photonic technology (ICAPT 2000), Québec City (CA), 12-16 Jun 2001. Lessard, R.A.; Lampropoulos, G.A. (eds.), (The International Society for Optical Engineering, Bellingham, WA, 2001) (SPIE Proceedings Series, 4087) p. 988-992

*Hanson, S.G.*, Miniaturized optical sensors for industrial use. In: New perspectives for optical metrology. International Balatonfüred workshop (HoloMet workshop), Balatonfüred (HU), 24-27 Jun 2001. Osten, W.; Jüptner, W. (eds.), (Bremer Institut für Angewandte Strahltechnik, Bremen, 2001) p. 87-93

*Jørgensen, T.M.; Linneberg, C.*, Feature weighted ensemble classifiers - a modified decision scheme. In: Proceedings. 2. International workshop on multiple classifier systems (MCS 2001), Cambridge (GB), 2-4 Jul 2001. Kittler, J.; Roli, F. (eds.), (Springer, Berlin, 2001) (Lecture Notes in Computer Science, 2096) p. 218-227

*Kitchen, S.R.; Hanson, S.G.; Hansen, R.S.*, Fourier plane filters and common path interferometry in vibrometers and electronic speckle interferometers. In: Optical engineering for sensing and nanotechnology. 2001 International conference on optical engineering for sensing and nanotechnology (ICOSN 2001), Yokohama (JP), 6-8 Jun 2001. Iwata, K. (ed.), (The International Society for Optical Engineering, Bellingham, WA, 2001) (SPIE Proceedings Series, 4416) p. 108-111

*Samsøe, E.; Petersen, P.M.; Andersen, P.E.; Andersson-Engels, S.; Svanberg, K.*, Novel diode laser system for photodynamic therapy. In: Laser-tissue interactions, therapeutic applications, and photodynamic therapy. International symposium, Munich (DE), 17-21 Jun 2001. Birngruber, R.; Bergh, H. van den (eds.), (International Society for Optical Engineering, Bellingham, WA, 2001) (SPIE Proceedings Series, v. 4433; Progress in Biomedical Optics and Imaging, v. 2, no. 33) p. 134-139

### 5.2.4 Publications for a broader readership

*Glückstad, J.; Mogensen, P.C.; Eriksen, R.L.*, The generalised phase contrast method and its applications. *DOPS-Nyt* (2001) v. 16 (no.1) p. 49-54

*Hansen, R.S.*, Wind turbine project turns to fusion technology. *Fusion Business* (2000) (no.10) p. 1 www.fusion.org.uk/industry/newsletters/may$_2$000/fusbus10.pdf

*Hansen, R.S.*, Risø. In: Making a difference. The EURATOM/UKAEA Fusion and Industry Programme. (Culham Science Centre, Abingdon, 2001) p. 31-32

*Samsøe, E.; Andersen, P.E.; Petersen, P.M.; Andersson-Engels, S.; Svanberg, K.*, A novel diode laser system for photodynamic therapy. *DOPS-Nyt* (2001) v. 16 (no.4) p. 34-37

*Thrane, L.; Andersen, P.E.; Jørgensen, T.M.; Tycho, A.; Levitz, D.; Yura, H.T.; Pedersen, F.*, Optical coherence tomography. *DOPS-Nyt* (2001) v. 16 (no.4) p. 13-18

### 5.2.5 Unpublished Danish lectures

*Andersen, F.*, Temperatur. Måling af temperatur og kalibrering af termometre. Ellab seminar, Rødovre (DK), Oct 2001. Unpublished.

*Andersen, F.; Kaiser, N.E.*, Temperatur. Måling af temperatur og kalibrering af termometre. Bie & Berntsen A/S seminar om temperaturmåling, Rødovre (DK), 25 Sep 2001. Unpublished.

*Andersen, F.; Kaiser, N.E.*, Temperatur. Måling af temperatur og kalibrering af termometre. Bie & Berntsen A/S seminar om temperaturmåling, Århus (DK), 25 Oct 2001. Unpublished.

*Angelsky, O.V.; Maksimyak, P.P.; Ryukhtin, V.V.; Burkovets, D.N.; Kovalchuk, A.V.; Hanson, S.G.*, Laser light scattering from fractal structures - two ways of analysis. DOPS annual meeting, Aarhus (DK), 22-23 Nov 2001. Unpublished. Abstract available

*Eriksen, R.L.*, Den optiske laser pincet. Møde i Naturvidenskabeligt Selskab Fyn, Odense (DK), 28 Feb 2001. Unpublished.

*Eriksen, R.L.; Mogensen, P.C.; Glückstad, J.*, Programmable optical tweezers. Biomedical optics '01, Risø (DK), 30 Oct 2001. Unpublished.

*Eriksen, R.L.; Mogensen, P.C.; Glückstad, J.*, Multiple beam optical tweezers. DOPS annual meeting, Aarhus (DK), 22-23 Nov 2001. Unpublished. Abstract available

*Hansen, R.S.; Frandsen, S.; Kristensen, L.; Miller, G.; Hansen, J.K.; Sangill, O.; Lading, P.*, Laser anemometry for performance testing of wind turbines (poster). DOPS annual meeting, Aarhus (DK), 22-23 Nov 2001. Unpublished. Abstract available

*Jensen, P.S.*, Dual-beam Fourier transform near-infrared spectroscopy of aqueous solutions (poster). DOPS annual meeting, Aarhus (DK), 22-23 Nov 2001. Unpublished. Abstract available

*Levitz, D.; Hansen, P.R.; Thrane, L.; Andersen, P.E.; Jørgensen, T.M.; Andersen, C.; Pedersen, F.*, Optical coherence tomography for intracoronary diagnostics. DOPS annual meeting, Aarhus (DK), 22-23 Nov 2001. Unpublished.

*Pranov, H.; Sørensen, H.S.; Andersen, P.E.; Bornhop, D.J.; Larsen, N.B.; Rasmussen, H.K.*, Micro Interferometric Backscatter Detection (MIBD) (poster). DOPS annual meeting, Aarhus (DK), 22-23 Nov 2001. Unpublished. Abstract available

*Samsøe, E.; Malm, P.; Andersen, P.E.; Petersen, P.M.; Andersson-Engels, S.*, Development of diode laser systems for photodynamic therapy (poster). DOPS annual meeting, Aarhus (DK), 22-23 Nov 2001. Unpublished. Abstract available

*Thrane, L.; Jørgensen, T.M.; Pedersen, F.; Larsen, H.E.; Levitz, D.; Andersen, P.E.*, 3D imaging of biological tissue using OCT (poster). DOPS annual meeting, Aarhus (DK), 22-23 Nov 2001. Unpublished. Abstract available

### 5.2.6 Unpublished international lectures

*Andersen, F.*, Hysteresis, hysteria or history for type K thermocouples. In: Abstracts. 8. International symposium on temperature and thermal measurements in industry and science (TEMPMEKO 2001), Berlin (DE), 19-21 Jun 2001. (Physikalisch-Technische Bundesanstalt, Berlin, 2001) p. 14

*Clausen, S.*, Measurement of spectral emissivity by a FTIR spectrometer. In: Abstracts. 8. International symposium on temperature and thermal measurements in industry and science (TEMPMEKO 2001), Berlin (DE), 19-21 Jun 2001. (Physikalisch-Technische Bundesanstalt, Berlin, 2001) p. 45

*Glückstad, J.*, Activities undertaken in the Danish Programmable Phase Optics project (invited talk). Optik-Kolloquium 2001, Stuttgart (DE), 28 Feb 2001. Unpublished. Abstract available

*Glückstad, J.*, The generalized phase contrast (GPC) method: Theory and applications (invited talk). In: Conference program. OSA annual meeting and exhibit 2001, Long Beach, CA (US), 14-18 Oct 2001. (Optical Society of America, Long Beach, CA, 2001) p. 62

*Glückstad, J.*, Photonics cryptization technology. Special symposium on photonics encryption technology, Kochi (JP), 31 Oct and 2 Nov 2001. Unpublished.

*Glückstad, J.*, Measurement results on the PAL-SLM. Meeting at Hamamatsu Photonics, Hamakita (JP), 11 Nov 2001. Unpublished.

*Glückstad, J.; Eriksen, R.L.; Mogensen, P.C.*, Phase-only spatial light modulation by the Reverse Phase Contrast method. In: Program and book of abstracts. 9. International topical meeting on optics of liquid crystals (OLC 2001), Sorrento (IT), 1-6 Oct 2001. (Società Italiana Cristalli Liquidi, [s.l.], 2001) 1 p.

*Glückstad, J.; Mogensen, P.C.*, A theoretical framework for optimising common path interferometers. Meeting at Hagen University, Abt. Optische Nachrichtentechnik, Hagen (DE), 27 Feb 2001. Unpublished. Abstract available

*Glückstad, J.; Mogensen, P.C.*, Compact optical encryption system using ferroelectric spatial light modulators. Forum for Advanced Cryptographic Theory (FACT), Chuo University, Dept. of Advanced Cryptography, Tokyo (JP), 22 Oct 2001. Unpublished.

*Ham, E.W.M. van der; Battuello, M.; Bosma, R.; Clausen, S.; Enouf, O.; Filipe, E.; Fischer, J.; Gutschwager, B.; Hirvonen, T.; Holtoug, J.U.; Ivarsson, J.; Machin, G.; McEvoy, H.; Pérez, J.; Ricolfi, T.; Ridoux, P.; Sadli, M.; Schmidt, V.; Staniewicz, C.; Struss, O.; Weckström, T.*, Intercomparison of local temperature scales with transfer radiation thermometers between -50 deg. C and 800 deg. C. In: Abstracts. 8. International symposium on temperature and thermal measurements in industry and science (TEMPMEKO 2001), Berlin (DE), 19-21 Jun 2001. (Physikalisch-Technische Bundesanstalt, Berlin, 2001) p. 77

*Hansen, R.S.*, A laser anemometer for control and performance. Measurements on wind turbines. 15. International conference on lasers and electrooptics in Europe in wind energy RTDF - from FP4 towards FP5, München (DE), 18-22 Jun 2001. Unpublished. Poster available

*Hansen, R.S.; Miller, G.*, A laser anemometer for control and performance measurements on wind turbines. In: Proceedings. 11. Coherent laser radar conference, Malvern (GB), 1-6 Jul 2001. (Defence Evaluation and Research Agency, Malvern, 2001) p. 123

*Hanson, S.G.*, Statistics for partially developed speckles: The impact on speckle-based measurements. 5. International conference on correlation optics 2001, Chernivtsi (UA), 10-13 May 2001. Unpublished.

*Hanson, S.G.*, Miniaturized optical sensors for micromeasurement. 4. International workshop on automatic processing of fringe patterns (FRINGE 2001), Bremen (DE), 17-19 Sep 2001. Unpublished.

*Jensen, P.S.*, Dual-beam FTIR. Biomedical optics '01, Risø (DK), 30 Oct 2001. Unpublished. Abstract available

*Jørgensen, T.M.*, Modeling OCT by rolling a dice (oral presentation). Biomedical optics '01, Risø (DK), 30 Oct 2001. Unpublished. Abstract available

*Jørgensen, T.M.; Thrane, L.; Ersbøll, B.*, Assessment of the intrinsic noise in optical coherence tomography images (oral presentation). 2. International workshop on computer assisted fundus image analysis (CAFIA-2), Copenhagen (DK), 5-7 Oct 2001. Unpublished. Abstract available

*Samsøe, E.*, A novel diode laser system for photodynamic therapy. IPA 8. World congress on photodynamic medicine, Vancouver (CA), 5-9 Jun 2001. Unpublished.

*Samsøe, E.*, A novel diode laser system for photodynamic therapy. European conference on biomedical optics 2001 (ECBO 01), München (DE), 17-21 Jun 2001. Unpublished.

*Sinzinger, S.; Glückstad, J.; Mogensen, P.C.*, Integrated microoptical systems for phase contrast imaging. Jahrestagung der deutschen Gesellschaft für angewandte Optik (DGaO), Göttingen (DE), 5-9 Jun 2001. Unpublished. Copy of poster available

*Thrane, L.*, True-reflection OCT imaging (oral presentation). Biomedical optics '01, Risø (DK), 30 Oct 2001. Unpublished. Abstract available

### 5.2.7 Internal publications

*Glückstad, J.; Mogensen, P.C.*, Optical encryption: A feasibility study and critical overview. A report compiled for OPTILINK. Risø-Dok--665 (2001) vp.

*Glückstad, J.; Sørensen, T.*, A system for electromagnetic field conversion. US provisional patent application 60/339104

*Hansen, R.S.; Frandsen, S.; Kristensen, L.; Miller, G.; Kjær Hansen, J.; Sangill, O.; Lading, P.*, Laser anemometry for control and performance testing of wind turbines. Risø-Dok-676 (2001) vp.

## 5.3 Plasma and fluid dynamics

### 5.3.1 International publications

*Andersen, A.; Ellegaard, C.; Jackson, A.D.; Schaadt, K.*, Random matrix theory and acoustic resonances in plates with an approximate symmetry. *Phys. Rev. E* (2001) v. 63 p. 066204.1-066204.11

*Bindslev, H.; Porte, L.; Hoekzema, A.; Machuzak, J.; Woskov, P.; van Eester, D.; Egedal, J.; Fessey, J.; Hughes, T.* "Fast ion collective Thomson scattering, JET results and TEXTOR plans", Fusion Engineering and Design, 53, 105-111 (2001)

*Clercx, H.J.H.; Nielsen, A.H.; Torres, D.J.; Coutsias, E.A.*, Two-dimensional turbulence in square and circular domains with no-slip walls. *Eur. J. Mech. B* (2001) v. 20 p. 557-576

*Dinesen, P.G.; Hesthaven, J.S.*, Fast and accurate modeling of waveguide grating couplers. 2. Three-dimensional vectorial case. *J. Opt. Soc. Am. A* (2001) v. 18 p. 2876-2885

*Ditkowski, A.; Dridi, K.H.; Hesthaven, J.S.*, Convergent Cartesian grid methods for Maxwell's equations in complex geometries. *J. Comput. Phys.* (2001) v. 170 p. 39-80

*Dridi, K.H.; Hesthaven, J.S.; Ditkowski, A.*, Staircase-free finite-difference time-domain formulation for general materials in complex geometries. *IEEE Trans. Antennas Propag.* (2001) v. 49 p. 749-756

*Germaschewski, K.; Grauer, R.; Bergé, L.; Mezentsev, V.K.; Juul Rasmussen, J.*, Splittings, coalescence, bunch and snake patterns in the 3D nonlinear Schrödinger equation with anisotropic dispersion. *Physica D* (2001) v. 151 p. 175-198

*Karpman, V.I.; Juul Rasmussen, J.; Shagalov, A.G.*, Dynamics of solitons and quasisolitons of the cubic third-order nonlinear Schrödinger equation. *Phys. Rev. E* (2001) v. 64 p. 026614.1-026614.13

*Klinger, T.; Schröder, C.; Block, D.; Greiner, F.; Piel, A.; Bonhomme, G.; Naulin, V.*, Chaos control and taming of turbulence in plasma devices. *Phys. Plasmas* (2001) v. 8 p. 1961-1968

*Korsholm, S.B.; Michelsen, P.K.; Naulin, V.; Juul Rasmussen, J.; Garcia, L.; Carreras, B.A.; Lynch, V.E.*, Reynolds stress and shear flow generation. *Plasma Phys. Control. Fusion* (2001) v. 43 p. 1379-1397

*Krolikowski, W.; Bang, O.; Juul Rasmussen, J.; Wyller, J.*, Modulational instability in nonlocal nonlinear Kerr media. *Phys. Rev. E* (2001) v. 64 p. 016612.1-016612.8

*Lodahl, P.; Bache, M.; Saffman, M.*, Spatiotemporal structures in the internally pumped optical parametric oscillator. *Phys. Rev. A* (2001) v. 63 p. 023815.1-023815.12

*Milovanov, A.V.; Juul Rasmussen J.*, Critical conducting networks in disordered solids: ac universality from topological arguments. *Phys. Rev. B* (2001) v. 64 p. 212203.1-212203.4

*Okkels, F.*, Temporal structures in shell models. *Phys. Rev. E* (2001) v. 63 p. 056214.1 - 056214.6

*Porte, L; Bindslev, H.; Hoekzema, F.; Machuzak, J.; Woskov, P.; Van Eester, D.,* "Implementation of collective Thomson scattering on the TEXTOR tokamak for energetic ion measurements", Review of Scientific Instruments, 72, 1148-1150 (2001)

*Ruban, V.P.*, Slow inviscid flows of a compressible fluid in spatially inhomogeneous systems. *Phys. Rev. E* (2001) v. 64 p. 036305.1-036305.7

*Ruban, V.P.; Podolsky, D.I.; Juul Rasmussen, J.*, Finite time singularities in a class of hydrodynamic models. *Phys. Rev. E* (2001) v. 63 p. 056306.1 - 056306.9

*Saffman, M.; Zoletnik, S.; Basse, N.P.; Svendsen,W.; Kocsis, G.; Endler, M.*, $CO_2$ laser based two-volume collective scattering instrument for spatially localized turbulence measurements. *Rev. Sci. Instrum.* (2001) v. 72 p. 2579-2592

*Schröder, C.; Klinger, T.; Block, D.; Piel, A.; Bonhomme, G.; Naulin, V.*, Mode selective control of drift wave turbulence. *Phys. Rev. Lett.* (2001) v. 86 p. 5711-5714

*Schwab, M.; Denz, C.; Saffman, M.*, Transverse modulational instability in counterpropagating two-wave mixing with frequency-detuned pump beams. *J. Opt. Soc. Am. B* (2001) v. 18 p. 628-638

*Sukhorukov, A.A.; Kivshar, Y.S.; Bang, O.; Juul Rasmussen, J.; Christiansen, P.L.*, Nonlinearity and disorder: Classification and stability of nonlinear impurity modes. *Phys. Rev. E* (2001) v. 63 p. 036601.1 - 036601.18

*Sykes, A.; Akers, R.J.; Appel, L.C.; Arends, E.R.; Carolan, P.G.; Conway, N.J.; Counsell, G.F.; Cunningham, G.; Dnestrovskij, A.; Dnestrovskij, Y.N.; Field, A.R.; Fielding, S.J.; Gryaznevich, M.P.; Korsholm, S.B.; Laird, E.; Martin, R.; Nightingale, M.P.S.; Roach, C.M.; Tournianski, M.R.; Walsh, M.J.; Warrick, C.D.; Wilson, H.R.; You, S.*, First results from MAST. *Nucl. Fusion* (2001) v. 41 p. 1423-1433

### 5.3.2 Danish publications

*Lomholt, S.*, Numerical investigations of macroscopic particle dynamics in microflows. Risø-R-1215(EN) (2001) 132 p. (ph.d. thesis) www.risoe.dk/rispubl/ofd/ris-r-1215.htm

*Lynov, J.P.; Singh, B.N (eds.)*, Association Euratom - Risø National Laboratory annual progress report 2000. Risø-R-1283(EN) (2001) 45 p. www.risoe.dk/rispubl/ofd/ris-r-1283.htm

*Lynov, J.P.; Singh, B.N (eds.)*, Association Euratom - Risø National Laboratory annual progress report 1999. Risø-R-1245(EN) (2001) 48 p. www.risoe.dk/rispubl/ofd/ris-r-1245.htm

### 5.3.3 Conference lectures

*Basse, N.P.; Michelsen, P.K.; Zoletnik, S.; Saffman, M.; Endler, M.; Hirsch, M.*, Spatial distribution of turbulence in the Wendelstein 7-AS stellarator (invited paper). In: Proceedings. Vol. 4. International conference on phenomena in ionized gases (25. ICPIG), Nagoya (JP), 17-22 Jul 2001. Goto, T. (ed.), (Nagoya University, Nagoya, 2001) p. 335-336

*Bindslev, H.; Porte, L.; Hoekzema, J.A.; Woskov, P.; Van Eester, D.; Messiaen, A.; Van Wassenhove, G.*, Fast ion dynamics in TEXTOR measured by collective Thomson scattering (oral presentation). In: Abstracts of invited and contributed papers. 28. European Physical Society conference on controlled fusion and plasma physics, Funchal (PT), 18-22 Jun 2001. Silva, C.; Varandas, C.; Campbell, D. (eds.), (Instituto Superior Tecnico, Funchal, 2001) p. 144

*Porte, L.; Bindslev, H.; Hoekzema, F.; Korsholm, S.B.; Kruyt, O.G.; Prins, R.; Woskov, P.*, Fast-ion collective Thomson scattering diagnostic on TEXTOR Tokamak (poster). In: Abstracts of invited and contributed papers. 28. European Physical Society conference on controlled fusion and plasma physics, Funchal (PT), 18-22 Jun 2001. Silva, C.; Varandas, C.; Campbell, D. (eds.), (Instituto Superior Tecnico, Funchal, 2001) p. 124

### 5.3.4 Publications for a broader readership

*Juul Rasmussen, J.*, De forunderlige hvirvler. *Aktuel Naturvidenskab* (2001) (no.2) p. 17-21

### 5.3.5 Unpublished Danish lectures

*Juul Rasmussen, J.*, Collapse dynamics in nonlinear Schroedinger equations with application to attractive Bose-Einstein condensates. NORDITA seminar, Copenhagen (DK), 22 Mar 2001. Unpublished.

*Michelsen, P.K.*, Status for fusionsforskningen. Møde i Kernefysisk Selskab, Ingeniørforeningen i Danmark, København (DK), 19 Mar 2001. Unpublished.

### 5.3.6 Unpublished international lectures

*Akers, R.J.; Appel, L.; Arends,E.R.; Carolan, P.G.; Conway, N.; Counsell, G.; Cunningham, G.; Dnestrovskij, A.; Dnestrovskij, Y.N.; Field, A.R.; Fielding, S.J.; Gryaznevich, M.; Kirk, A.; Korsholm, S.; Laird, E.; Martin, R.; Roach, C.; Sykes, A.; Walsh, M.J.; Warrick, C.*, Confinement in L and H-mode MAST plasmas (poster). In: Abstracts of invited and contributed papers. 28. European Physical Society conference on controlled fusion and plasma physics, Funchal (PT), 18-22 Jun 2001. Silva, C.; Varandas, C.; Campbell, D. (eds.), (Instituto Superior Tecnico, Funchal, 2001) p. 176

*Andersen, A.*, The bathtub vortex. Institut seminar at Eindhoven University of Technology, Department of Physics, Eindhoven (DK), 13 Sep 2001. Unpublished.

*Andersen, A.; Bohr, T.; Lautrup, B.; Juul Rasmussen, J.; Stenum, B.*, The flow structure of a bathtub vortex. 54. Annual meeting of the APS Division of Fluid Dynamics, San Diego (CA), 18-20 Nov 2001. Unpublished. Abstract available

*Andersen, A.; Bohr, T.; Juul Rasmussen, J.; Stenum, B.*, Bathtub vortices. Nonlinear science festival 3, Lyngby (DK), 12-15 Jun 2001. Unpublished. Abstract available

*Bache, M.; Lodahl, P.; Saffman, M.*, Spiral waves in optical second-harmonic generation. Nonlinear science festival 3, Lyngby (DK), 12-15 Jun 2001. Unpublished. Abstract available

*Basse, N.P.; Zoletnik, S.; Saffman, M.; Antar, G.; Michelsen, P.K.*, Temporal separation of turbulent time series: Measurements and simulations. In: Book of abstracts. 9. European fusion theory conference (EFTC), Elsinore (DK), 17-19 Oct 2001. (Risø National Laboratory, Optics and Fluid Dynamics Department, Roskilde, 2001) p. O-9

*Basse, N.P.; Zoletnik, S.; Saffman, M.; Endler, M.; Hirsch, M.*, Separation of L- and H-mode density fluctuations in dithering Wendelstein 7-AS plasmas (poster). In: Abstracts of invited and contributed papers. 28. European Physical Society conference on controlled fusion and plasma physics, Funchal (PT), 18-22 Jun 2001. Silva, C.; Varandas, C.; Campbell, D. (eds.), (Instituto Superior Tecnico, Funchal, 2001) p. 584

*Benilov, E.; Juul Rasmussen, J.*, Does a sheared current stabilise inversely stratified fluid?. EGS 2001, 26. General assembly, Nice (FR), 25-30 Mar 2001. Unpublished.

*Bindslev, H.; Porte, L.; Hoekzema, J. A.; Woskov, P.* "Fast ion dynamics measured by Collective Thomson Scattering of mm waves", Invited Lecture at the 10th International Symposium on Laser-Aided Plasma Diagnostics (LAPD-10), Fukuoka, Japan, 24-28 September 2001

*Bindslev, H.; Porte, L.; Hoekzema, J. A.; Van Eester, D.; Woskov, P.* "Fast ion dynamics measured by Collective Thomson Scattering", Invited Oral at the International conference on Advanced Diagnostics for Magnetic and Inertial Fusion, 3-7 September 2001, Varenna, Italy.

*Bindslev, H.* "Assessing and Optimising Diagnostic Capabilities of Interdependent Systems", Invited oral at the Wendelstein 7-X data validation workshop Greifswald, 30 July – 1 August 2001

*Bindslev*, H. "Fast ion dynamics measured by collective Thomson scattering", Oral at the 2001 US - European Transport Task Force Meeting, 16-19 May 2001, University of Alaska, Fairbanks.

*Bindslev, H.* "Fast ion dynamics measured by collective Thomson scattering", Invited Oral at the IEA-DED & IEA-TEXTOR workshop, Jülich, 26-28 March 2001.

*Bindslev, H.*, Fast ion dynamics measured by collective Thomson scattering (invited talk). 43. Annual meeting of the APS Division of Plasma Physics, Long Beach, CA (US), 29 Oct - 2 Nov 2001. Unpublished. Abstract available

*Bindslev, H.; Porte, L.; Hoekzema, J.A.; Woskov, P.; Eester, D. Van; Messiaen, A.; Wassenhove, G. Van*, Fast ion dynamics in TEXTOR measured by collective Thomson scattering (oral presentation). In: Abstracts of invited and contributed papers. 28. European Physical Society conference on controlled fusion and plasma physics, Funchal (PT), 18-22 Jun 2001. Silva, C.; Varandas, C.; Campbell, D. (eds.), (Instituto Superior Tecnico, Funchal, 2001) p. 144

*Dinesen, P.G.; Hesthaven, J.S.*, High-order methods for the analysis of diffractive optics. In: Book of abstracts. International conference on spectral and high order methods (ICOSAHOM-01), Uppsala (SE), 11-15 Jun 2001. (Uppsala University, Uppsala, 2001) 2 p.

*Donné, A. J. H.; Jaspers, R.; Barth, C. J.; Bindslev, H.; Elzendoorn, B. S. Q.; van Gorkom, J. C.; van der Meiden, H. J.; Oyevaar, T.; van de Pol, M. J.; Udintsev, V. S.; Widdershoven, H. L. M.; Biel, W.; Finken, K. H.; Krämer-Flecken, A.; Kreter, A. et al.*, " New diagnostics for physics studies on TEXTOR-94", Review of Scientific Instruments, 72, 1046-1053 (2001)

*Juul Rasmussen, J.*, Generation of large scale flows and transport barriers in plasma turbulence. Workshop on simulation of plasma turbulence and comparison with experiment, Kiel (DE), 7-9 Mar 2001. Unpublished.

*Juul Rasmussen, J.*, Collapse dynamics in nonlinear Schrödinger equations. Seminar at University of Linköping, Department of Physics and Measurement Technology, Linköping (SE), 22 Nov 2001. Unpublished.

*Juul Rasmussen, J.*, Turbulent equipartition (invited talk). Annual meeting og the Swedish Fusion Research Unit, Stockholm (SE), 7-8 Nov 2001. Unpublished.

*Juul Rasmussen, J.*, Fusion research at Risø. Annual meeting og the Swedish Fusion Research Unit, Stockholm (SE), 7-8 Nov 2001. Unpublished.

*Juul Rasmussen, J.; Naulin, V.; Nycander, J.*, Turbulent equipartition and the dynamics of transport barriers in electrostatic turbulence (poster). In: Book of abstracts. 9. European fusion theory conference (EFTC), Elsinore (DK), 17-19 Oct 2001. (Risø National Laboratory, Optics and Fluid Dynamics Department, Roskilde, 2001) ((EN)) p. P1-13

*Juul Rasmussen, J.; Naulin, V.*, Transport of momentum and particles in electrostatic drift wave turbulence. 4. International workshop on nonlinear waves and chaos in space plasmas, Tromsø (NO), 17-22 Jun 2001. Unpublished. Abstract available

*Juul Rasmussen, J.; Naulin, V.; Nielsen, A.H.*, Dynamics of vortex interactins in two-dimensional flows. In: Programme and book of abstracts. International topical conference on plasma physics: New plasma horizons, Faro (PT), 3-7 Sep 2001. (University of Algarve, Faro, 2001) 1 p.

*Juul Rasmussen, J.; Naulin, V.*, Particle diffusion and density flux in anisotropic turbulence dominated by vortical structures. EUROMECH workshop 428: Transport by coherent structures in environmental and geophysical flows, Torino (IT), 26-29 Sep 2001. Unpublished. Abstract available

*Korsholm, S.B.; Michelsen, P.K.; Naulin, V.; Juul Rasmussen, J.*, Reynolds stress and effects of external and self-generated shear flows (poster). In: Book of abstracts. 9. European fusion theory conference (EFTC), Elsinore (DK), 17-19 Oct 2001. (Risø National Laboratory, Optics and Fluid Dynamics Department, Roskilde, 2001) p. P1-6

*Korsholm, S.B.; Michelsen, P.K.; Naulin, V.; Juul Rasmussen, J.*, Analysis of determination of Reynolds stress in drift wave turbulence (poster). In: Abstracts of invited and contributed papers. 28. European Physical Society conference on controlled fusion and plasma physics, Funchal (PT), 18-22 Jun 2001. Silva, C.; Varandas, C.; Campbell, D. (eds.), (Instituto Superior Tecnico, Funchal, 2001) p. 650

*Lehane, I.; Mansfield, M.W.D.; Meyer, H.; Carolan, P.G.; Arends, E.R.; Korsholm, S.B.*, Impurity radiation amp; Transport in the MAST Tokamak (poster). 43. Annual meeting of the APS Division of Plasma Physics, Long Beach, CA (US), 29 Oct - 2 Nov 2001. Unpublished. Abstract available

*Naulin, V.*, Taming driftwave turbulence: Numerical simulations and experiment. 2001 US - European Transport Task Force meeting, Fairbanks, AK (US), 16-19 May 2001. Unpublished.

*Naulin, V.*, Stabilization of Rayleigh Taylor types of instability by shearing. Seminar on dynamics of complex systems, University of Alaska, Fairbanks, AK (US), 21-23 May 2001. Unpublished.

*Naulin, V.*, Turbulent transport: From fluxes to diffusion coefficients. Workshop on simulation of plasma turbulence and comparison with experiment, Kiel (DE), 7-9 Mar 2001. Unpublished.

*Naulin, V.*, Driving forces and stabilizing agents in turbulence and their signatures. Workshop on simulation of plasma turbulence and comparison with experiment, Kiel (DE), 7-9 Mar 2001. Unpublished.

*Naulin, V.*, Flows and transport in 3D drift Alfven turbulence. Theorie Seminar at Max Planck Institut für Plasmaphysik, Zinnowitz (DE), 19-23 Nov 2001. Unpublished.

*Naulin, V.*, Flows and transport in 3D drift Alfven turbulence. Seminar at IPP Greifswald, Greifswald (DE), 11 Oct 2001. Unpublished.

*Naulin, V.; Basu, R.; Jessen, T.; Michelsen, P.K.; Nielsen, A.H.; Juul Rasmussen, J.*, Particle diffusion and density flux in strong drift-wave turbulence containing vortical structures (poster). In: Book of abstracts. 9. European fusion theory conference (EFTC), Elsinore (DK), 17-19 Oct 2001. (Risø National Laboratory, Optics and Fluid Dynamics Department, Roskilde, 2001) p. P1-11

*Naulin, V.; Korsholm, S.B.; Michelsen, P.K.; Juul Rasmussen, J.*, Flows and transport in 3D drift Alfvén turbulence (invited talk). In: Book of abstracts. 9. European fusion theory conference (EFTC), Elsinore (DK), 17-19 Oct 2001. (Risø National Laboratory, Optics and Fluid Dynamics Department, Roskilde, 2001) p. I-4

*Naulin, V.; Schröder, C.; Klinger, T.; Blick, D.; Piel, A.; Bonhomme, G.; Korsholm, S.B.*, Taming driftwave turbulence: Numerical simulations and experiment (poster). In: Abstracts of invited and contributed papers. 28. European Physical Society conference on controlled fusion and plasma physics, Funchal (PT), 18-22 Jun 2001. Silva, C.; Varandas, C.; Campbell, D. (eds.), (Instituto Superior Tecnico, Funchal, 2001) p. 519

*Nielsen, A.H.; Clercx, H.J.H.; Coutsias, E.A.*, Vortex evolution in forced 2D bounded flow. EGS 2001, 26. General assembly, Nice (FR), 25-30 Mar 2001. Unpublished. Abstract available

*Nielsen, A.H.; Clercx, H.J.H.; Coutsias, E.A.*, A dipole interacting with a curved no-slip wall. New trands in no-slip vortex flows programme workshop, Eindhoven (NL), 17-18 Sep 2001. Unpublished.

*Nielsen, S.A.; Hesthaven, J.S.; Lynov, J.P.*, Multidomain pseudospectral simulation of ultrasonic fields in discontinuous solids. In: Book of abstracts. International conference on spectral and high order methods (ICOSAHOM-01), Uppsala (SE), 11-15 Jun 2001. (Uppsala University, Uppsala, 2001) 2 p.

*Nikolov, N.I.; Bang, O.*, Supercontinuum generation in crystal fibres. International workshop on nonlinear photonic crystals, Lyngby (DK), 25-26 Oct 2001. Unpublished. Abstract available

*Porte, L.; Bindslev, H.; Hoekzema, F.; Korsholm, S.B.; Kruyt, O.G.; Prins, R.; Woskov, P.*, Fast-ion collective Thomson scattering diagnostic on TEXTOR Tokamak (poster). In: Abstracts of invited and contributed papers. 28. European Physical Society conference on controlled fusion and plasma physics, Funchal (PT), 18-22 Jun 2001. Silva, C.; Varandas, C.; Campbell, D. (eds.), (Instituto Superior Tecnico, Funchal, 2001) p. 124

*Porte, L.; Bindslev, H.; Hoekzema, F.; Machuzak, J.; Woskov, P.* "Fast-Ion Collective Thomson Scattering Diagnostic on TEXTOR Tokamak", poster at the 28th EPS (see above) (P1.110)

*Senchenko, S.*, Stability of weak turbulence Kolmogorov spectra. Nonlinear science festival 3, Lyngby (DK), 12-15 Jun 2001. Unpublished. Abstract available

*Senchenko, S.*, Stability of weak turbulence Kolmogorov spectra. In: Europhysics conference abstracts, vol. 25G. International conference on waves and wave turbulence, Nyborg (DK), 12-15 Aug 2001. (European Physical Society, Paris, 2001) p. 21

*Thomassen, J.Q.; Jespersen, T.S.; Andersen, A.; Bohr, T.*, Vortex dynamics around a solid ripple in an oscillatory flow. Workshop: Discussions on the formation and dynamics of ripples, dunes and related systems, Paris (FR), 2-5 May 2001. Unpublished.

# 6. Personnel

**Scientific staff**

Andersen, Peter E.
Bak, Jimmy
Bindslev, Henrik (from 1 May)
Clausen, Sønnik
Daria, Vincent (from 1 November)
Dinesen, Palle (until 31 January)
Glückstad, Jesper
Hansen, René Skov
Hanson, Steen Grüner
Jakobsen, Michael Linde
Jensen, Sussie Juul (until 31 January)
Johansen, Per Michael
Jørgensen, Thomas Martini
Kirkegaard, Mogens
Larsen, Henning
Lynov, Jens-Peter
Michelsen, Poul K.
Naulin, Volker
Nielsen, Anders H.
Nielsen, Birgitte Thestrup (from 1 April)
Pedersen, Henrik Chresten
Petersen, Paul Michael
Ramanujam, P.S.
Rasmussen, Jens Juul
Schou, Jørgen
Stenum, Bjarne

**Post Doctoral Research Fellows**

Bardenshtein, Alexander (from 1 March)
Chi, Mingjun
Christensen, Bo Toftmann (from 1 July)
Horvath, Robert (from 1 November)
Kjærgaard, Niels (from 17 September)
Mogensen, Paul Christian (until 30 September)
Nielsen, Birgitte Thestrup (until 31 March)
Thrane, Lars
Tycho, Andreas (from 1 October)

**Industrial Post Doctoral Research Fellows**

Dridi, Kim (until 31 April)
Nielsen, Steen Arnfred (until 30 June)

**PhD students**

Andersen, Anders
Andersen, Eva Samsøe
Bache, Morten
Basse, Nils
Christensen, Bo Toftman
Eriksen, René Lynge
Jensen, Peter Snoer
Jespersen, Kim G.
Korsholm, Søren Bang
Nikolov, Nikola Ivanov (from 1 February)
Okkels, Fridolin (until 27 April)
Senchenko, Sergey (from 1 March)

**Industrial PhD students**

Kitchen, Steven R.
Linneberg, Christian (until 31 March)

**Technical staff**

Andersen, Finn
Eilertsen, Erik
Eliasen, Finn
Jessen, Martin
Knudsen, Lene (from 1 March)
Nimb, Søren (from 1 June)
Nordskov, Arne
Pedersen, Finn
Petersen, Torben D.
Rasmussen, Erling
Sass, Bjarne
Stubager, Jørgen
Thorsen, Jess

**Apprentice**

Pedersen, Søren Peo

**Administrative staff**

Astradsson, Lone
Carlsen, Heidi
Skaarup, Bitten

**Students working for the Master's Degree**

Andersen, Marie Lund (1 January – 31 May)
Apitz, Dirk (from 1 November)
Basu, Ronni (from 5 February)
Levitz, David (1 June - 12 December)
Malm, Per (from 1 September)
Nikolaisen, Jeppe (from 26 October)

Osten, Stefan (1 June – 19 October)
Pranov, Henrik (from 1 July)
Sørensen, Henrik Schiøtt (from 1 July)

**Guest scientists**

Bornhop, Darryl, Texas Tech University, USA
Chakrabarti, Nikhil, Saha Institute of Nuclear Physics, India
Coutsias, Evangelos A., University of New Mexico, USA
Doggett, Brendan, Trinity College, Ireland
Garcia, Odd Erik, The University of Tromsø, Norway
Hesthaven, Jan, Brown University, Rhode Island, USA
Karpman, Vladimir, Racah Institute of Physics, Israel
Milovanov, Alexander, Space Science Institute, Russia
Montgomery, David, Dartmouth College, New Hampshire, USA, USA
Nielsen, Martin E., Purup-Eskofot, Denmark
Paulig, Thomas, University of Technology Chemnitz, Germany
Pécseli, Hans, University of Oslo, Norway
Podivilov, Evgeny, Institute of Automation and Electrometry, Russia
Ratynskaia, Svetlana, The University of Tromsø, Norway
Ruban, Victor P., Landau Institute for Theoretical Physics, Russia
Rypdal, Kristoffer, The University of Tromsø, Norway
Sajti, Szilàrd, Technical University of Budapest, Hungary
Shagalov, Arkadi G., Institute of Metal Physics, Russia
Wyller, John, Agricultural University of Norway, Norway
Yura, Harold T., The Aerospace Corporation, USA
Yurasova, Irina, Institute of Radiophysics, Russia

**Short-term visitors**

Baragiola, Raul, University of Virginia, USA
Bergé, Luc, Commissariat à l'Energie Atomique, Centre d'Etudes de Limeil-Valenton, France
Birngruber, Reginald, Medical Laser Center Lübeck GmbH, Germany
Bortwick, Stephen, Honeywell Control Systems, Scotland
Früh, Wolf-Gerrit, Heriot-Watt University, United Kingdom
Germashewskii, Kai, University of Düsseldorf, Germany
Grauer, Rainer, University of Düsseldorf, Germany
Kuznetsov, Eugenie A., Landau Institute for Theoretical Physics, Russia
McNamara, Honeywell Control Systems, Scotland
Mezentsev, Vladimir K., Aston University, United Kingdom
Schrøder, Christina, University of Greifswald, Germany

**Bibliographic Data Sheet** **Risø-R-1314(EN)**

Title and authors

Optics and Fluid Dynamics Department
Annual Progress Report for 2001

Edited by H. Bindslev, S.G. Hanson, J.P. Lynov, P.M. Petersen and B. Skaarup

| ISBN | ISSN |
|---|---|
| 87-550-2993-0 (Internet) | 0106-2840; 0906-1797 |

| Department or group | Date |
|---|---|
| Optics and Fluid Dynamics Department | March 2002 |

| Pages | Tables | Illustrations | References |
|---|---|---|---|
| 94 | | 62 | 71 |

Abstract (max. 2000 characters)

The Optics and Fluid Dynamics Department performs basic and applied research within three scientific programmes: (1) laser systems and optical materials, (2) optical diagnostics and information processing and (3) plasma and fluid dynamics. The department has core competences in: optical sensors, optical materials, optical storage, biooptics, numerical modelling and information processing, non-linear dynamics and fusion plasma physics. The research is supported by several EU programmes, including EURATOM, by Danish research councils and by industry. A summary of the activities in 2001 is presented.

Descriptors INIS/EDB

DYNAMICS; FLUIDS; LASERS; NONLINEAR OPTICS; NONLINEAR PROBLEMS; NUMERICAL SOLUTION; PLASMA; PROGRESS REPORT; RESEARCH PROGRAMMES; RISOE NATIONAL LABORATORY; THERMONUCLEAR REACTIONS